Bézier- and B-spline Techniques

Errata

Hartmut Prautzsch
Wolfgang Boehm
Marco Paluszny

April 2, 2005

1 Geometric fundamentals

1.1 Affine spaces — 1.2 Affine combinations — 1.3 Affine maps — 1.4 Parametric curves and surfaces — 1.5 Problems

The world can be seen as a space of points while vectors describe the directions and lengths of line segments between pairs of points. The interpretation of the world as a point space, and not as a vector space, has the advantage that any point can serve as the origin. This fact is also reflected by the symmetry of barycentric coordinates.

Since this book relies heavily on the concept of point or affine spaces, this chapter provides a brief recapitulation of their fundamental properties that are used throughout the book.

1.1 Affine spaces

An **affine space** $\mathcal{A}$ is a point space with an underlying vector space $\mathbf{V}$. Here we consider only finite-dimensional spaces over $\mathbb{R}$, which implies that points as well as vectors can be represented by the elements of some $\mathbb{R}^n$. Thus, any $\mathbf{x} \in \mathbb{R}^n$ represents a point or a vector, depending on the context. Moreover, we only work with such a coordinate representation and, therefore, simply regard $\mathcal{A}$ and $\mathbf{V}$ as some $\mathbb{R}^n$.

Given two points $\mathbf{p}$ and $\mathbf{q}$, the vector pointing from $\mathbf{p}$ to $\mathbf{q}$ is obtained as their difference,

$$\mathbf{v} = \mathbf{q} - \mathbf{p} \ ,$$

as illustrated in Figure 1.1. Note that a vector can be added to a point, but the sum of two points is undefined.

One can distinguish between points and vectors by **extended coordinates** with

$$\mathbb{x} = \begin{bmatrix} \mathbf{x} \\ e \end{bmatrix} \quad \text{representing a} \quad \begin{cases} \text{point} \\ \text{vector} \end{cases} \quad \text{if} \quad e = \begin{cases} 1 \\ 0 \end{cases} \ .$$

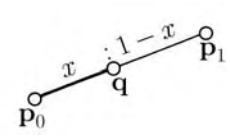

Figure 1.2: Linear interpolation and ratio.

any m points of $\mathcal{A}$. Then, the **weighted sum**

$$\mathbf{a} = \sum \mathbf{a}_i \alpha_i \quad \text{represents a} \quad \begin{cases} \text{point} \\ \text{vector} \end{cases} \quad \text{if} \quad \sum \alpha_i = \begin{cases} 1 \\ 0 \end{cases} .$$

If the weights sum to one, then $\mathbf{a} = \sum \mathbf{a}_i \alpha_i$ is called an **affine combination**. If, in addition, the weights are non-negative, then $\mathbf{a}$ is called a **convex combination**. It lies in the **convex hull** of the points $\mathbf{a}_i$, see Problem 4.

1.3 Affine maps

Let $\mathcal{A}$ and $\mathcal{B}$ be affine spaces, $\mathbf{U}$ and $\mathbf{V}$ be the underlying vector spaces and m and n be the corresponding dimensions, respectively. Then, a map $\Phi : \mathcal{A} \to \mathcal{B}$ is called **affine** if it can be represented by an $n \times m$ matrix A and a point $\mathbf{a}$ of $\mathcal{B}$ such that

$$\mathbf{y} = \Phi(\mathbf{x}) = \mathbf{a} + A\mathbf{x} \ ,$$

where $\mathbf{a}$ represents the image of the origin of $\mathcal{A}$.

The linear map $\varphi : \mathbf{U} \to \mathbf{V}$ given by

$$\mathbf{v} = \varphi(\mathbf{u}) = A\mathbf{u}$$

is called the **underlying linear map** of Φ. Using extended coordinates, both maps have the same matrix representation, which is given by

$$\begin{bmatrix} \mathbf{y} \\ 1 \end{bmatrix} = \begin{bmatrix} A & \mathbf{a} \\ \mathbf{o}^t & 1 \end{bmatrix} \begin{bmatrix} \mathbf{x} \\ 1 \end{bmatrix}, \quad \begin{bmatrix} \mathbf{v} \\ 0 \end{bmatrix} = \begin{bmatrix} A & \mathbf{a} \\ \mathbf{o}^t & 1 \end{bmatrix} \begin{bmatrix} \mathbf{u} \\ 0 \end{bmatrix} \ ,$$

and more concisely written as

$$\mathtt{y} = \mathbb{A}\mathtt{x} \ , \qquad \mathtt{v} = \mathbb{A}\mathtt{u} \ .$$

The following two properties are immediate consequences of the matrix representation.

An affine map Φ commutes with affine combinations, i.e.,

$$\Phi(\sum \mathbf{a}_i \alpha_i) = \sum \Phi(\mathbf{a}_i)\alpha_i \ .$$

And

an affine map is completely determined by a frame of $\dim \mathcal{A} + 1$ independent points $\mathbf{p}_0 \ldots \mathbf{p}_m$ and its image $\mathbf{q}_0 \ldots \mathbf{q}_m$.

The first property even characterizes affine maps, see Problem 5. The second property is due to the fact that the matrix $\mathbb{A}$ can be written as

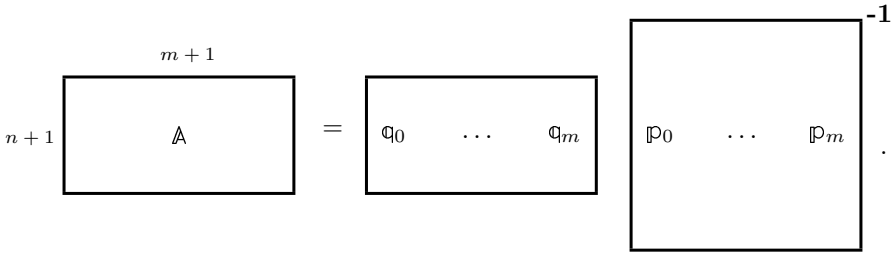

1.4 Parametric curves and surfaces

An element $\mathbf{x}$ of $\mathbb{R}^d$ whose coordinates depend on a parameter t traces out a **parametric curve**,

$$\mathbf{x}(t) = \begin{bmatrix} x_1(t) \\ \vdots \\ x_d(t) \end{bmatrix} .$$

Usually, we visualize $\mathbf{x}(t)$ as a point. In particular, if the coordinate functions $x_i(t)$ are polynomials of degree n or less than n, then $\mathbf{x}(t)$ is called a **polynomial curve** of degree n in t.

The **graph** of a function $x(t)$ is a special parametric curve in $\mathbb{R}^2$, which is given by

$$\mathbf{x}(t) = \begin{bmatrix} t \\ x(t) \end{bmatrix} .$$

Such a planar curve is often referred to as **functional curve**.

2.5 Singular parametrization

Consider a polynomial curve

$$\mathbf{b}(t) = \sum_{i=0}^{n} \mathbf{b}_i B_i^n(t)$$

and its derivative

$$\dot{\mathbf{b}}(t) = n \sum_{i=0}^{n-1} \triangle\mathbf{b}_i B_i^{n-1}(t) \ ,$$

where the dot indicates differentiation with respect to the parameter t.

If $\triangle\mathbf{b}_0 = \mathbf{o}$, then $\dot{\mathbf{b}}(t)$ is zero at $t = 0$. However, with the singular reparametrization $t = \sqrt{s}$, one gets

$$\frac{d}{ds}\mathbf{b}(t(0)) = n \cdot \triangle\mathbf{b}_1 \ .$$

Thus, if $\triangle\mathbf{b}_0 = \mathbf{o}$ and $\triangle\mathbf{b}_1 \neq \mathbf{o}$, then the curve $\mathbf{b}(t)$ has a tangent at $t = 0$ that is directed towards $\mathbf{b}_2$, as illustrated in Figure 2.9.

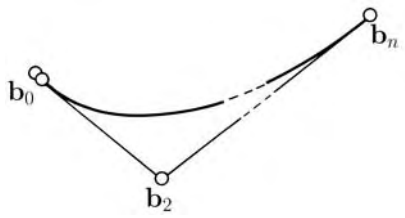

Figure 2.9: Singular parametrization.

Remark 6: If $\triangle\mathbf{b}_0 = \triangle\mathbf{b}_1 = \mathbf{o}$ and $\triangle\mathbf{b}_2 \neq \mathbf{o}$, then the tangent of $\mathbf{b}(t)$ at $t = 0$ is directed towards $\mathbf{b}_3$, etc.

2.6 A tetrahedral algorithm

Computing differences and the affine combinations of de Casteljau's algorithm can be combined. Namely, the rth derivative of a curve

$$\mathbf{b}(u) = \sum \mathbf{b}_i^0 B_i^n(t) \ , \quad t = \frac{u-a}{b-a} \ ,$$

at any u can be computed with de Casteljau's algorithm applied to multiples of the differences $\Delta^k\mathbf{b}_i$. Since the computation of affine combinations of

Remark 8: If $\mathbf{a}_2 = \cdots = \mathbf{a}_n = \mathbf{o}$ and $\mathbf{a}_1 \neq \mathbf{o}$, then $\mathbf{b}(\mathrm{t})$ is a linear polynomial represented over $[0, 1]$ by the Bézier points

$$\mathbf{b}_j = \mathbf{a}_0 + j\mathbf{a}_1 \ ,$$

as illustrated in Figure 2.12.

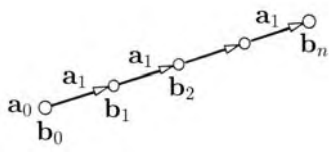

Figure 2.12: Equidistant Bézier points on a line.

Remark 9: Conversely, if the $n + 1$ Bézier points $\mathbf{b}_i$ lie equidistantly on a line, then $\mathbf{b}(\mathrm{t})$ is a linear polynomial, which can be written as

$$\mathbf{b}(t) = (1 - t)\mathbf{b}_0 + t\mathbf{b}_n \ .$$

This property is referred to as the **linear precision** of the Bézier representation.

Remark 10: As a consequence of Remark 8, the functional curve

$$\mathbf{b}(t) = \begin{bmatrix} t \\ b(t) \end{bmatrix}, \qquad b(t) = \sum b_i B_i^n(t) \ ,$$

has the Bézier points $[i/n \ \ b_i]^t$, as illustrated in Figure 2.13. The coefficients b_i are referred to as the **Bézier ordinates** of $b(t)$, and i/n as the **Bézier abscissae**.

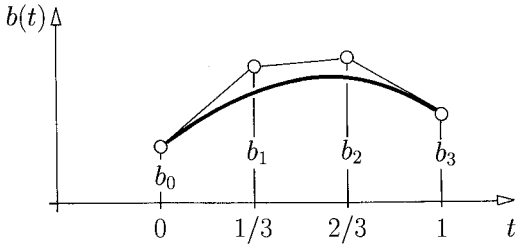

Figure 2.13: Bézier representation of a functional curve.

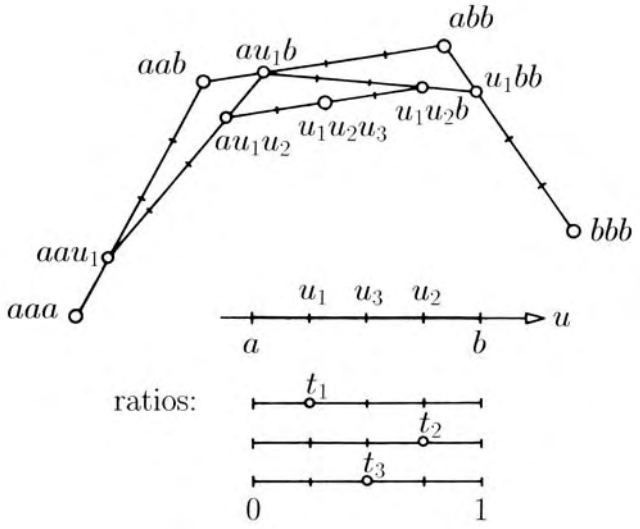

Figure 3.1: Main theorem, illustration.

In de Casteljau's array,

$$\begin{array}{lll} \mathbf{b}_0^0 & & \\ \mathbf{b}_1^0 & \mathbf{b}_0^1 & \\ \vdots & & \ddots \\ \mathbf{b}_n^0 & \mathbf{b}_{n-1}^1 \cdots & \mathbf{b}_0^n = \mathbf{b}(c) \end{array}$$

used to compute a point $\mathbf{b}(c)$, the Bézier points

$$\mathbf{b}_0^i = \mathbf{b}[a \overset{n-i}{\ldots} a\, c \overset{i}{\ldots} c] \quad \text{and} \quad \mathbf{b}_i^{n-i} = \mathbf{b}[c \overset{n-i}{\ldots} c\, b \overset{i}{\ldots} b]$$

of the curve segments over $[a, c]$ and $[c, b]$ are found in the upper diagonal and bottom row, respectively.

The computation of the Bézier points over the two intervals $[a, c]$ and $[c, b]$ is called **subdivision**. The corresponding construction is shown in Figure 3.2. Again, the points

$$\mathbf{b}_i^k = \mathbf{b}[a \overset{n-i-k}{\ldots} a\, c \overset{k}{\ldots} c\, b \overset{i}{\ldots} b]$$

are labelled by their arguments. Note that the figure is still correct if we interchange b and c.

On subdividing $\mathbf{b}(u)$ repeatedly, one can obtain the Bézier polygons of $\mathbf{b}(u)$ over any number of abutting intervals $[a_0, a_1], [a_1, a_2], \ldots, [a_{k-1}, a_k]$.

Together, these polygons form the **composite Bézier polygon** of $\mathbf{b}$ over

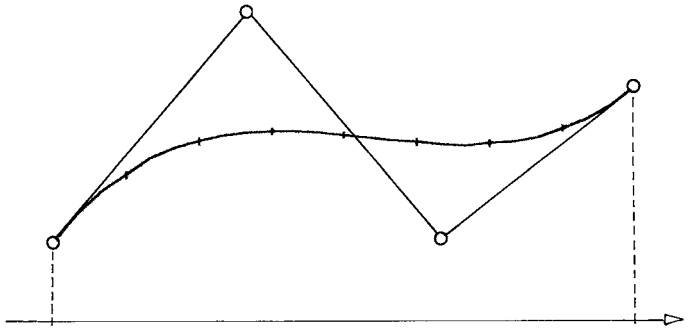

Figure 3.3: Subdividing a Bézier polygon three-times.

ment $\mathbf{b}_0\mathbf{b}_n$ when this criterion is satisfied. A bound of its deviation from the curve is given by the following theorem:

Let $\mathbf{l}(t) = \mathbf{b}_0(1-t) + \mathbf{b}_n t$ *be the linear interpolant of* $\mathbf{b}(t)$*. Then,*

$$\begin{aligned} \sup_{0\le t\le 1} \|\mathbf{b}(t) - \mathbf{l}(t)\| &\le \frac{1}{8} \sup_{0\le t\le 1} \|\ddot{\mathbf{b}}(t)\| \\ &\le \frac{1}{8} n(n-1) \max_{i=0,\ldots,n-2} \|\Delta^2 \mathbf{b}_i\| \ , \end{aligned}$$

where $\|\cdot\|$ *denotes the supremum, sum, or Euclidean norm.*

For a proof, we refer to [Boor '78, p. 39] and [Filip et al. '86].

Remark 4: If $\mathbf{b}(u)$ has the Bézier points $\mathbf{b}_i$ over $[a, b]$ and the Bézier points $\mathbf{c}_i$ over some subinterval $[c, c+h]$, then the differences $\|\Delta^2 \mathbf{c}_i\|$ are bounded by $(h/(b-a))^2 \max \|\Delta^2 \mathbf{b}_i\|$, see Problem 3. Hence, the approximation order of a linear interpolant is quadratic. Moreover, the approximation order is only quadratic, in general. Thus, due to Remark 3, the composite Bézier polygon over $[0, \frac{1}{2^m}, \ldots, 1]$ is, asymptotically, as good an approximation as the secant polygon with vertices

$$\mathbf{b}(\frac{i}{(n2^m)}), \quad i = 0, 1, \ldots, n2^m \ .$$

Remark 5: Essentially, the above plotting routine only evaluates convex combinations of the form $(\mathbf{a}+\mathbf{b})/2$. Thus, one can accelerate the procedure if the divisions by 2 are realized by bit shifts. Then there are roughly $(n+1)/2$ vector additions and 1 division per vertex of the polygon in this plotting routine.

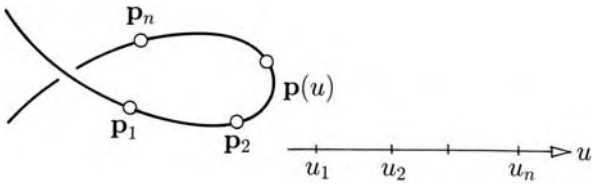

Figure 4.1: Interpolating curve

For a proof, write the **interpolation conditions** in matrix notation,

$$\begin{bmatrix} C_1(u_1) & \dots & C_n(u_1) \\ \vdots & & \vdots \\ C_1(u_n) & \dots & C_n(u_n) \end{bmatrix} \begin{bmatrix} \mathbf{x}_1^t \\ \vdots \\ \mathbf{x}_n^t \end{bmatrix} = \begin{bmatrix} \mathbf{p}_1^t \\ \vdots \\ \mathbf{p}_n^t \end{bmatrix} ,$$

or more concisely,

$$CX = P \ ,$$

which represents d simultaneous linear systems for the d columns of X. The existence of the solution follows from the linear independence of $C_1, \dots, C_n$ over $u_1, \dots, u_n$. ◇

Remark 1: If the C_i are linearly independent polynomials of degree $n-1$, then the matrix C is invertible for any n distinct values $u_1, \dots, u_n$. Namely, the homogeneous system $C\mathbf{x} = \mathbf{o}$ (for a single column $\mathbf{x}$) has only the trivial solution $\mathbf{x} = \mathbf{o}$ since the zero polynomial is the only polynomial of degree $n-1$ with n roots.

Remark 2: Two points can be interpolated by a line, three points by a parabola, four points by a cubic, and so on.

4.2 Lagrange form

A fundamental and simple method to obtain a polynomial interpolant is due to Lagrange. Given $n+1$ points $\mathbf{p}_i$ with corresponding parameter values u_i, $i = 0, \dots, n$, the interpolating polynomial curve of degree n is

$$\mathbf{p}(u) = \sum_{i=0}^{n} \mathbf{p}_i L_i^n(u) \ ,$$

where the **Lagrange polynomials** $L_i^n(u), i = 0, \dots, n$, are defined by the interpolation conditions

$$L_i^n(u_k) = \begin{cases} 1 & \text{if} \quad k = i \\ 0 & \quad\quad k \neq i \end{cases} .$$

Proof: Let $\mathbf{x}, \mathbf{y}$ be a solution of (2). Further, let $\mathbf{x}+\mathbf{h}$ be any other point satisfying the constraints

$$D[\mathbf{x}+\mathbf{h}] = \mathbf{q} \ .$$

This implies $D\mathbf{h} = \mathbf{o}$. Further, let

$$\begin{aligned} \overline{\mathbf{r}} &= C[\mathbf{x}+\mathbf{h}] - \mathbf{p} \\ &= \mathbf{r} + C\mathbf{h} \ . \end{aligned}$$

Then it follows that

$$\overline{\mathbf{r}}^t\overline{\mathbf{r}} = \mathbf{r}^t\mathbf{r} + 2\mathbf{r}^tC\mathbf{h} + \mathbf{h}^tC^tC\mathbf{h} \ .$$

The last term is non-negative, and the second term is zero since, under assumption (2),

$$\mathbf{h}^tC^t\mathbf{r} = \mathbf{h}^tC^t[C\mathbf{x}-\mathbf{p}] = -\mathbf{h}^tD^t\mathbf{y} = 0 \ .$$

Hence, $\mathbf{r}^t\mathbf{r}$ is minimal. $\diamond$

Remark 11: If there are no constraints, i.e., $D = O$ and $\mathbf{q} = \mathbf{o}$, then the linear system (2) reduces to the so-called **Gaussian normal equations**

$$C^tC\mathbf{x} = C^t\mathbf{p} \ .$$

Remark 12: If C is the identity matrix and if $D\mathbf{x} = \mathbf{q}$ is an underdetermined system, then (2) consists of the **correlate equations**

$$\mathbf{x} = \mathbf{p} - D^t\mathbf{y}$$

and the **normal equations**

$$D\mathbf{p} - DD^t\mathbf{y} = \mathbf{q} \ ,$$

which one obtains by substituting the correlate equations into the constraints $D\mathbf{x} = \mathbf{q}$.

Remark 13: Let W be an $m \times m$ diagonal weight matrix. Then, as a consequence of the theorem above, the weighted residual

$$W\mathbf{r} = WC\mathbf{x} - W\mathbf{p}$$

becomes minimal under the condition $D\mathbf{x} = \mathbf{q}$ for the solution $\mathbf{x}, \mathbf{y}$ of the weighted equation

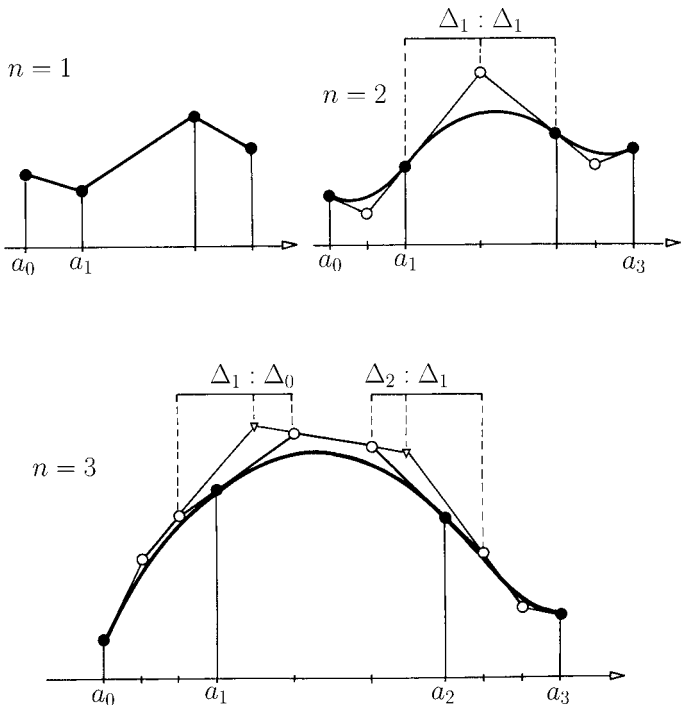

Figure 5.1: Spline functions of degree 1, 2 and 3.

5.2 B-splines

As with the Bézier representation of polynomial curves, it is desirable to write a spline $\mathbf{s}(u)$ as an affine combination of some control points $\mathbf{c}_i$, namely

$$\mathbf{s}(u) = \sum \mathbf{c}_i N_i^n(u) \ ,$$

where the $N_i^n(u)$ are basis spline functions with minimal support and certain continuity properties. Schoenberg introduced the name B-splines for these functions [Schoenberg '67]. Their Bézier polygons can be constructed by Stärk's theorem.

Figure 5.3 shows a piecewise cubic C^2 B-spline. Stärk's theorem is only needed for the Bézier ordinates, while the abscissae are given by Remark 8 in 2.8.

For higher degree this construction, albeit possible, becomes much less obvious and more complicated, see [**?**]. Therefore, we use a recurrence relation, which was found independently by de Boor and Mansfield [Boor '72] in 1970 and Cox [Cox '72] in 1971. We define B-splines from that relation and derive

5.7 B-spline properties

We summarize the basic properties of B-splines.

- The B-splines of degree n with a given knot sequence that do not vanish over some knot interval are **linearly independent** over this interval.
- A dimension count shows that the B-splines $N_0^n, \ldots, N_m^n$ with the knots $a_0, \ldots, a_{m+n+1}$ form a **basis** for all splines of degree n with support $[a_0, a_{m+n+1}]$ and the same knots.
- Similarly, the B-splines $N_0^n, \ldots, N_m^n$ over the knots $a_0, \ldots, a_{m+n+1}$ restricted to the interval $[a_n, a_{m+1})$ form a **basis** for all splines of degree n restricted to the same interval.
- The B-splines of degree n form a **partition of unity**, i.e.,

$$\sum_{i=0}^{m} N_i^n(u) = 1, \quad \text{for} \quad u \in [a_n, a_{m+1}) \ .$$

- A spline $\mathbf{s}[a_n, a_{m+1}]$ of degree n with n**-fold end knots**,

$$(a_0 =)a_1 = \ \ldots \ = a_n \quad \text{and} \quad a_{m+1} = \ \ldots \ = a_{m+n}(= a_{m+n+1})$$

  has the same end points and end tangents as its control polygon.
- The **end knots** a_0 and a_{m+n+1} **have no influence** on N_0^n and N_m^n over the interval $[a_n, a_{m+1}]$.
- The B-splines are **positive** over the interior of their support,

$$N_i^n(u) > 0 \quad \text{for} \quad u \in (a_i, a_{i+n+1}) \ .$$

- The B-splines have **compact support**,

$$\text{supp} N_i^n = [a_i, a_{i+n+1}] \ .$$

- The B-splines satisfy the **de Boor, Mansfield, Cox recursion formula**

$$N_i^n(u) = \alpha_i^{n-1} N_i^{n-1}(u) + (1 - \alpha_{i+1}^{n-1}) N_{i+1}^{n-1}(u) \ ,$$

  where $\alpha_i^{n-1} = (u - a_i)/(a_{i+n} - a_i)$ represents the local parameter over the support of N_i^{n-1}.
- The **derivative** of a single B-spline is given by

$$\frac{d}{du} N_i^n(u) = \frac{n}{a_{i+n} - a_i} N_i^{n-1}(u) - \frac{n}{a_{i+n+1} - a_{i+1}} N_{i+1}^{n-1}(u) \ .$$

ure 5.8 shows the example $s(u) = N_2^3(u)$. Other examples are shown in Figure 5.1.

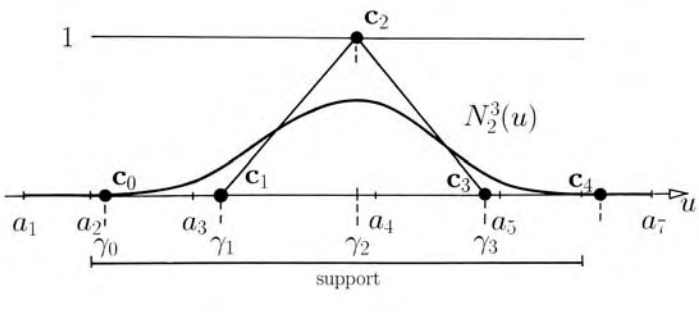

Figure 5.8: Control points of the cubic B-spline $N_2^3(u)$.

5.9 The complete de Boor algorithm

The Taylor expansion of a polynomial spline segment

$$\mathbf{s}_n(u) = \sum_{i=0}^{n} \mathbf{c}_i N_i^n(u) \ , \quad u \in [a_n, a_{n+1}) \ ,$$

can be computed at any $u \in \mathbb{R}$ following the ideas presented in 2.6 for Bézier curves.

Let $\mathbf{s}_n[u_1 \ldots u_n]$ be the polar form of $\mathbf{s}_n$ and consider the points and vectors

$$\mathbf{c}_{r,i,k} = \mathbf{s}_n[\varepsilon \overset{r}{\ldots} \varepsilon \, a_{i+1} \ldots a_{i+n-r-k} \, u \overset{k}{\ldots} u],$$

where ε denotes the direction $1 - 0$, for $i = r + k, \ldots, n$. It follows that

$$\frac{d^r}{du^r}\mathbf{s}_n(u) \quad = \quad \frac{n!}{(n-r)!}\mathbf{c}_{r,n,n-r} \ ,$$

and the Taylor expansion is given by

$$\mathbf{s}_n(u+h) = \sum_{r=0}^{n} \mathbf{c}_{r,n,n-r} \binom{n}{r} h^r \ .$$

The points and vectors $\mathbf{c}_{rik}$ can again be arranged conveniently in a tetrahedral array, see Figure 5.9, where $n = 2$ and $\varepsilon 4$ stands for $\mathbf{s}_n[\varepsilon \, a_4]$, etc.

This array, first considered by Sablonniere in 1978 [Sablonniere '78], is composed of $\binom{n+2}{3}$ subtetrahedra and contains the given control points $\mathbf{c}_i = \mathbf{c}_{0,i,0}$

versa, it suffices to compute, for example, only the left and top faces of the tetrahedral array, see [Lee '82, Boehm '84b].

Remark 9: If one first computes the rear face and then the bottom (or top) face of the tetrahedral array, one needs to solve formula (2) above (or (3)) for $\mathbf{c}_{r+1,i,k}$ (or $\mathbf{c}_{r,i-1,k}$). This is impossible if $u = a_{i+n-r-k}$ (or $u = a_i$). Hence, the derivatives of the polynomial $\mathbf{s}_n$ cannot be computed in this fashion for $u = a_{n+1}, \ldots, a_{2n}$ (or $u = a_0, \ldots, a_{n-1}$).

5.10 Conversions between Bézier and B-spline representations

There is also a tetrahedral algorithm to convert a B-spline representation into a Bézier representation and vice versa [Boehm '77, Sablonniere '78]. It can be derived similarly as the algorithm in 5.9. Let the notations be as in 5.9 and let

$$\mathbf{q}_{rik} = \mathbf{s}_n[a \overset{r}{\ldots} a\, a_{i+1} \ \ldots \ a_{i+n-r-k}\, b \overset{k}{\ldots} b]$$

for $i = r + k, \ldots, n$. Thus, the control points of the spline are given by

$$\mathbf{c}_i = \mathbf{q}_{0i0} \ ,$$

and the Bézier points of the polynomial $\mathbf{s}_n$ over $[a, b]$ are given by

$$\mathbf{b}_j = \mathbf{q}_{n-j,n,j} \ .$$

Again, the points $\mathbf{q}_{rik}$ are conveniently arranged in a tetrahedral array, as illustrated below in Figure 5.10 for $n = 2$, where $a3, ab$, etc. stand for $\mathbf{q}_{120}$, $\mathbf{q}_{101}$, etc.

The left face is computed according to the rule

$$\mathbf{q}_{r+1,i,k} = (1-\alpha)\mathbf{q}_{r,i-1,k} + \alpha\, \mathbf{q}_{r,i,k} \ , \qquad \alpha = \frac{a - a_i}{a_{i+n-r-k} - a_i} \ ,$$

and the bottom face according to the rule

$$\mathbf{q}_{r,i,k+1} = (1-\gamma)\mathbf{q}_{r+1,i,k} + \gamma\, \mathbf{q}_{r,i,k} \ , \qquad \gamma = \frac{b - a}{a_{i+n-r-k} - a} \ .$$

Conversely, one can compute the B-spline control points from the Bézier points. First, one solves the two formulae above for $\mathbf{q}_{r,i-1,k}$ and $\mathbf{q}_{rik}$. Second, one applies the formulae to compute the bottom and then the left face.

algorithm [Cohen et al. '80]. Note that the affine combinations of the Oslo-algorithm are, in general, not convex. Further improvements are necessary to avoid non-convex combinations.

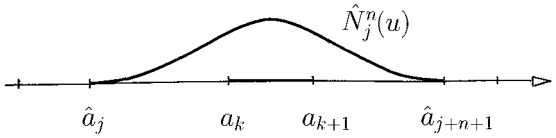

Figure 6.3: Choosing a_k for the construction of $\hat{\mathbf{c}}_j$.

6.3 Convergence under knot insertion

In this section, we generalize the ideas used in 3.3. Consider the spline $\mathbf{s}(u) = \sum_i \mathbf{c}_i N_i^n(u)$ with some knot sequence (a_i). On inserting more and more knots such that the knot sequence becomes dense eventually, the sequence of the corresponding control polygons converges to the spline $\mathbf{s}$ with the rate of convergence being quadratic in the maximum knot distance.

More precisely, let $[a, b]$ be some interval, let $h = \max\{\Delta a_i | [a_i, a_{i+1}] \subset [a, b]\}$, and let $\gamma_i = (a_{i+1} + \cdots + a_{i+n})/n$ be the Greville abscissae.

Then one has

$$\max \|\mathbf{s}(\gamma_i) - \mathbf{c}_i\| = O(h^2) \ ,$$

where the maximum is taken over all i such that $[a_{i+1}, a_{i+n}] \subset [a, b]$.

For the proof, which is due to [Schaback '93], consider a control point $\mathbf{c}_i = \mathbf{s}_r[a_{i+1} \ldots a_{i+n}]$, where $\mathbf{s}_r$ is the symmetric polynomial of $\mathbf{s}$ restricted to the knot interval $[a_r, a_{r+1})$ containing γ_i. Since

$$\frac{\partial}{\partial u_1}\mathbf{s}_r[u \ldots u] = \cdots = \frac{\partial}{\partial u_n}\mathbf{s}_r[u \ldots u] \ ,$$

the Taylor expansion of $\mathbf{s}_r$ around $[\gamma_i \ldots \gamma_i]$ is of the form

$$\begin{aligned} \mathbf{c}_i &= \mathbf{s}_r[\gamma_i \ldots \gamma_i] + \sum_{j=i+1}^{i+n} (a_j - \gamma_i)\frac{\partial}{\partial u_1}\mathbf{s}_r[\gamma_i \ldots \gamma_i] + O(h^2) \\ &= \mathbf{s}(\gamma_i) + O(h^2) \ , \end{aligned}$$

which proves the assertion. $\diamond$

6.4 A degree elevation algorithm

Due to the basis properties of B-splines, we can write a spline

$$\mathbf{s}(u) = \sum_i \mathbf{c}_i N_i^n(u)$$

with some knot sequence (a_i) also as a linear combination of B-splines of degree $n+1$,

$$\mathbf{s}(u) = \sum_j \mathbf{d}_j \hat{N}_j^{n+1}(u) \ ,$$

with the knot sequence $(\hat{a}_j)$ obtained from (a_i) by raising the multiplicity of each knot a_i by one, as illustrated in Figure 6.4.

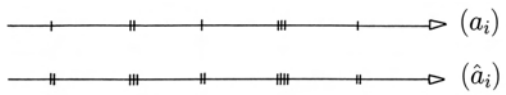

Figure 6.4: Knot sequences for degree elevation.

The main theorem from 5.5 and formula (2) from Section 3.11 tell us that

$$\begin{aligned} \mathbf{d}_j &= \mathbf{s}_r[\hat{a}_{j+1} \quad \dots \quad \hat{a}_{j+n+1}] \\ &= \frac{1}{n+1} \sum_{k=1}^{n+1} \mathbf{s}_r[\hat{a}_{j+1} \dots \hat{a}_k^* \dots \hat{a}_{j+n+1}] \ , \end{aligned}$$

where $\mathbf{s}_r[u_1 \dots u_n]$ and $\mathbf{s}_r[u_1 \dots u_{n+1}]$, respectively, denote the n- and $(n+1)$-variate polar forms of a polynomial segment of the spline $\mathbf{s}(u)$ that depends on $\mathbf{d}_j$. Each point

$$\mathbf{s}_r[\hat{a}_{j+1} \dots \hat{a}_k^* \dots \hat{a}_{j+n}]$$

can be computed by the generalized de Boor algorithm given in Remark 5 from Section 5.5, where one needs to insert at most $\lfloor (n-1)/2 \rfloor$ knots. For a uniform cubic spline with two segments, this algorithm is first described in [Ramshaw '87, pp. 109f] and in [**?**] for five segments.

Remark 4: The number of operations for the algorithm above is of order $O(n^2)$ per new control point $\hat{\mathbf{c}}_i$. It is possible to organize the computations more efficiently such that only $O(n)$ operations are needed, see [Prautzsch et al. '91, **?**, **?**].

Remark 5: Different $O(n^2)$ algorithms are derived in [Prautzsch '84a, Cohen et al. '85, Piegel & Tiller '94].

the fact that $\sum_{i_1=1}^{m} \ldots \sum_{i_k=1}^{m} (a_{i_1} - \gamma_0) \ldots (a_{i_k} - \gamma_0) = 0$, we obtain

$$\|\mathbf{c}_0 - \mathbf{s}(\gamma_0)\| \leq \sum_{k=2}^{n} \frac{h^k}{k!} \frac{m^k - (m \ldots (m-k+1))}{m \ldots (m-k+1)} \sup \|\mathbf{s}^{(k)}(u)\| ,$$

which proves the claim above. $\diamond$

6.7 Interpolation

Splines are often used to solve interpolation problems. Of particular interest is the uniqueness of a spline interpolant. Let $N_0^n, \ldots, N_m^n$ be the B-splines of degree n with the knots $a_0, \ldots, a_{m+n+1}$ and let $\mathbf{p}_0, \ldots, \mathbf{p}_m$ be given points with associated interpolation abscissae $u_0 < \ldots < u_m$. We wish to find a spline $\mathbf{s} = \sum_{i=0}^{m} \mathbf{c}_i N_i^n$ solving the interpolation problem

$$\mathbf{s}(u_j) = \sum_{i=0}^{m} \mathbf{c}_i N_i^n(u_j) = \mathbf{p}_j \ .$$

This means solving the following linear system

$$\begin{bmatrix} N_0^n(u_0) \cdots N_m^n(u_0) \\ \vdots \qquad\qquad \vdots \\ N_0^n(u_m) \cdots N_m^n(u_m) \end{bmatrix} \begin{bmatrix} \mathbf{c}_0^t \\ \vdots \\ \mathbf{c}_m^t \end{bmatrix} = \begin{bmatrix} \mathbf{p}_0^t \\ \vdots \\ \mathbf{p}_m^t \end{bmatrix} , \tag{2}$$

which we abbreviate by $NC = P$. Note that this linear system consists of several systems, one for each column of C. The matrix N is called **collocation matrix**.

The **Schoenberg-Whitney theorem** from 1953 establishes when the interpolation problem has a unique solution [Schoenberg et al. '53].

> *The matrix N is invertible if and only if N has a positive diagonal, which means that* $N_i^n(u_i) \neq 0$ *for all* i.

Note that if the N_i^n are continuous, then the condition $N_i^n(u_i) \neq 0$ is equivalent to the requirement $u_i \in (a_i, a_{i+n+1})$.

For a proof of the theorem, we follow [Powell '81]. Let $N_i^n(u_i) = 0$ for some i and assume $a_{i+n+1} \leq u_i$. Then, it follows that

$$N_0^n(u_j) = \cdots = N_i^n(u_j) = 0 \quad \text{for all} \quad j \geq i \ ,$$

i.e.,

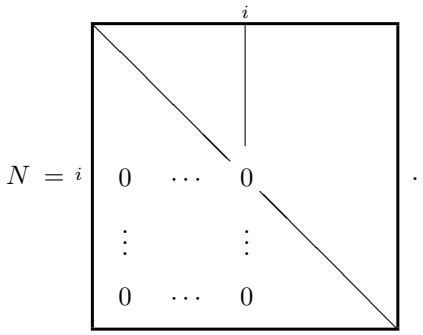

Hence, standard linear algebra shows that N is singular. Similarly, N is also singular if $u_i \leq a_i$.

For the converse, let N be singular and $\mathbf{c}$ be a non-trivial column solving the (single) homogenous system

$$N\mathbf{c} = \mathbf{o} \ .$$

For the moment, we assume that no $n+1$ consecutive coordinates of $\mathbf{c}$ are zero. Then, the variation diminishing property, see Problem 4, implies that the spline

$$\sum_{i=0}^{m} c_i N_i^n$$

has at most m zeroes in (a_0, a_{m+n+1}) if $a_0 < a_{n-1}$ or $[a_0, a_{m+n+1})$ if $a_0 = \cdots = a_{n-1}$. Thus, at least one u_i lies outside the support of the corresponding B-spline N_i^n. If

$$c_r = \cdots = c_{r+n} = 0 \ ,$$

then one can consider the splines

$$\sum_{i=0}^{r-1} c_i N_i^n \quad \text{and} \quad \sum_{i=r+n+1}^{m} c_i N_i^n$$

instead, which are zero at $u_0, \ldots, u_{r-1}$ and $u_{r+n+1}, \ldots, u_m$, respectively. $\diamond$

Remark 6: A solution of the system $NC = P$ above is not necessarily affinely invariant. This is only guaranteed if N is regular and if the rows sum to one, i.e., if

$$N\mathbf{e} = \mathbf{e} \ , \quad \text{where} \quad \mathbf{e} = [1 \ \ldots \ 1]^t \ .$$

Namely, the row condition $N\mathbf{e} = \mathbf{e}$ implies $\mathbf{e} = N^{-1}\mathbf{e}$, which means that the $\mathbf{c}_i$ given by $C = N^{-1}P$ are affine combinations of the $\mathbf{p}_i$. The row condition is satisfied if $a_n \leq u_i < a_{m+1}$ as illustrated in Figure 6.6.

Remark 7: The matrix N is **totally positive**, see [Karlin '68, Boor '76b].

7 Smooth curves

7.1 Contact of order r — 7.2 Arc length parametrization — 7.3 Gamma splines — 7.4 Gamma B-splines — 7.5 Nu-splines — 7.6 The Frenet frame — 7.7 Frenet frame continuity — 7.8 Osculants and symmetric polynomials — 7.9 Geometric meaning of the main theorem — 7.10 Splines with arbitrary connection matrices — 7.11 Knot insertion — 7.12 Basis splines — 7.13 Problems

There are several ways to define smoothness. Stärk's simple C^r condition establishes a very simple construction of a smooth curve continuation. More generally, a curve is said to be GC^r if it has an r times continuously differentiable parametrization. An even more general smoothness concept is based on the continuity of higher order geometric invariants. Piecewise polynomial curves with this general smoothness can be nicely studied using a geometric interpretation of symmetric polynomials.

7.1 Contact of order r

Two curves $\mathbf{p} = \mathbf{p}(s)$ and $\mathbf{q} = \mathbf{q}(t)$, which are r times differentiable at $s = t = 0$, are said to have **contact of order** r or to have a general C^r joint at 0, short a GC^r **joint**, if $\dot{\mathbf{q}}(0) \neq \mathbf{o}$ and there exists a reparametrization $s(t)$ with $s(0) = 0$ such that $\mathbf{p}(s(t))$ and $\mathbf{q}(t)$ have identical derivatives at 0 up to order r. As before, we denote derivatives with respect to s and t by primes or dots, respectively.

Because of the chain and product rules, contact of order r at $s = t = 0$ means that

$$\begin{array}{lllllll} \mathbf{p} & & & & & = & \mathbf{q} \\ \mathbf{p}'\dot{s} & & & & & = & \dot{\mathbf{q}} \\ \mathbf{p}'\ddot{s} & + & \mathbf{p}''\dot{s}^2 & & & = & \ddot{\mathbf{q}} \\ \mathbf{p}'\dddot{s} & + & 3\mathbf{p}''\dot{s}\ddot{s} & + & \mathbf{p}'''\dot{s}^3 & = & \dddot{\mathbf{q}} \\ & & \vdots & & & & \vdots \end{array} .$$

Remark 18: Because of Remark 16, there are at most m, possibly coalescing, osculating flats $\mathcal{P}_{a_1}^{n-1}, \ldots, \mathcal{P}_{a_m}^{n-1}$ whose intersection contains any given subspace of dimension $n-m$.

Remark 19: Moreover, it can be shown that the intersection of any osculating flat $\mathcal{P}_u^{n-r}$ with an m-dimensional subspace is of dimension $m-r$, except for at most finitely many n, see [Prautzsch '02].

Remark 20: The geometric approach to B-splines discussed above can be used in a more general form also for Tchebycheffian splines,
see [Pottmann '93, Mazure et al. '96].

Remark 21: The Bézier points $\mathbf{b}_i$ of a cubic curve $\mathbf{p}(u)$ spanning $\mathbb{R}^3$ are given by the 3rd osculants

$$\begin{array}{lcll} \mathbf{b}_0 & = & \mathbf{p}_{000} & = & \mathcal{P}_0^0 \ , \\ \mathbf{b}_1 & = & \mathbf{p}_{001} & = & \mathcal{P}_0^1 \cap \mathcal{P}_1^2 \ , \\ \mathbf{b}_2 & = & \mathbf{p}_{011} & = & \mathcal{P}_0^2 \cap \mathcal{P}_1^1 \quad \text{and} \\ \mathbf{b}_3 & = & \mathbf{p}_{111} & = & \mathcal{P}_1^0 \ , \end{array}$$

see Figure 7.9 for an illustration.

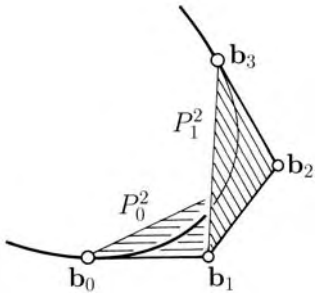

Figure 7.9: Osculating flats.

7.10 Splines with arbitrary connection matrices

Let a_i be simple knots such that $a_i < a_{i+1}$. Further, let $\mathbf{s}(u)$ be a continuous curve that is polynomial of degree n over each knot interval $[a_i, a_{i+1}]$ and whose left- and right-hand side derivatives up to order $n-1$ at the knots are related by arbitrary non-singular connection matrices. Thus, the curve $\mathbf{s}$ has a well-defined $(n-1)$th osculating flat at each knot a_i, denoted by $\mathcal{S}_i$ or $\mathcal{S}_{a_i}$, but it need not be Frenet frame continuous!

Further, we assume that the polynomial segments of $\mathbf{s}$ span n-dimensional

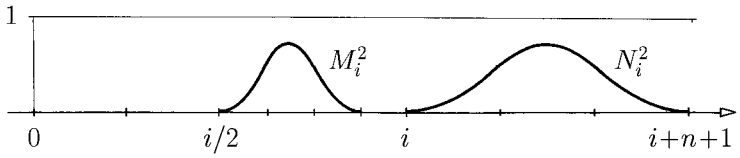

Figure 8.2: Scaled uniform B-spline.

Constructing the finer representation

$$\mathbf{s}^n(u) = \sum \mathbf{b}_i^n M_i^n(u)$$

is rather simple. For $n = 0$, one has

$$\begin{aligned} \mathbf{s}^n(u) &= \sum \mathbf{c}_i N_i^0(u) \\ &= \sum \mathbf{c}_i (M_{2i}^0(u) + M_{2i+1}^0(u)) \end{aligned}$$

and, therefore,

$$\mathbf{b}_{2i}^0 = \mathbf{b}_{2i+1}^0 = \mathbf{c}_i \ .$$

For $n = j + 1 > 0$, the recursion formula for uniform B-splines implies that

$$\begin{aligned} \mathbf{s}^n(u) &= \sum \mathbf{c}_i N_i^{j+1}(u) \\ &= \int_{\mathbb{R}} \sum \mathbf{c}_i N_i^j(u-t) N^0(t) dt \\ &= \int_{\mathbb{R}} \sum \mathbf{b}_i^j M_i^j(u-t)[M_0^0(t) + M_1^0(t)] dt \\ &= \frac{1}{2} \sum \mathbf{b}_i^j [M_i^{j+1}(u) + M_{i+1}^{j+1}(u)] \\ &= \sum \frac{1}{2}(\mathbf{b}_{i-1}^j + \mathbf{b}_i^j) M_i^{j+1}(u) \end{aligned}$$

and, therefore,

$$\mathbf{b}_i^{j+1} = \frac{1}{2}(\mathbf{b}_{i-1}^j + \mathbf{b}_i^j) \ .$$

This recursive computation of the $\mathbf{b}_i^n$ is the **algorithm of Lane and Riesenfeld** [Lane et al. '80].

> *Given a control polygon, first* **double** *all control points and then construct the polygons connecting the* **midpoints** *n times repeat-*

edly.

Figure 8.3 shows the corresponding construction for $n = 3$. Solid dots mark given points and their doubles, empty circles midpoints and small empty circles points constructed in the preceding step. The first m steps of this algorithm are the same for all uniform splines of degree n, where $m > n$.

Remark 1: The construction for $n = 2$ bears **Chaikin's** name [Chaikin '74] but has already been investigated by de Rham [Rham '47].

Remark 2: One has

$$\mathbf{s}^{n+1}(u) = \int_{u-1}^{u} \mathbf{s}^n(t)dt = \mathbf{s}^n * N^0 = \mathbf{s}^0 * N^n \quad .$$

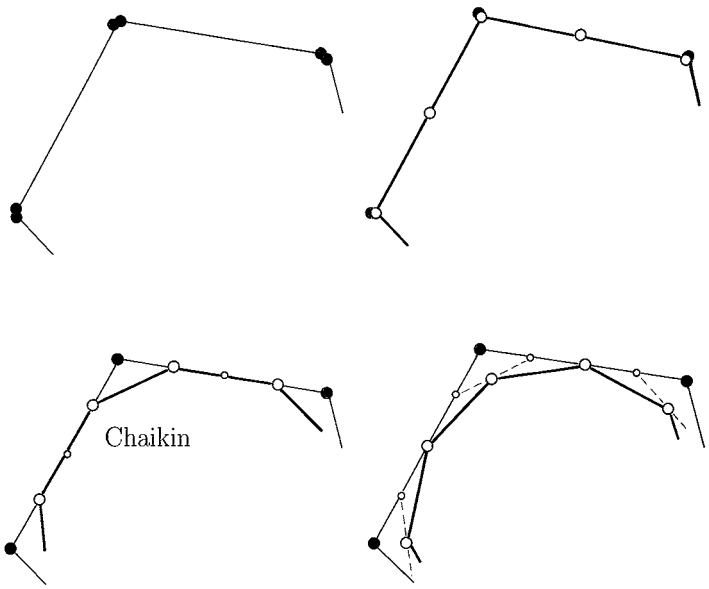

Figure 8.3: Uniform subdivision.

8.3 Repeated subdivision

The uniform subdivision algorithm can be described in matrix notation. Let

$$C = [\ldots \quad \mathbf{c}_{-1}\,\mathbf{c}_0\,\mathbf{c}_1 \quad \ldots]$$

and

$$B_n = [\qquad \ldots \quad \mathbf{b}^n_{-1}\,\mathbf{b}^n_0\,\mathbf{b}^n_1 \quad \ldots \qquad]$$

8.4 The subdivision matrix

The subdivision matrix $S_1 = D \cdot M$ for piecewise linear splines can be read off directly from Figure 8.3,

$$S_1 = \frac{1}{2}\begin{bmatrix} \cdot & \cdot & \cdot & & & & & \\ & & 1 & 2 & 1 & & & \\ & & & & 1 & 2 & 1 & \\ & & & & & \cdot & \cdot & \cdot \end{bmatrix} .$$

Similarly, the subdivision matrix S_2 for piecewise quadratic splines (Chaikin's algorithm) is obtained as

$$S_2 = \frac{1}{4}\begin{bmatrix} \cdot & \cdot & \cdot & \cdot & & & & & \\ & & 1 & 3 & 3 & 1 & & & \\ & & & & 1 & 3 & 3 & 1 & \\ & & & & & \cdot & \cdot & \cdot & \cdot \end{bmatrix} .$$

In general, the matrix S_n is of the form

$$S_n = \begin{bmatrix} \cdots & & & & & & & \\ a_0 & a_1 & \cdots & a_{n+1} & & & & \\ & a_0 & a_1 & \cdots & a_{n+1} & & & \\ & & & & & \cdots & & \end{bmatrix} ,$$

where a_i represents the scaled binomial coefficient

$$a_i = \frac{1}{2^n}\binom{n+1}{i} .$$

Another derivation of S_n is given in Remark 5 of 8.8.

Multiplying a control polygon C by the subdivision matrix S_n leads to the so-called **refinement equations**

$$\mathbf{b}_{2i}^n = \sum_j \mathbf{c}_j a_{2i-2j} \quad \text{and} \quad \mathbf{b}_{2i+1}^n = \sum_j \mathbf{c}_j a_{2i+1-2j} \ ,$$

which can be combined into one equation for the new control points,

$$\mathbf{b}_i^n = \sum_j \mathbf{c}_j a_{i-2j} \ .$$

This sequence is said to converge uniformly to a continuous curve $\mathbf{c}(u)$ if

$$\sup_i \| \mathbf{c}_i^k - \mathbf{c}(2^{-k}i) \| \underset{k\to\infty}{\longrightarrow} 0 \ .$$

Uniform convergence of the polygons C_k to $\mathbf{c}(u)$, implies that the piecewise linear splines

$$\mathbf{c}_k(u) = \sum_i \mathbf{c}_i^k N_i^1(u)$$

also converge uniformly to $\mathbf{c}(u)$ over each compact interval since $\mathbf{c}(u)$ is uniformly continuous over compact intervals.

Further, an important necessary and sufficient criterion for uniform convergence is the following [Dyn et al. '91][Micchelli et al. '87].

> *The polygons C_k converge uniformly to a uniformly continuous curve $\mathbf{c}(u)$ if and only if the difference polygons ∇C_k converge uniformly to zero.*

A proof is given in 15.3, see also Problems 3 and 4.

8.7 Convergence theorems

Let $C_k = [\dots \mathbf{c}_i^k \dots], k = 0, 1, \dots,$ be arbitrary polygons, not necessarily obtained by subdivision, and assume that the second divided difference polygons $2^k\nabla^2 C_k$ converge uniformly to zero. Due to 8.6, this means that the first divided difference polygons $2^k\nabla C_k$ converge uniformly to a uniformly continuous curve, say $\mathbf{d}(u)$. Therefore, the first difference polygons ∇C_k converge uniformly to zero and the polygons C_k to a uniformly continuous curve $\mathbf{c}$.

This fact implies that the piecewise constant splines

$$\mathbf{d}_k(u) = \sum 2^k \nabla \mathbf{c}_i^k N_i^0(2^k u)$$

and the piecewise linear splines

$$\mathbf{c}_k(u) = \sum \mathbf{c}_i^k N_i^1(2^k u)$$

converge uniformly to $\mathbf{d}(u)$ and $\mathbf{c}(u)$, respectively. Since

$$\mathbf{c}_k(u) = \mathbf{c}_{-1}^k + \int_0^u \mathbf{d}_k(t)\, dt \ ,$$

and since integration commutes with the limit of a uniformly converging

differences $\nabla \mathbf{b}_i$ by z^i and summing over all i results in the Laurent polynomial

$$\nabla \mathbf{b}(z) = \sum_i \nabla \mathbf{b}_i z^i = \mathbf{b}(z)(1-z) \ .$$

Substituting the above equation for $\mathbf{b}(z)$ gives

$$\begin{aligned} \nabla \mathbf{b}(z) &= \mathbf{c}(z^2)\alpha(z)(1-z) \\ &= \nabla \mathbf{c}(z^2)\alpha(z)\frac{1-z}{1-z^2} \\ &= \nabla \mathbf{c}(z^2)\frac{\alpha(z)}{1+z} \ . \end{aligned}$$

The assumption $\sum \alpha_{2i} = \sum \alpha_{2i+1} = 1$ made in 8.5 is equivalent to

$$\alpha(-1) = 0 \quad \text{and} \quad \alpha(1) = 2 \ .$$

Therefore, $(1+z)$ is a factor of $\alpha(z)$, which implies that

$$\beta(z) = \frac{\alpha(z)}{1+z}$$

is the **characteristic polynomial of the difference scheme** associated with S.

Remark 4: The subdivision matrix D for piecewise constant splines over $\mathbb{Z}$ is given in 8.3. It has the characteristic polynomial

$$\sigma_0(z) = (1+z) \ .$$

Remark 5: The matrix $\frac{1}{2}S_{n-1}$ defined in 8.4 represents the difference scheme underlying the subdivision algorithm for splines of degree n over $\mathbb{Z}$, see 8.5. Hence, the characteristic polynomial $\sigma_n(z)$ of S_n is given by

$$\begin{aligned} \sigma_n &= \frac{1}{2}(1+z)\sigma_{n-1}(z) \\ &= \frac{1}{4}(1+z)^2\sigma_{n-2}(z) \\ &\vdots \\ &= 2^{-n}(1+z)^n\sigma_0(z) = 2^{-n}(1+z)^{n+1} \ , \end{aligned}$$

which, again, proves the identity $a_i = 2^{-n}\binom{n+1}{i}$ in 8.4.

8.10 Analyzing the four-point scheme

From the definition of the four-point scheme one can easily read off its characteristic polynomial,

$$\begin{aligned}\alpha(z) &= -\omega + (1/2+\omega)z^2 + z^3 + (1/2+\omega)z^4 - \omega z^6 \\ &= (1+z)\beta(z) \ ,\end{aligned}$$

where

$$\beta(z) = -\omega + \omega z + 1/2z^2 + 1/2z^3 + \omega z^4 - \omega z^5$$

is the characteristic polynomial of the difference scheme. Thus, it follows that

$$\begin{aligned}\|\nabla \mathbf{p}_{2i}^{k+1}\| &= \| -\omega\nabla\mathbf{p}_i^k + 1/2\nabla\mathbf{p}_{i-1}^k + \omega\nabla\mathbf{p}_{i-2}^k\| \\ &\leq (1/2 + 2|\omega|)\sup_i \|\nabla\mathbf{p}_i^k\|\end{aligned}$$

and, similarly,

$$\|\nabla \mathbf{p}_{2i+1}^{k+1}\| \leq (1/2+2|\omega|)\sup_i \|\nabla\mathbf{p}_i^k\| \ .$$

Hence, for $|\omega| < 1/4$, the difference polygons ∇P_k converge to zero and the polygons P_k to a continuous curve. Further, according to 8.7 differentiability depends on the second differences $2^k\nabla^2 P_k$. Due to 8.8, the associated subdivision scheme has the characteristic polynomial

$$\gamma(z) = \frac{2\beta(z)}{1+z} = -2\omega + 4\omega z + (1-4\omega)z^2 + 4\omega z^3 - 2\omega z^4 \ .$$

Again, one can show that the differences $2^k\nabla^2 P_k$ go to zero if $0 < \omega < 1/8$. Hence, the four-point scheme produces C^1 interpolants in this case.

Remark 8: One can show [Dyn et al. '91] that the four-point scheme produces C^1 interpolants also if $0 < \omega < (\sqrt{5}-1)/8 \approx 0.15$. However, the four-point scheme does not produce C^2 curves in general.

Remark 9: Kobbelt's $2k$-point schemes produce C^{k-1} interpolants, see [Kobbelt '94].

8.11 Problems

1 The uniform B-spline N^n can be obtained by n-fold convolution of N^0 with itself,

$$N^n = N^0 * \overset{n}{\ldots} * N^0 \ .$$

2 Use the recursion formula for uniform B-splines in 8.1 to show that for

$n \geq 0$

$$\sum_i N_i^n = 1 \quad \text{and} \quad \int_{\mathbb{R}} N_i^n = 1$$

and that for $n \geq 1$

$$\sum_i (i + \frac{n+1}{2}) N_i^n(u) = u \ .$$

3 Use the notation of 8.6 to show that $\|\mathbf{c}_{2i}^{k+1} - \mathbf{c}_i^k\|$ and $\|\mathbf{c}_{2i+1}^{k+1} - 1/2(\mathbf{c}_i^k + \mathbf{c}_{i+1}^k)\|$ are bounded by some multiple of $\sup_i \|\mathbf{c}_i^k\| \cdot \sum_i |\alpha_i|$.

4 Conclude from Problem 3 that the piecewise linear curves $\sum \mathbf{c}_i^k N_i^1(2^k u)$ converge uniformly if the differences $\nabla \mathbf{c}_i^k$ converge uniformly to zero.

5 Let S_k be the matrix of the subdivision algorithm for uniform splines of degree k, as given in 8.4 and consider the sequence of polygons

$$C_k = C_{k-1} S_k, \ k = 1, 2, 3, \ldots \quad ,$$

where $C_0 = [\ldots \mathbf{c}_i \ldots]$ is an arbitrary control polygon. Show that the polygons C_k converge to a C^∞ curve [**?**].

6 Consider the uniform splines $\mathbf{s}_n = \sum \mathbf{c}_i N_i^n(u)$ of degree n over $\mathbb{Z}$. For any integer $r \in \mathbf{N}$, let

$$\mathbf{s}_n = \sum \mathbf{b}_i^n N_i^n(ru)$$

be the corresponding representations over $\frac{1}{r}\mathbb{Z}$. Show that the control points $\mathbf{b}_i^n$ can be computed by the recursion

$$\begin{aligned} \mathbf{b}_{ri}^0 &= \cdots = \mathbf{b}_{ri+r-1}^0 = \mathbf{c}_i \\ \mathbf{b}_i^{n+1} &= \frac{1}{r}(\mathbf{b}_{i-r+1}^n + \cdots + \mathbf{b}_i^n) \ , \end{aligned}$$

7 Consider two subdivision matrices R and S with characteristic polynomials $\alpha(z)$ and $(1+z)\alpha(z)/2$, respectively. Given a polygon C, let the polygons CR^k converge to a curve $\mathbf{c}(u)$. Show that the polygons CS^k converge to the curve $\mathbf{d}(u) = \int_{u-1}^u \mathbf{c}(u)du$.

This means

$$\mathbf{b}(c_1, d_1) = \mathbf{b}_{00}, \quad \mathbf{b}(c_1, d_2) = \mathbf{b}_{0n} \ , \quad \text{etc.}$$

Since the Bernstein polynomials sum to one,

- *their products form a* **partition of unity**,

$$\sum_{\mathbf{i}} B_{\mathbf{i}}^{\mathbf{m}} = \sum_{j} 1 \cdot B_j^n = 1 \ .$$

- *Thus,* $\mathbf{b}(\mathbf{u})$ *is an* **affine combination** *of its Bézier points and the Bézier representation is* **affinely invariant**.

Since the Bernstein polynomials are non-negative in $[0, 1]$, it follows that

- $\mathbf{b}(\mathbf{u})$ *is a* **convex combination** *of the* $\mathbf{b_i}$ *for every* $\mathbf{u} \in [\mathbf{c}, \mathbf{d}]$.

Hence,

- *the patch* $\mathbf{b}[\mathbf{c}, \mathbf{d}]$ *lies in the* **convex hull** *of its Bézier points.*

Remark 4: Using the convex hull property separately for each coordinate a bounding box is obtained for the surface patch $\mathbf{b}[\mathbf{c}, \mathbf{d}]$,

$$\mathbf{b}(\mathbf{u}) \in [\min_{\mathbf{i}} \mathbf{b_i}, \max_{\mathbf{i}} \mathbf{b_i}] \quad \text{for} \qquad \mathbf{u} \in [\mathbf{c}, \mathbf{d}] \ ,$$

which is illustrated in Figure 9.5.

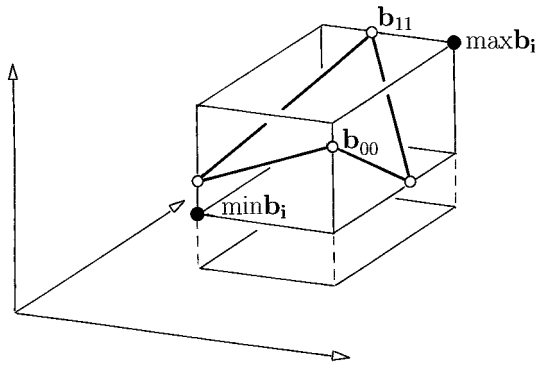

Figure 9.5: A bounding box.

9.3 Tensor product polar forms

Let $A_0(u), \ldots, A_m(u)$ and $B_0(v), \ldots, B_n(v)$ be bases for the space of all polynomials up to degree m and n, respectively. Further, let

$$A_i[u_1 \ldots u_m] \quad \text{and} \quad B_j[v_1 \ldots v_n]$$

be the corresponding polar forms. Then, any tensor product surface

$$\mathbf{b}(u,v) = \sum_i \sum_j \mathbf{b}_{ij} A_i(u) B_j(v)$$

has the **tensor product polar form**

$$\mathbf{b}[u_1 \ldots u_m, v_1 \ldots v_n] = \sum_i \sum_j \mathbf{b}_{ij} A_i[u_1 \ldots u_m] B_j[v_1 \ldots v_n] \ .$$

This polar form has the following three properties.

- $\mathbf{b}[u_1 \ldots u_m, v_1 \ldots v_n]$ *agrees with* $\mathbf{b}(u,v)$ *on its* **diagonal**,

which means $\mathbf{b}[u \ldots u, v \ldots v] = \mathbf{b}(u,v)$.

- $\mathbf{b}[u_1 \ldots u_m, v_1 \ldots v_n]$ *is* **symmetric** *in the variables* u_i *and symmetric in the variables* v_j,

which means that

$$\mathbf{b}[s_1 \ldots s_m, t_1 \ldots t_n] = \mathbf{b}[u_1 \ldots u_m, v_1 \ldots v_n]$$

for any permutations $(s_1, \ldots, s_m)$ and $(t_1, \ldots, t_n)$ of $(u_1, \ldots, u_m)$ and $(v_1, \ldots, v_n)$, respectively.

- $\mathbf{b}[u_1 \ldots u_m, v_1 \ldots v_n]$ *is* **affine** *in each variable.*

The Bézier points of $\mathbf{b}(u,v)$ over some interval $[a,b] \times [c,d]$ can easily be obtained by the main theorem 3.2. For any fixed u, the polynomial $\mathbf{b}(v) = \mathbf{b}(u,v)$ has the Bézier points

$$\mathbf{b}_j(u) = \mathbf{b}[\underbrace{u \ldots u}_{m}, \underbrace{c \ldots c}_{n-j} \underbrace{d \ldots d}_{j}], \ j = 0, \ldots, n \ ,$$

and, for each j, these polynomials $\mathbf{b}_j(u)$ have the Bézier points

$$\mathbf{b}_{ij} = \mathbf{b}[\underbrace{a \ldots a}_{m-i} \underbrace{b \ldots b}_{i}, \underbrace{c \ldots c}_{n-j} \underbrace{d \ldots d}_{j}] \ .$$

Thus, we have proved the following form of the **main theorem**

A tensor product polynomial $\mathbf{b}(u,v)$ *with tensor product polar form* $\mathbf{b}[u_1 \dots u_m, v_1 \dots v_n]$ *has the Bézier points*

$$\mathbf{b}_{ij} = \mathbf{b}[a \overset{m-i}{\dots} a b \overset{i}{\dots} b, c \overset{n-j}{\dots} c d \overset{j}{\dots} d]$$

over any interval $[a,b] \times [c,d]$.

Any tensor product polar form $\mathbf{b}[u_1 \dots u_m, v_1 \dots v_n]$ can be computed by the generalized de Casteljau algorithm from the points

$$\mathbf{b}_j(u) = \mathbf{b}[u_1 \dots u_m, c \overset{m-j}{\dots} c d \overset{j}{\dots} d] \ , \ j = 0, \dots, m \ ,$$

and these from the Bézier points $\mathbf{b}_{ij}$. Since the Bézier points are unique, any tensor product polynomial $\mathbf{b}(u,v)$ of degree $\leq (m,n)$ has a unique tensor product polar form $\mathbf{b}[u_1 \dots u_m, v_1 \dots v_n]$.

9.4 Conversion to and from monomial form

The monomial form of a polynomial tensor product surface

$$\mathbf{b}(u,v) = \sum_{k=0}^{m} \sum_{l=0}^{n} \mathbf{a}_{kl} \binom{m}{k} \binom{n}{l} u^k v^l$$

can be written more concisely with bold vector notation as

$$\mathbf{b}(\mathbf{u}) = \sum_{\mathbf{k}=\mathbf{0}}^{\mathbf{m}} \mathbf{a}_{\mathbf{k}} \binom{\mathbf{m}}{\mathbf{k}} \mathbf{u}^{\mathbf{k}} \ ,$$

where $\mathbf{u} = (u,v), \mathbf{k} = (k,l)$ and $\mathbf{m} = (m,n)$.

The conversion of the monomial form to the Bézier representation of $\mathbf{b}(\mathbf{u})$ over $[0,1]^2$ is straightforward. Applying the conversion formula in 2.8 for univariate polynomials twice gives

$$\mathbf{b}(\mathbf{u}) = \sum_{\mathbf{i}=\mathbf{0}}^{\mathbf{m}} \mathbf{b}_{\mathbf{i}} B_{\mathbf{i}}^{\mathbf{m}}(\mathbf{u}) \ ,$$

where

$$\mathbf{b}_{\mathbf{i}} = \sum_{\mathbf{k}=\mathbf{0}}^{\mathbf{i}} \binom{\mathbf{i}}{\mathbf{k}} \mathbf{a}_{\mathbf{k}} \ .$$

Similarly, by applying the conversion formula in 2.9 twice, we obtain the

converse relation

$$\mathbf{a_k} = \sum_{\mathbf{i=0}}^{\mathbf{k}} (-1)^{k+l-i-j} \binom{\mathbf{k}}{\mathbf{i}} \mathbf{b_i} \ .$$

Remark 5: If $\mathbf{b}(\mathbf{u})$ is a bilinear polynomial, i.e., a biaffine map, then $\mathbf{a_k} = \mathbf{0}$ for all $\mathbf{k} \not\leq (1,1)$. Hence, $\mathbf{b}(\mathbf{u})$ has the Bézier points

$$\begin{aligned} \mathbf{b}_{ij} &= \mathbf{a}_{00} + i\mathbf{a}_{10} + j\mathbf{a}_{01} + ij\mathbf{a}_{11} \\ &= \mathbf{b}(i/m, j/n) \ . \end{aligned}$$

This property is referred to as the **bilinear precision** of the Bézier representation.

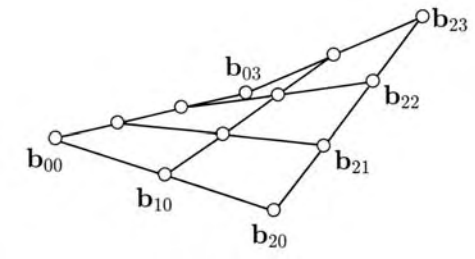

Figure 9.6: Uniform Bézier net on a bilinear interpolant.

9.5 The de Casteljau algorithm

A bivariate polynomial surface in Bézier representation,

$$\mathbf{b}(\mathbf{u}) = \sum_{\mathbf{i}} \mathbf{b_i} B_{\mathbf{i}}^{\mathbf{m}}(\mathbf{s}) \ ,$$

can be evaluated at any $\mathbf{s} = (s,t)$ by $(m+2)$ or $(n+2)$ applications of de Casteljau's algorithm for curves. This leads to the following surface algorithm

Use de Casteljau's curve algorithm to compute

1. *the points* $\mathbf{b}_i = \sum_{j=0}^{n} \mathbf{b}_{ij} B_j^n(t)$ *and*
2. *the surface point* $\mathbf{b}(\mathbf{u}) = \sum_{i=0}^{m} \mathbf{b}_i B_i^m(s)$.

Remark 6: For example, consider the polynomial $b(s,t) = \sum b_{ij} B_{ij}^{3,2}(s,t)$ whose Bézier matrix $[b_{ij}]$ appears in the upper left corner of Figure 9.7. This Figure illustrates the algorithm above by showing the $8 = 4 \cdot 2$ de Casteljau

9.8 Piecewise bicubic C^1 interpolation

Interpolation schemes for curves can be extended in a straightforward manner to tensor product schemes. We describe the principle for the example of the cubic interpolation scheme discussed in 4.5.

Given $(m+1)\times(n+1)$ interpolation points $\mathbf{p}_{ij}$ with corresponding parameter values (u_i, v_j), for $i = 0, \ldots, m$ and $j = 0, \ldots, n$, we construct a piecewise bicubic C^1 surface $\mathbf{s}(u, v)$ such that $\mathbf{s}(u_i, v_j) = \mathbf{p}_{ij}$. More exactly, we construct for all (i, j) the Bézier points $\mathbf{b}_{3i,3j}, \ldots, \mathbf{b}_{3i+3,3j+3}$ defining the bicubic segment of $\mathbf{s}$ over the interval $[u_i, u_{i+1}] \times [v_j, v_{j+1}]$.

Let $P = [\mathbf{p}_{ij}]$ be the $(m + 1) \times (n + 1)$ matrix formed by the interpolation points. Note that the entries are coordinate columns rather than scalars, in general. Further, let S and T be the $(m+1)\times(3m+1)$ and $(n+1)\times(3n+1)$ matrices of two linear interpolation schemes over the abscissae $u_0, \ldots, u_m$ and $v_0, \ldots, v_n$, respectively, as described in 4.5, Remark 9.

Then, the tensor product interpolation scheme based on S and T is as follows.

1 Interpolate every column of P by computing $A = S^t P$.

2 Interpolate every row of A by computing $B = AT$.

The desired Bézier points are the entries of $B = [\mathbf{b}_{ij}] = S^t P T$. See Figure 9.12 for an illustration.

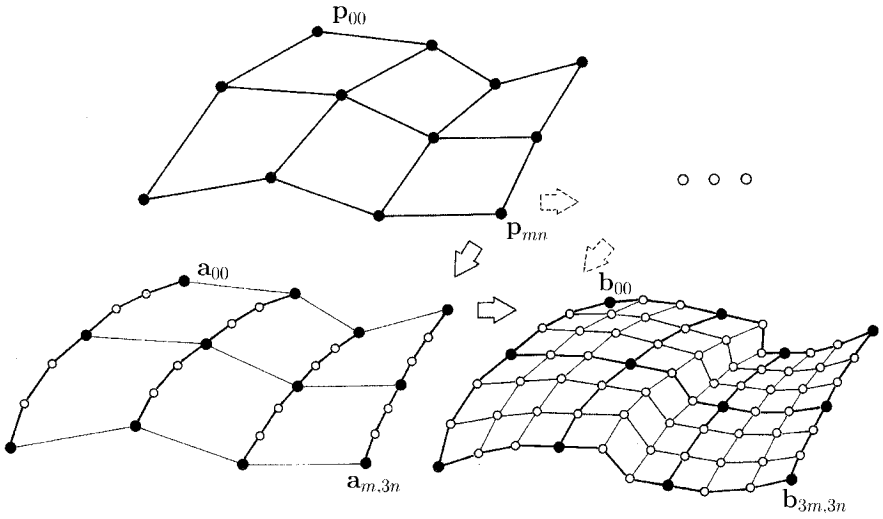

Figure 9.12: Tensor product interpolation scheme.

Row and column interpolation are interchangeable. Namely, row interpolation gives $C^t = PT$ and subsequent column interpolation $B = S^t C = S^t P T$.

describe how to build such spline surfaces, which can be used to interpolate the vertices of arbitrary quadrilateral nets.

Any piecewise bicubic surface with simple C^1 joints is completely determined by the inner Bézier points of each patch. These are marked by ∘ in Figure 9.16. The boundary Bézier points marked by □ and ●, respectively, can be computed as the midpoints of two adjacent Bézier points, respectively.

The inner Bézier points next to a vertex surrounded by three or more than four patches must coincide in order to obtain C^1 joints along all patch boundary curves emanating from this so-called **extraordinary vertex**. Moreover, the patches around an extraordinary vertex have a common tangent plane at this vertex only if the interior Bézier points connected by dashed lines in Figure 9.16 are all coplanar and if they satisfy the conditions given in 9.10.

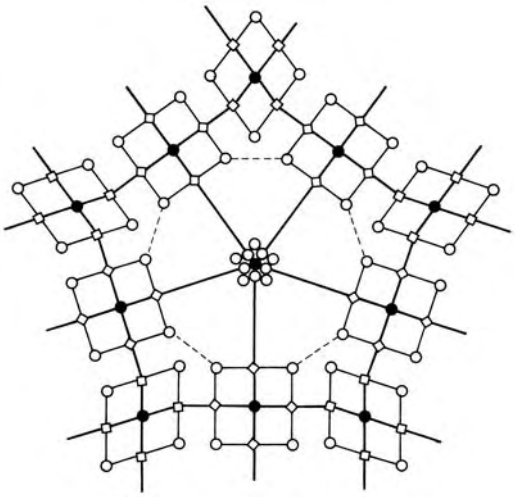

Figure 9.16: A bicubic C^1 spline.

Remark 12: The coplanarity condition above can, in general, only be satisfied if each patch has at most one extraordinary vertex. This assumption is always satisfied if one subdivides each patch into four subpatches.

Remark 13: The inner Bézier points ∘ determine the spline surface completely. However, they must meet certain restrictions for the spline to be a C^1 surface. Therefore, Reif calls these points **quasi control points**.

Remark 14: Reif has also developed a projection mapping arbitrary control nets onto quasi control nets satisfying the conditions above, see Problem 6. A more general method is presented in 14.6.

This property is referred to as the **linear precision** of the Bézier representation.

Remark 2: As a consequence of the linear precision, a functional surface

$$\mathbf{b}(\mathbf{x}) = \begin{bmatrix} \mathbf{x} \\ b(\mathbf{x}) \end{bmatrix} \quad , \quad \text{where} \quad b(\mathbf{x}) = \sum b_{\mathfrak{i}} B^n_{\mathfrak{i}} \quad ,$$

has the Bézier points $[\mathbf{a}^t_{\mathfrak{i}} \; b_{\mathfrak{i}}]^t$, where $n\mathbf{a}_{\mathfrak{i}} = [\mathbf{a}_0 \ldots \mathbf{a}_d]\mathfrak{i}$, as illustrated in Figure 10.5. The $b_{\mathfrak{i}}$ are called **Bézier ordinates** and the corresponding points $\mathbf{a}_{\mathfrak{i}}$ the **Bézier abscissae** of $b(\mathbf{x})$.

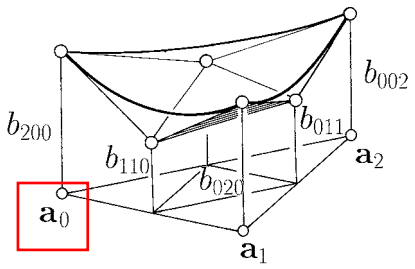

Figure 10.5: A quadratic function with its Bézier polyhedron.

10.4 The de Casteljau algorithm

A Bézier simplex $\mathbf{b} = \sum \mathbf{b}_{\mathfrak{i}} B^n_{\mathfrak{i}}$ can be evaluated by a generalization of de Casteljau's algorithm. Using the recurrence relation of the Bernstein polynomials repeatedly as in the case of curves, we first obtain

$$\begin{aligned} \mathbf{b}(\mathbf{x}) &= \sum_{|\mathfrak{i}|=n} \mathbf{b}_{\mathfrak{i}} B^n_{\mathfrak{i}}(\mathfrak{u}) \\ &= \sum_{|\mathfrak{i}|=n-1} \mathbf{b}_{\mathfrak{i}} B^{n-1}_{\mathfrak{i}}(\mathfrak{u}) \end{aligned}$$

and after $n-2$ further steps

$$\mathbf{b}(\mathbf{x}) = \sum_{|\mathfrak{i}|=0} \mathbf{b}_{\mathfrak{i}} B^0_{\mathfrak{i}}(\mathfrak{u}) = \mathbf{b}_{000} \quad ,$$

where

$$\mathbf{b}_{\mathfrak{i}} = [\mathbf{b}_{\mathfrak{i}+\mathfrak{e}_0} \ldots \mathbf{b}_{\mathfrak{i}+\mathfrak{e}_d}]\mathfrak{u} \quad .$$

An example is illustrated in Figure 10.6.

The intermediate points $\mathbf{b}_{\mathfrak{i}}, |\mathfrak{i}| = n, \ldots, 0$, of the de Casteljau algorithm in

Its **derivative** with respect to t at $t = 0$ is given by

$$\begin{aligned} D_{\mathbf{v}}\mathbf{b}(\mathbf{p}) &= \frac{\mathrm{d}}{\mathrm{d}t}\mathbf{b}\left(\mathbf{x}(t)\right)\Big|_{t=0} \\ &= v_0\frac{\partial}{\partial u_0}\mathbf{b} + \cdots + v_d\frac{\partial}{\partial u_d}\mathbf{b} \\ &= n\sum_{\mathbb{j}}\mathbf{c}_{\mathbb{j}}B_{\mathbb{j}}^{n-1} \ , \end{aligned}$$

where

$$\mathbf{c}_{\mathbb{j}} = v_0\mathbf{b}_{\mathbb{j}+\mathbb{e}_0} + \cdots + v_d\mathbf{b}_{\mathbb{j}+\mathbb{e}_d} \ ,$$

which we abbreviate by $\mathbf{c}_{\mathbb{j}} = \Delta_{\mathbf{v}}\mathbf{b}_{\mathbb{j}}$ as illustrated in Figure 10.7.

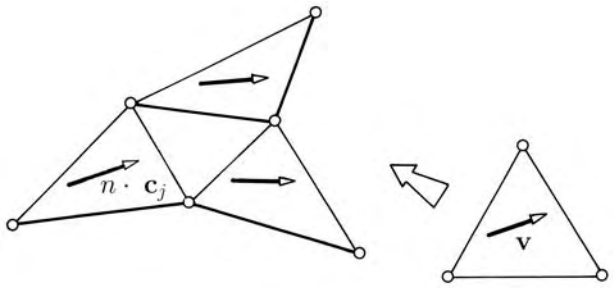

Figure 10.7: The differences $\mathbf{c}_{\mathbb{j}}$.

Similarly, one can compute higher derivatives. An rth directional derivative $D_{\mathbf{v}_1} \ldots D_{\mathbf{v}_r}\mathbf{b}$ has the Bézier coefficients $\Delta^{\mathbf{v}_1} \ldots \Delta^{\mathbf{v}_r}\mathbf{b}_{\mathbb{j}}$, where $|\mathbb{j}| = n - r$. The difference operator $\Delta^{\mathbf{v}}$ commutes with the steps of the de Casteljau algorithm since the computation of affine combinations of affine combinations is commutative, see 2.6.

Hence, we can compute an rth derivative also by first computing $n - r$ steps of the de Casteljau algorithm and then r differencing steps. In particular, it follows that the points $\mathbf{b}_{10\ldots0}, \ldots, \mathbf{b}_{0\ldots01}$ computed in the next to last step of the de Casteljau algorithm span the tangent plane of $\mathbf{b}$ at $\mathbf{x}$.

Remark 3: If $d = 2$, we can view the Bézier net of a polynomial $\mathbf{b}(\mathbf{x}) = \sum \mathbf{b}_{\mathbb{i}}B_{\mathbb{i}}^n(\mathbb{u})$ as a piecewise linear function $\mathbf{p}(\mathbf{x})$ over $\mathbf{a}_0\mathbf{a}_1\mathbf{a}_2$. Then,

> *the directional derivative $D_{\mathbf{v}}\mathbf{p}(\mathbf{x})$ of the Bézier net contains the Bézier points of $D_{\mathbf{v}}\mathbf{b}(\mathbf{x})$.*

This fact is illustrated in Figure 10.8 for a functional surface.

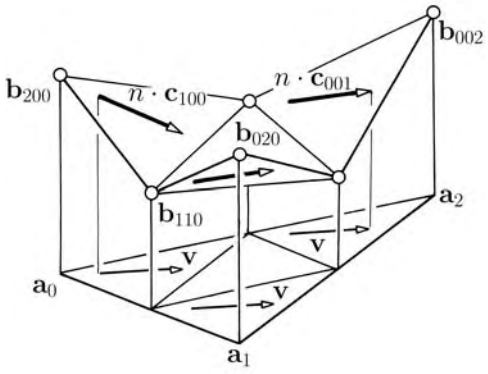

Figure 10.8: A Bézier net with its derivative.

10.6 Convexity

In the following we restrict ourselves to bivariate functions. Hence, we set $d = 2$ and $\mathbb{u} = [u, v, w]^t$.

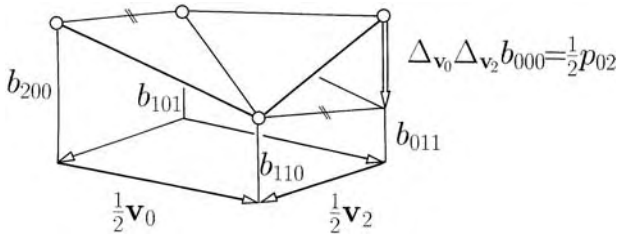

Figure 10.9: Convexity of a Bézier net.

Given the Bézier representation of a polynomial over some triangle $\mathbf{a}_0\mathbf{a}_1\mathbf{a}_2$, there is a piecewise linear polynomial $p(\mathbf{x})$ that interpolates the Bézier ordinates $b_{\mathbb{i}}$ at the corresponding abscissae $A\mathbb{i}/n$. We call it the **Bézier polyhedron** of $b(\mathbf{x})$ over A and show that

a polynomial $b(\mathbf{x})$ *is convex if its Bézier polyhedron* $p(\mathbf{x})$ *is convex.*

The converse does not hold in general, see 3.13 Problem 11.

For a proof, let

$$\mathbf{v}_0 = \mathbf{a}_2 - \mathbf{a}_1 \ , \quad \mathbf{v}_1 = \mathbf{a}_0 - \mathbf{a}_2 \ , \quad \mathbf{v}_2 = \mathbf{a}_1 - \mathbf{a}_0$$

10.7 Limitations of the convexity property

Functional polynomials with a convex Bézier polyhedron are convex, as we have seen. The converse, however, is not true in general. Consider the quadratic polynomial

$$b = 3B_{200} - B_{101} + 3B_{002} \ ,$$

which is shown with its Bézier polyhedron in Figure 10.11.

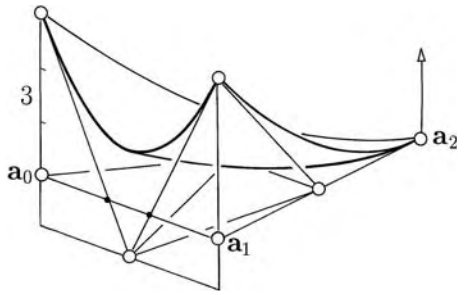

Figure 10.11: A convex polynomial patch with non-convex Bézier net.

Obviously, the Bézier polyhedron is not convex, but b is convex. Namely, the second partial derivatives are $b_{00} = b_{11} = 6$ and $b_{01} = 2$. Thus, for any $\mathbf{v} = \alpha\mathbf{v}_0 + \beta\mathbf{v}_1 \neq \mathbf{o}$ it follows that

$$\begin{aligned} D_{\mathbf{v}} D_{\mathbf{v}} b &= \alpha^2 b_{00} + 2\alpha\beta b_{01} + \beta^2 b_{11} \\ &= 4(\alpha^2 + \beta^2) + 2(\alpha + \beta)^2 > 0 \ , \end{aligned}$$

which means that b is even strictly convex.

The Bézier polyhedra of all higher degree representations of b are also **not** convex since for any nth degree representation of the constant polynomial $b_{01} = 2$ all Bézier ordinates equal 2. This result is striking since the nth degree Bézier polyhedra of b converge to b if n goes to infinity, see 11.9. Thus, we have a sequence of non-convex functions with a strictly convex limit.

Another negative result is due to Grandine [Grandine '89]. Consider a non-convex quadrilateral **abdc**, as the ones illustrated in Figure 10.12, and let b and c be polynomials with C^1 contact along the line **ad**. Then, if b and c have convex Bézier nets over **adc** and **abd**, respectively, they must be linear over **ad**.

Because of the C^1 contact, we have $b_{14} = c_{14} (= D_{\mathbf{v}_1} D_{\mathbf{v}_4} c)$ along **ad**. Since there are positive constants α and β such that $\mathbf{v}_1 = \alpha\mathbf{v}_2 + \beta\mathbf{v}_4$, the convexity

Remark 2: The barycentric coordinate vector $\mathbb{u}$ and the affine coordinate vector $\mathbf{x}$ are related by two transformations, given by

$$\mathbf{x} = \mathbf{x}(\mathbb{u}) = [\mathbf{a}_0\mathbf{a}_1\mathbf{a}_2]\mathbb{u} \quad \text{and} \quad \mathbb{u} = \mathbb{u}(\mathbf{x}) = \mathbb{p} + [\mathbb{v}_1\mathbb{v}_2]\mathbf{x} \ ,$$

where $\mathbb{p}; \mathbb{v}_1, \mathbb{v}_2$ represents the affine coordinate system in barycentric coordinates. Since these transformations are affine, one can transform a polar form $\mathbf{a}[\mathbf{x}_1 \dots \mathbf{x}_n]$, given by affine coordinates, to the corresponding polar form $\mathbf{b}[\mathbb{u}_1 \dots \mathbb{u}_n] = \mathbf{a}[A\mathbb{u}_1 \dots A\mathbb{u}_n]$ and vice versa, i.e., $\mathbf{a}[\mathbf{x}_1 \dots \mathbf{x}_n] = \mathbf{b}[\mathbb{u}(\mathbf{x}_1) \dots \mathbb{u}(\mathbf{x}_n)]$.

11.2 The main theorem

The uniqueness of the symmetric polynomials and their relationship to the Bézier representation is given by the following extension of the **main theorem**.

> *For every polynomial surface* $\mathbf{b}(\mathbf{x})$ *of degree* $\leq n$*, there exists only one symmetric* n*-variate multiaffine polynomial* $\mathbf{b}[\mathbf{x}_1 \dots \mathbf{x}_n]$ *with diagonal* $\mathbf{b}[\mathbf{x} \dots \mathbf{x}] = \mathbf{b}(\mathbf{x})$*, and the points*
>
> $$\mathbf{b}^0_{\mathbb{i}} = \mathbf{b}[\mathbf{p} \ .^{i}. \ \mathbf{p}\ \mathbf{q} \ .^{j}. \ \mathbf{q}\ \mathbf{r} \ .^{k}. \ \mathbf{r}]$$
>
> *are the Bézier points of* $\mathbf{b}(\mathbf{x})$ *over* $\mathbf{pqr}$*.*

Proof: Consider the points

$$\mathbf{b}^l_{\mathbb{i}} = \mathbf{b}[\mathbf{p} \ .^{i}. \ \mathbf{p}\ \mathbf{q} \ .^{j}. \ \mathbf{q}\ \mathbf{r} \ .^{k}. \ \mathbf{r}\ \mathbf{x}_1 \ .^{l}. \ \mathbf{x}_l] \ , \qquad i+j+k+l = n \ .$$

Since $\mathbf{b}^n_{\mathbb{o}} = \mathbf{b}[\mathbf{x}_1 \dots \mathbf{x}_n]$ is symmetric and multiaffine, it can be computed from the points $\mathbf{b}^0_{\mathbb{i}}$ by the recursion formula

$$\mathbf{b}^l_{\mathbb{i}} = u_l\mathbf{b}^{l-1}_{\mathbb{i}+\mathbb{e}_1} + v_l\mathbf{b}^{l-1}_{\mathbb{i}+\mathbb{e}_2} + w_l\mathbf{b}^{l-1}_{\mathbb{i}+\mathbb{e}_3} \ , \tag{1}$$

where u_l, v_l, w_l are the barycentric coordinates of $\mathbf{x}_l$ with respect to $\mathbf{pq}$, see Figure 11.1, where the points $\mathbf{b}[\mathbf{x}_1\mathbf{x}_2\mathbf{x}_3]$ are labelled by their arguments $\mathbf{x}_1\mathbf{x}_2\mathbf{x}_3$. Thus, different symmetric multiaffine maps must differ at some argument $[\mathbf{p} \ .^{i}. \ \mathbf{p}\ \mathbf{q} \ .^{j}. \ \mathbf{q}\ \mathbf{r} \ .^{k}. \ \mathbf{r}]$.

If all $\mathbf{x}_l$ equal $\mathbf{x}$, then the recursion formula above reduces to de Casteljau's algorithm for the computation of $\mathbf{b}(\mathbf{x})$. Consequently, since the Bézier representation is unique, the points $\mathbf{b}^0_{\mathbb{i}}$ are the Bézier points of $\mathbf{b}(\mathbf{x})$ over $\mathbf{pqr}$ and, furthermore, there can be only one symmetric n-affine polynomial with the diagonal $\mathbf{b}(\mathbf{x})$. $\diamond$

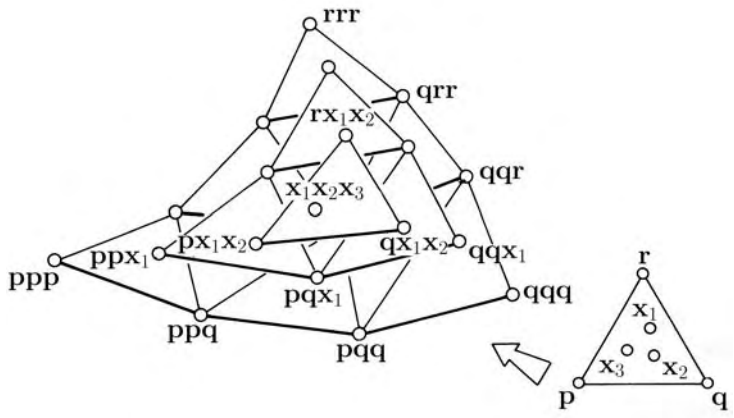

Figure 11.1: The generalized de Casteljau algorithm.

11.3 Subdivision and reparametrization

Recursion formula (1), which is illustrated in Figure 11.1, reveals another important property of de Casteljau's algorithm. The computation of $\mathbf{b}(\mathbf{x})$ generates also the Bézier points

$$\mathbf{b}[\mathbf{p} \overset{i}{\cdot\cdot} \mathbf{p}\,\mathbf{q} \overset{j}{\cdot\cdot} \mathbf{q}\,\mathbf{x} \overset{k}{\cdot\cdot} \mathbf{x}], \quad \mathbf{b}[\mathbf{p} \overset{i}{\cdot\cdot} \mathbf{p}\,\mathbf{x} \overset{j}{\cdot\cdot} \mathbf{x}\,\mathbf{r} \overset{k}{\cdot\cdot} \mathbf{r}] \ ,$$

and

$$\mathbf{b}[\mathbf{x} \overset{i}{\cdot\cdot} \mathbf{x}\,\mathbf{q} \overset{j}{\cdot\cdot} \mathbf{q}\,\mathbf{r} \overset{k}{\cdot\cdot} \mathbf{r}]$$

of $\mathbf{b}$ over $\mathbf{pqx}$, $\mathbf{pxr}$, and $\mathbf{xqr}$, respectively. Figure 11.2 shows an example for $n = 3$.

The Bézier nets of $\mathbf{b}(\mathbf{x})$ over $\mathbf{pqx}$, $\mathbf{pxr}$, and $\mathbf{xqr}$ form one connected net. It is folded if $\mathbf{x}$ lies outside $\mathbf{pqr}$. The computation of this composed net will be referred to as the **subdivision** of the Bézier net over $\mathbf{pqr}$ in $\mathbf{x}$.

One can compute the Bézier net of a polynomial surface $\mathbf{b}$ over a second triangle $\mathbf{xyz}$ by repeated subdivision from the net over $\mathbf{pqr}$, see [Prautzsch '84a, Boehm et al. '84]. First one subdivides the net over $\mathbf{pqr}$ in $\mathbf{x}$, then one subdivides the net over $\mathbf{xqr}$ in $\mathbf{y}$, and, finally, one subdivides the net over $\mathbf{xyr}$ in $\mathbf{z}$, see Figure 11.3.

A permutation of $\mathbf{pqr}$ and $\mathbf{xyz}$ results in a different construction. If possible, one should subdivide at interior points in order to avoid non-convex combinations.

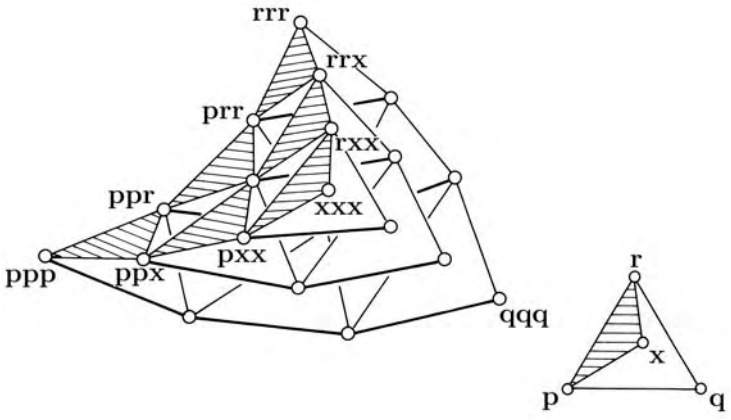

Figure 11.2: Subdividing a Bézier net.

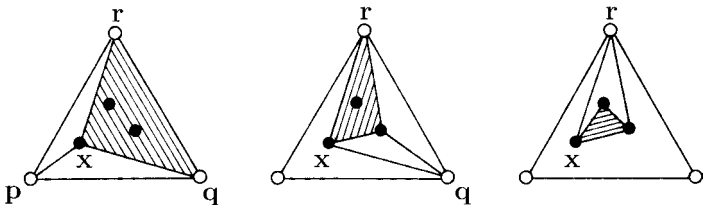

Figure 11.3: Reparametrization by repeated subdivision.

Figure 11.4 shows a situation, where it is impossible to avoid non-convex combinations with the above construction, no matter how one permutes **pqr** and **xyz**.

Remark 3: The construction above requires one to compute $3 \cdot \binom{n+2}{3} = O(n^3)$ affine combinations.

Remark 4: Every single Bézier point $\mathbf{b}[\mathbf{x} \,.^{i}.\, \mathbf{x}\,\mathbf{y} \,.^{j}.\, \mathbf{y}\,\mathbf{z} \,.^{k}.\, \mathbf{z}]$ of $\mathbf{b}$ over **xyz** can also be computed by the generalized de Casteljau algorithm, see Figure 11.1. The affine combinations computed by this algorithm are convex if $\mathbf{x}, \mathbf{y}$ and $\mathbf{z}$ all lie in the triangle **pqr**.

Remark 5: To compute the Bézier net over **xyz** by $\binom{n+2}{2}$ applications of the generalized de Casteljau algorithm, one needs to compute $\binom{n+2}{2} \cdot \binom{n+3}{3} = O(n^5)$ affine combinations.

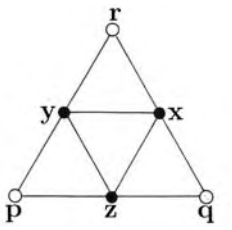

Figure 11.4: Special reference triangles.

11.4 Convergence under subdivision

The Bézier net of $\mathbf{b}(\mathbf{x})$ over a triangle **pqr** is a good approximation of the patch $\mathbf{b}$ if the triangle is sufficiently small. To make this statement precise, let **pqr** be any triangle in some fixed bounded region and let h be its diameter. Furthermore, let

$$\mathbf{i} = \mathbf{p}\frac{i}{n} + \mathbf{q}\frac{j}{n} + \mathbf{r}\frac{k}{n}$$

represent the point with barycentric coordinates $\mathfrak{i}/n$. Then,

there is a constant M not depending on **pq** *such that*

$$\max_{\mathfrak{i}} \|\mathbf{b}(\mathbf{i}) - \mathbf{b}_{\mathfrak{i}}\| \leq Mh^2 \quad .$$

For a proof, let D be the differential of $\mathbf{b}[\mathbf{x}\,\mathbf{i}\,\ldots\,\mathbf{i}] = \cdots = \mathbf{b}[\mathbf{i}\,\ldots\,\mathbf{i}\,\mathbf{x}]$ at $\mathbf{x} = \mathbf{i}$. Expanding the symmetric polynomial $\mathbf{b}[\mathbf{x}_1\,\ldots\,\mathbf{x}_n]$ around $[\mathbf{i}\,\ldots\,\mathbf{i}]$, we obtain

$$\begin{aligned} \mathbf{b}_{\mathfrak{i}} &= \mathbf{b}[\mathbf{i}\,\ldots\,\mathbf{i}] + iD[\mathbf{p}-\mathbf{i}] + jD[\mathbf{q}-\mathbf{i}] + kD[\mathbf{r}-\mathbf{i}] + O(h^2) \\ &= \mathbf{b}(\mathbf{i}) + O(h^2) \quad , \end{aligned}$$

which concludes the proof. ◇

An application of this approximation property is discussed in the following section.

11.5 Surface generation

As a consequence of section 11.4, repeated subdivision of a Bézier net produces arbitrarily good approximations of the underlying surface. We discuss three subdivision strategies.

(1) Subdividing triangles at their centers, as illustrated in Figure 11.5, leaves the maximum diameter of the reference triangles unchanged. Hence, the

The derivatives of $\mathbf{b}$ *and* $\mathbf{c}$ *up to order* r *agree over* $\mathbf{qr}$ *if and only if for all* $l = 0, \ldots, n-r$ *the two polynomials* $\mathbf{b}[\mathbf{x}\ \overset{r}{\ldots}\ \mathbf{xq}\ \overset{l}{\ldots}\ \mathbf{qr}\ \overset{n-r-l}{\ldots}\ \mathbf{r}]$ *and* $\mathbf{c}[\mathbf{x}\ \overset{r}{\ldots}\ \mathbf{xq}\ \overset{l}{\ldots}\ \mathbf{qr}\ \overset{n-r-l}{\ldots}\ \mathbf{r}]$ *are equal.*

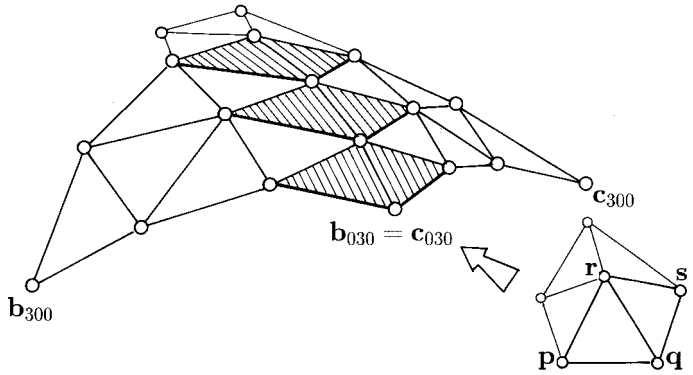

Figure 11.8: Sabin's simple C^1 joint.

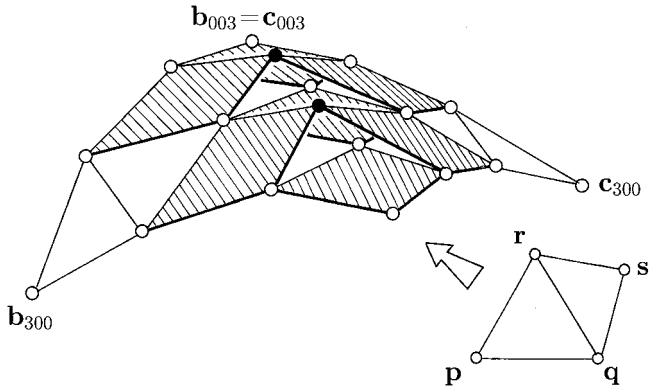

Figure 11.9: Farin's simple C^2 joint.

Remark 6: The shaded quadrilaterals in Figure 11.8 and 11.9 are different affine images of the quadrilateral **pqrs**. Consequently, any m triangular patches $\mathbf{b}^i(\mathbf{x})$, $i = 1, \ldots, m$, enclosing a common vertex have simple C^1 joints at this vertex if and only if their parameter triangles form an m-gon that is an affine image of the m-gon formed by the respective corner triangles of the associated Bézier nets.

Remark 7: Since two polynomials are equal if and only if their polar forms

are equal, $\mathbf{b}(\mathbf{x})$ and $\mathbf{c}(\mathbf{x})$ have identical derivatives up to order r over the line $\mathbf{qr}$ if and only if their polar forms satisfy the equation

$$\mathbf{b}[\mathbf{x}_1\ \ldots\ \mathbf{x}_r\ \mathbf{q}\overset{j}{\cdot\cdot}\mathbf{q}\,\mathbf{r}\overset{k}{\cdot\cdot}\mathbf{r}] = \mathbf{c}[\mathbf{x}_1\ \ldots\ \mathbf{x}_r\ \mathbf{q}\overset{j}{\cdot\cdot}\mathbf{q}\,\mathbf{r}\overset{k}{\cdot\cdot}\mathbf{r}]$$

for arbitrary variables $\mathbf{x}_1, \ldots, \mathbf{x}_r$ and for all j and k with $r + j + k = n$. This condition is used in [Lai '91] to characterize multivariate C^r splines over arbitrary triangulations.

11.8 Degree elevation

A polynomial surface of degree n also has a Bézier representation of any degree m higher than n. As in the case of curves, a conversion to a higher degree representation is called degree **elevation**.

Given an nth degree Bézier representation,

$$\mathbf{b}(\mathbf{x}) = \sum \mathbf{b}_{\mathbb{i}} B^n_{\mathbb{i}}(\mathbb{u}) \ , \quad \mathbf{x} = [\mathbf{pqr}]\mathbb{u} \ ,$$

of some polynomial surface $\mathbf{b}(\mathbb{u})$ over a triangle $\mathbf{pqr}$, we show how to obtain its Bézier representation of degree $n+1$. In analogy to the derivation for curves in 3.11, we use the symmetric polynomial $\mathbf{b}[\mathbf{x}_1\ \ldots\ \mathbf{x}_n]$ of $\mathbf{b}(\mathbf{x})$. The polynomial

$$\mathbf{c}[\mathbf{x}_0\ \ldots\ \mathbf{x}_n] = \frac{1}{n+1}\sum_{l=0}^{n} \mathbf{b}[\mathbf{x}_0\ \ldots\ \mathbf{x}_l^*\ \ldots\ \mathbf{x}_n]$$

is multiaffine, symmetric and agrees with $\mathbf{b}(\mathbf{x})$ on its diagonal. Hence, due to the main theorem in 11.2, it follows that the points

$$\mathbf{b}_{\mathbb{j}} = \mathbf{c}[\mathbf{p}\overset{j_0}{\cdot\cdot}\mathbf{p}\,\mathbf{q}\overset{j_1}{\cdot\cdot}\mathbf{q}\,\mathbf{r}\overset{j_2}{\cdot\cdot}\mathbf{r}]$$

are the Bézier points of $\mathbf{b}(\mathbf{x})$ over $\mathbf{pqr}$ in its representation for degree $n+1$. Consequently,

$$\begin{aligned}\mathbf{b}_{\mathbb{j}} = \quad & \frac{j_0}{n+1}\mathbf{b}[\mathbf{p}\overset{j_0-1}{\cdot\cdot}\mathbf{p}\,\mathbf{q}\overset{j_1}{\cdot\cdot}\mathbf{q}\,\mathbf{r}\overset{j_2}{\cdot\cdot}\mathbf{r}] \\ + \quad & \frac{j_1}{n+1}\mathbf{b}[\mathbf{p}\overset{j_0}{\cdot\cdot}\mathbf{p}\,\mathbf{q}\overset{j_1-1}{\cdot\cdot}\mathbf{q}\,\mathbf{r}\overset{j_2}{\cdot\cdot}\mathbf{r}] \\ + \quad & \frac{j_2}{n+1}\mathbf{b}[\mathbf{p}\overset{j_0}{\cdot\cdot}\mathbf{p}\,\mathbf{q}\overset{j_1}{\cdot\cdot}\mathbf{q}\,\mathbf{r}\overset{j_2-1}{\cdot\cdot}\mathbf{r}] \ .\end{aligned}$$

Figure 11.10 illustrates the associated construction for $n = 2$.

be written as

$$\binom{n}{\mathbf{i}}\left(\frac{k_1}{m}\cdots\frac{k_1-i_1+1}{m-i_1+1}\right)\left(\frac{k_2}{m-i_1}\cdots\frac{k_2-i_2+1}{m-i_1-i_2+1}\right)\left(\frac{k_3}{m-i_1-i_2}\cdots\frac{k_3-i_3+1}{m-n+1}\right),$$

from which we conclude that

$$\beta_{\mathbf{i}\mathbb{k}} \le \binom{n}{\mathbf{i}}\left(\frac{k_1}{m}+\frac{n}{m-n}\right)^{i_1}\left(\frac{k_2}{m}+\frac{n}{m-n}\right)^{i_2}\left(\frac{k_3}{m}+\frac{n}{m-n}\right)^{i_3}$$

and

$$\beta_{\mathbf{i}\mathbb{k}} \ge \binom{n}{\mathbf{i}}\left(\frac{k_1}{m}-\frac{n}{m}\right)^{i_1}\left(\frac{k_2}{m}-\frac{n}{m}\right)^{i_2}\left(\frac{k_3}{m}-\frac{n}{m}\right)^{i_3} .$$

Thus, we find

$$\beta_{\mathbf{i}\mathbb{k}} = B^n_{\mathbf{i}}(\mathbb{k}/m) + O(1/m)$$

and, therefore,

$$\mathbf{d}_{\mathbb{k}} = \sum \mathbf{b}_{\mathbf{i}} B^n_{\mathbf{i}}(\mathbb{k}/m) + O(1/m) \ .$$

Consequently, the mth degree Bézier nets of $\mathbf{b}(\mathbf{x})$ converge to $\mathbf{b}(\mathbf{x})$ linearly in $1/m$, see [Farin '79, Trump et al. '96].

11.10 Conversion to tensor product Bézier representation

Let $\mathbf{b}(\mathbf{x})$ be a bivariate polynomial with polar form $\mathbf{b}[\mathbf{x}_1 \dots \mathbf{x}_n]$, and let $\mathbf{x}_{st} = \mathbf{x}(s,t)$ be any biaffine map that maps the unit square $[0,1]^2$ onto a convex quadrilateral, see Figure 11.11. Then the reparametrized polynomial

$$\mathbf{c}(s,t) = \mathbf{b}(\mathbf{x}(s,t))$$

is a tensor product polynomial of degree (n,n) in (s,t). Its tensor product polar form is given by

$$\mathbf{c}[s_1 \dots s_n, t_1 \dots t_n] = \frac{1}{n!}\sum_{\tau} \mathbf{b}[\mathbf{x}(s_1,\tau_1)\dots\mathbf{x}(s_n,\tau_n)] \ ,$$

where the sum extends over all permutations $(\tau_1,\dots,\tau_n)$ of $(t_1,\dots,t_n)$. To verify this, one checks that $\mathbf{c}$ satisfies the three characterizing properties: the diagonal, symmetry and affinity property.

Knowing the tensor product polar form, we can apply the main theorem 9.3 to obtain the Bézier points of $\mathbf{c}(s,t)$ over $[0,1]^2$. These are the points

$$\mathbf{c}_{ij} = \mathbf{c}[0\overset{n-i}{\dots}01\overset{i}{\dots}1, 0\overset{n-j}{\dots}01\overset{j}{\dots}1] \ ,$$

12 Interpolation

12.1 Hermite interpolation — 12.2 The Clough-Tocher interpolant — 12.3 The Powell-Sabin interpolant — 12.4 Surfaces of arbitrary topology — 12.5 Singular parametrization — 12.6 Quintic C^1 splines of arbitrary topology — 12.7 Problems

Given the values and derivatives of a bivariate function, it is quite easy to construct smooth piecewise polynomial interpolants using their Bézier representation. However, there is no straightforward extension to arbitrary parametric surfaces as, for example, spheres. General C^r joints or singular parametrizations are necessary to build such interpolants.

12.1 Triangular Hermite interpolation

Given a triangulation $\mathcal{T}$ of some polygonal domain in $\mathbb{R}^2$, one can construct a piecewise polynomial surface of degree $4r+1$ that interpolates any given derivatives up to order $2r$ at the vertices of $\mathcal{T}$ and is r-times differentiable. The Bézier representation is a very handy tool to describe this construction.

Figure 12.1 shows one triangle of a triangulation and the Bézier abscissae, see 10.3, of the interpolant over that triangle for $r = 2$.

There are three kinds of Bézier abscissae. The Bézier ordinates at the abscissae $\bullet$ are defined by the prescribed derivatives, the Bézier ordinate at $\circ$ can be chosen arbitrarily, and the Bézier ordinates at the abscissae $\boldsymbol{\cdot}, \boldsymbol{\cdot}, \boldsymbol{\cdot}$ depend on the corresponding ordinates over the adjacent triangles according to the C^r-conditions. One can choose the ordinates at $\boldsymbol{\cdot}, \boldsymbol{\cdot}, \boldsymbol{\cdot}$ in one triangle arbitrarily. Then, the corresponding Bézier ordinates in the adjacent triangles are determined by the C^r-conditions.

$$\mathbf{b}_{00n} = \mathbf{b}_{1,0,n-1} = \mathbf{b}_{0,1,n-1}$$

and

$$\mathbf{b}_{1,1,n-2} = \alpha\mathbf{b}_{2,0,n-2} + \beta\mathbf{b}_{0,2,n-2} + \gamma\mathbf{b}_{00n}$$

with $\alpha, \beta > 0$, $\alpha+\beta+\gamma = 1$ and independent points $\mathbf{b}_{00n}, \mathbf{b}_{2,0,n-2}, \mathbf{b}_{0,2,n-2}$. The derivatives of $\mathbf{b}(u, v)$ vanish at $\mathbf{u} = (u, v) = (0, 0)$. However, there exists a reparametrization $\mathbf{u}(\mathbf{x})$ such that $\mathbf{c}(\mathbf{x}) = \mathbf{b}(\mathbf{u}(\mathbf{x}))$ is regular at $\mathbf{x} = \mathbf{u}^{-1}(\mathbf{o})$. After a suitable affine transformation, we obtain

$$\mathbf{b}_{00n} = \mathbf{0} \ , \quad \mathbf{b}_{2,0,n-2} = \frac{2}{n(n-1)} \begin{bmatrix} 1 \\ 0 \\ 0 \end{bmatrix} \ , \quad \mathbf{b}_{0,2,n-2} = \frac{2}{n(n-1)} \begin{bmatrix} 0 \\ 1 \\ 0 \end{bmatrix} \ .$$

Hence, the Taylor expansion of $\mathbf{b}(\mathbf{u})$ at $\mathbf{u} = (0, 0)$ is of the form

$$\mathbf{b}(\mathbf{u}) = \begin{bmatrix} \mathbf{x}(\mathbf{u}) \\ 0 \end{bmatrix} + \mathbf{d}(\mathbf{u}) \ ,$$

where

$$\mathbf{x}(\mathbf{u}) = \begin{bmatrix} u^2 + 2\alpha uv \\ v^2 + 2\beta uv \end{bmatrix} = O(\|\mathbf{u}\|^2)$$

and $\|\mathbf{d}(\mathbf{u})\| = O(\|\mathbf{u}\|^3)$. Obviously, x and y are strictly monotone in u and v for $u, v \geq 0$. Hence, $\mathbf{x}(\mathbf{u})$ is one-to-one for $u, v \geq 0$. Furthermore, $\mathbf{x}(\mathbf{u})$ is regular for $\mathbf{u} \neq \mathbf{0}$. Consequently, $\mathbf{c}(\mathbf{x}) = \mathbf{d}(\mathbf{u}(\mathbf{x}))$ is continuously differentiable if $\mathbf{c}(\mathbf{x})$ has continuous partial derivatives. These partials are given by

$$[\mathbf{c}_x \mathbf{c}_y] = [\mathbf{d}_u \mathbf{d}_v] \begin{bmatrix} x_u & x_v \\ y_u & y_v \end{bmatrix}^{-1} = \frac{1}{x_u y_v - x_v y_u} [\mathbf{d}_u \mathbf{d}_v] \begin{bmatrix} y_v & -x_v \\ -y_u & x_u \end{bmatrix} \ ,$$

which shows that

$$\|\mathbf{c}_x\| = O(\|\mathbf{u}\|) = O(\sqrt{\|\mathbf{x}\|}) \ .$$

The same argument can be made for $\mathbf{d}_y$. Hence, $\mathbf{c}(\mathbf{x})$ and, therefore, $\mathbf{b}(\mathbf{u}(\mathbf{x}))$ are continuously differentiable.

Remark 2: Even if $\alpha, \beta < 0$ and $4\alpha\beta > 1$, one can show that $\mathbf{b}(\mathbf{u})$ has a continuous tangent plane [Reif '95a].

12.6 Quintic C^1 splines of arbitrary topology

Singular parametrizations can be used to construct arbitrary C^1 surfaces composed of triangular patches with prescribed positions and tangent planes at their vertices. The following description of one such surface construction

One says that $\mathbf{p}$ and $\mathbf{q}$ have a **general $\mathbf{C^1}$** or **geometric $\mathbf{C^1}$**- or, in short, **$\mathbf{G^1}$ joint** in $x = 0$ if they have equal normals along this parameter line, i.e., if

$$\frac{\mathbf{p}_x \times \mathbf{p}_y}{\|\mathbf{p}_x \times \mathbf{p}_y\|} = \frac{\mathbf{q}_x \times \mathbf{q}_y}{\|\mathbf{q}_x \times \mathbf{q}_y\|} \quad \text{for} \quad x = 0 \ .$$

Equivalently, one can characterize G^1-continuity by requiring that there are **connection functions** $\lambda(y), \mu(y)$ and $\nu(y)$ such that for $x = 0$ and all y

$$\lambda \mathbf{p}_x = \mu \mathbf{q}_x + \nu \mathbf{q}_y \quad \text{and} \quad \lambda\mu > 0 \ , \tag{1}$$

except for isolated zeros.

In particular, if $\mathbf{p}$ *and* $\mathbf{q}$ *have a* G^1 *joint and are polynomials, then the connection functions are also polynomials, and, up to a common factor, we have*

$$\begin{aligned} \text{degree } \lambda &\leq \text{degree } \mathbf{q}_x(0,y) + \text{degree } \mathbf{q}_y(0,y) \ , \\ \text{degree } \mu &\leq \text{degree } \mathbf{p}_x(0,y) + \text{degree } \mathbf{q}_y(0,y) \ , \\ \text{degree } \nu &\leq \text{degree } \mathbf{p}_x(0,y) + \text{degree } \mathbf{q}_x(0,y) \ . \end{aligned}$$

For a proof, we compute the vector product of equation (1) with $\mathbf{q}_x$ and $\mathbf{q}_y$. This gives

$$\begin{aligned} \lambda \mathbf{p}_x \times \mathbf{q}_x &= \nu \mathbf{q}_y \times \mathbf{q}_x \ , \quad \text{and} \\ \lambda \mathbf{p}_x \times \mathbf{q}_y &= \mu \mathbf{q}_x \times \mathbf{q}_y \ . \end{aligned}$$

Recall that $\mathbf{q}$ is regular. Hence, at least one coordinate, say the first of $[\mathbf{q}_x \times \mathbf{q}_y]$, denoted by $[\mathbf{q}_x \times \mathbf{q}_y]_1$, is non-zero. Since equation (1) can be multiplied by a factor, we may assume that

$$\lambda = [\mathbf{q}_x \times \mathbf{q}_y]_1 \ .$$

This implies

$$\mu = [\mathbf{p}_x \times \mathbf{q}_y]_1 \quad \text{and} \quad \nu = -[\mathbf{p}_x \times \mathbf{q}_x]_1 \ ,$$

which proves the assertion. $\diamond$

Remark 1: Often, one sets $\lambda = 1$. Then μ and ν are rational, in general.

Remark 2: The proof given above also holds for rational polynomials $\mathbf{p}$ and $\mathbf{q}$. Then, the functions λ, μ and ν are rational up to a common factor with the same degree estimates as above.

Remark 3: Any G^1 joint is a simple C^1 joint after a suitable parameter transformation. Namely, if $\mathbf{p}$ and $\mathbf{q}$ satisfy the G^1-condition (1), then $\mathbf{a}(x,y) = \mathbf{p}(\lambda x, y)$ and $\mathbf{b}(x,y) = \mathbf{q}(\mu x, \nu x + y)$ have a simple C^1 joint, see 9.7 and 11.7.

Remark 4: Whether two patches have a G^1 joint does not depend on their parametrization. However, the connection functions do depend on the parametrization. The maximum degree of the connection function is invariant under affine reparametrization.

13.2 Joining two triangular cubic patches

Consider two triangular cubic patches

$$\mathbf{p}(\mathbb{u}) = \sum \mathbf{p}_{\mathbb{i}} B^3_{\mathbb{i}}(\mathbb{u}) \quad \text{and} \quad \mathbf{q}(\mathbb{u}) = \sum \mathbf{q}_{\mathbb{i}} B^3_{\mathbb{i}}(\mathbb{u}) \ ,$$

where $\mathbb{0} \leq \mathbb{i} = (i,j,k)$ and $|\mathbb{i}| = i+j+k = 3$ and $\mathbf{p}_{\mathbb{i}} = \mathbf{q}_{\mathbb{i}}$ for $i = 0$ such that $\mathbf{p}$ and $\mathbf{q}$ join continuously at $u = 0$ and have common tangent planes at $\mathbb{e}_1 = (0,1,0)$ and $\mathbb{e}_2 = (0,0,1)$. This configuration is illustrated in Figure 13.2. The shaded quadrilaterals are planar but not necessarily affine.

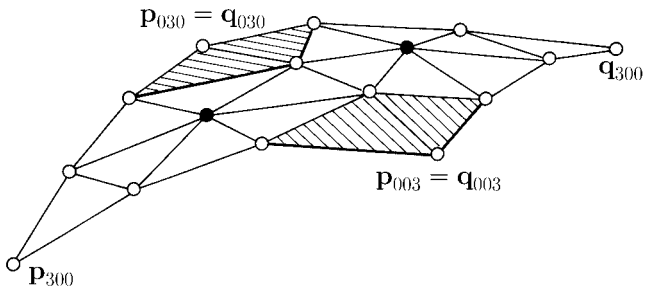

Figure 13.2: Moving interior Bézier points so as to achieve a G^1 joint.

In general, we can move both interior points $\mathbf{p}_{111}$ *and* $\mathbf{q}_{111}$ *so that* $\mathbf{p}$ *and* $\mathbf{q}$ *join* G^1*-continuously along* $u = 0$.

In particular, we show how to obtain such a smooth joint with linear connection functions $\lambda(v)$, $\mu(v)$ and $\nu(v)$. Then, the G^1-condition for $\mathbf{p}$ and $\mathbf{q}$ along $u = 0$ becomes a cubic equation in $w = 1 - v$. Denoting the partial derivatives with respect to the directions $\mathbb{e}_0 - \mathbb{e}_2$ and $\mathbb{e}_2 - \mathbb{e}_1$ by subindices 0 and 1, respectively, this cubic equation is

$$\lambda \mathbf{p}_0 = \mu \mathbf{q}_0 - \nu \mathbf{q}_1 \ , \quad \lambda\mu > 0 \ .$$

At $v = 0$, we know the derivatives $\mathbf{p}_0, \mathbf{q}_0$ and $\mathbf{q}_1$. Hence, this equation establishes a linear system for $\lambda_0 = \lambda(0)$, $\mu_0 = \mu(0)$ and $\nu_0 = \nu(0)$, with a one parameter family of solutions. Similarly, there is a one parameter family

of solutions λ_1, μ_1 and ν_1 at $v = 1$. We choose arbitrary solutions at $v = 0$ and $v = 1$, which determine the linear functions λ, μ and ν. Since a cubic is determined by its values and derivatives at two points, here $v = 0$ and $v = 1$, we are also interested in the derivative and, therefore, differentiate the G^1-condition along $u = 0$. Thus, we obtain

$$\lambda \mathbf{p}_{01} - \mu \mathbf{q}_{01} = \nu \mathbf{q}_{11} + \nu' \mathbf{q}_1 - \lambda' \mathbf{p}_0 + \mu' \mathbf{q}_0 \ .$$

Expressing $\mathbf{p}_{01}$, $\mathbf{q}_{01}$ etc. in terms of the Bézier points, we obtain at $\mathbb{e}_1$ the equations

$$\begin{aligned} \mathbf{p}_{01} &= 6(\mathbf{p}_{003} + \mathbf{p}_{111} - \mathbf{p}_{012} - \mathbf{p}_{102}) \ , \\ \mathbf{q}_{01} &= 6(\mathbf{q}_{021} + \mathbf{q}_{111} - \mathbf{q}_{012} - \mathbf{q}_{120}) \\ &\text{etc.} \end{aligned}$$

and similar expressions for $\mathbf{p}_{01}, \mathbf{q}_{01}$, etc. at $\mathbb{e}_2$. The points $\mathbf{q}_{11}, \mathbf{q}_1, \mathbf{q}_0$, and $\mathbf{p}_0$ do not depend on $\mathbf{p}_{111}$ and $\mathbf{q}_{111}$ for $v = 0$ and $v = 1$. Substituting these expressions into the differentiated G^1-condition leads to a linear system for $\mathbf{p}_{111}$ and $\mathbf{q}_{111}$ given by

$$[\mathbf{p}_{111}\mathbf{q}_{111}] \begin{bmatrix} \lambda_0 & \lambda_1 \\ -\mu_0 & -\mu_1 \end{bmatrix} = [\mathbf{w}_0 \mathbf{w}_1] \ ,$$

where $\mathbf{w}_0$ and $\mathbf{w}_1$ are combinations of known Bézier points $\mathbf{p}_{ijk}$ and $\mathbf{q}_{ijk}$, except $\mathbf{p}_{111}$ and $\mathbf{q}_{111}$. This system has a solution if the matrix

$$\begin{bmatrix} \lambda_0 & \lambda_1 \\ -\mu_0 & -\mu_1 \end{bmatrix}$$

is invertible. Hence, a solution exists, unless $\lambda(y) : \mu(y) = \textit{constant}$. Only for the configuration illustrated in Figure 13.3, a solution might not exist. $\diamond$

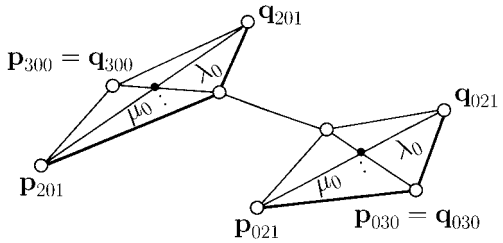

Figure 13.3: Critical configuration.

In fact, there is no solution if $\lambda(y) : \mu(y)$ is constant, if both quadrilaterals are not affine and if the common boundary $\mathbf{p}(0, y) = \mathbf{q}(0, y)$ is a regular cubic, i.e., if $\mathbf{q}_y(0, y)$ is a quadratic not passing through the origin.

Namely, rewriting the G^1-condition as

$$\mathbf{p}_x - \frac{\mu}{\lambda}\mathbf{q}_x = \frac{\nu}{\lambda}\mathbf{q}_y$$

results in a quadratic on the left. Since $\mathbf{q}_y$ is also quadratic without real root, it follows that ν/λ must be constant. This, finally, contradicts the assumption that the two quadrilaterals shown in Figure 13.3 are not affine.

If $\mathbf{q}(0, y)$ is quadratic or non-regular, a solution exists with linear functions λ, μ and ν, see Problem 3.

13.3 A triangular G^1 interpolant

In 1985, Bruce Piper [Piper '87] presented a scheme to construct a piecewise quartic G^1 surface interpolating a triangular network of cubic curves, as illustrated in Figure 13.4. We review the basic construction, but rule out critical situations so that cubic patches suffice.

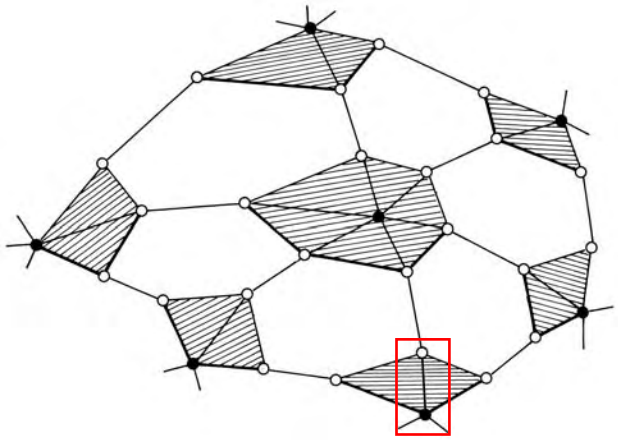

Figure 13.4: A triangular G^1-net of cubic curves.

Adjacent "triangles" of a cubic net exhibit the configurations discussed in 13.2. For simplicity, we assume that there are no critical configurations as in Figure 13.3. Then, any "triangle" can be interpolated by a macro patch consisting of three cubic patches, as described below. Figure 13.5 shows the Bézier points of such a macro patch schematically.

The Bézier points ○ on the boundary are given by the cubic net. The Bézier points ● are the centroids of their three neighbors ○ with which they form a planar quadrilateral which is shaded in the Figure.

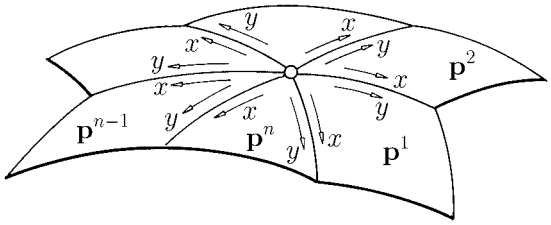

Figure 13.6: A vertex enclosed by n patches, where $n = 6$.

For $z = 0$, these equations form the cyclic linear system

$$[\mathbf{p}^1_{xy} \dots \mathbf{p}^n_{xy}] \begin{bmatrix} \lambda_1 & & -\mu_1 \\ -\mu_2 & \lambda_2 & \\ & \ddots & \\ & -\mu_n & \lambda_n \end{bmatrix} [\mathbf{r}_1 \dots \mathbf{r}_n] \ ,$$

where

$$\mathbf{r}_i = -\lambda'_i \mathbf{p}^i_x + \mu'_i \mathbf{p}^{i+1}_y + \nu'_i \mathbf{p}^{i+1}_x + \nu_i \mathbf{p}^{i+1}_{xx} \ .$$

We abbreviate this system by $TA = R$.

13.5 The parity phenomenon

The cyclic matrix A of the twist constraints exhibits the following phenomenon. The rank of A is n if n is odd, and it is $n - 1$ if n is even. Thus, A is non-singular only for odd n. Consequently, the twist constraints are solvable if the number n of patches is odd, while, in general, there is no solution if the number is even. In order to verify this surprising fact, we observe that

$$\begin{aligned} \det A &= \lambda_1 \dots \lambda_n - \mu_1 \dots \mu_n \\ &= \Pi\lambda_i - \Pi\mu_i \ . \end{aligned}$$

Computing, the vector product of

$$\lambda_i \mathbf{p}^i_x = \mu_i \mathbf{p}^{i+1}_y + \nu_i \mathbf{p}^{i+1}_x \ ,$$

with $\mathbf{p}^{i+1}_x = \mathbf{p}^i_y$ gives

$$\lambda_i : \mu_i = [\mathbf{p}^{i+2}_x \times \mathbf{p}^{i+1}_x] : [\mathbf{p}^i_x \times \mathbf{p}^{i+1}_x] \ ,$$

which implies that

$$\Pi\lambda_i : \Pi\mu_i = (-1)^n$$

14 G^k-constructions

14.1 The general C^k joint — 14.2 G^k joints by cross curves — 14.3 G^k joints by the chain rule — 14.4 G^k surfaces of arbitrary topology — 14.5 Smooth n-sided patches — 14.6 Multi-sided patches in the plane — 14.7 Problems

Two patches join smoothly if they can be (re-)parametrized so that their derivatives up to some order are identical along a common boundary curve. For any fixed reparametrization, this smoothness condition means that the derivatives of both patches at any common point are related by a linear transformation. This is analogous to the curve case.

In this chapter, we discuss these smoothness conditions and use them to build surfaces of arbitrary topological form and arbitrarily high smoothness order.

14.1 The general C^k joint

Two regular patches $\mathbf{p}$ and $\mathbf{q}$ with a common boundary curve $\mathbf{b}$ are said to have a **general C^k joint** along $\mathbf{b}$ if they have a simple C^k joint locally for each point $\mathbf{b}_0$ on $\mathbf{b}$ after some regular reparametrization. This means that, locally, there are regular reparametrizations $\mathbf{u}$ and $\mathbf{v}$ such that $\mathbf{p}\circ\mathbf{u}$ and $\mathbf{q}\circ\mathbf{v}$ have identical derivatives up to order k along $\mathbf{b}$, see Figure 14.1. It suffices to reparametrize only one patch, for example $\mathbf{q}$ by $\mathbf{v}\circ\mathbf{u}^{-1}$, see Figure 14.2. A general C^k joint is also referred to as a **G^k joint**.

If $\mathbf{p}$ and $\mathbf{q}$ have a G^k joint at some point $\mathbf{b}_0$, we obtain a local C^k parametrization $\mathbf{r}(x,y)$ of the union of both patches simply by a non-tangential projection π into some plane P, as illustrated in Figure 14.3.

The regular C^k-maps $\phi = \pi\circ\mathbf{p}\circ\mathbf{u}$ and $\psi = \pi\circ\mathbf{q}\circ\mathbf{v}$, have a C^k joint along $\pi(\mathbf{b})$ in a neighborhood of $\pi(\mathbf{b}_0)$. Therefore,

$$\mathbf{r}(x,y) = \begin{cases} \mathbf{p}\circ\mathbf{u}\circ\phi^{-1}(x,y) & \text{if } (x,y) \text{ lies in } \pi(\mathbf{p}) \\ \mathbf{q}\circ\mathbf{v}\circ\psi^{-1}(x,y) & \text{if } (x,y) \text{ lies in } \pi(\mathbf{q}) \end{cases}$$

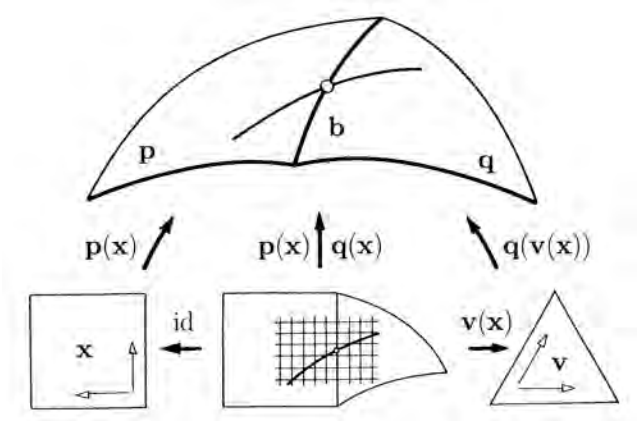

Figure 14.2: A general C^k joint brought into a simple form.

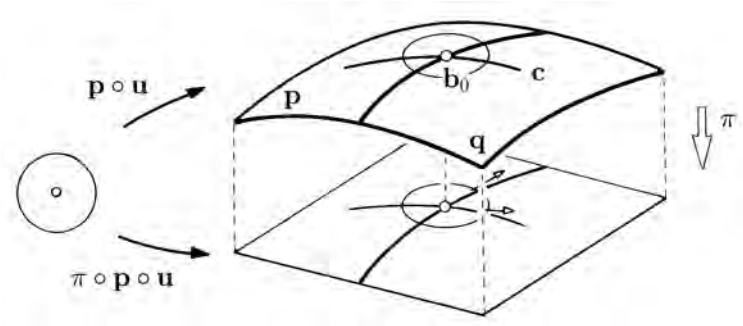

Figure 14.3: Parametrization by projection.

be any partial derivatives of $\mathbf{p}$ and $\mathbf{q}$ of order $i + j = k - 1$. Then, the induction assumption implies that

$$\overline{\mathbf{p}}(\pi\mathbf{b}(t)) = \overline{\mathbf{q}}(\pi\mathbf{b}(t)) \ .$$

Differentiating this equation with respect to t, we obtain for $t = t_0$

$$\overline{\mathbf{p}}_x(\mathbf{o}) = \overline{\mathbf{q}}_x(\mathbf{o}) \ .$$

Hence, almost all k-th partial derivatives of $\mathbf{p}$ and $\mathbf{q}$ are equal and we need to show that

$$\frac{\partial^k}{\partial y^k}[\mathbf{p}(\mathbf{o}) - \mathbf{q}(\mathbf{o})] = \mathbf{o} \ .$$

mials of certain degrees.

The G^k-conditions are simpler if $\mathbf{u}$ is linear in x. In this case, $\mathbf{u}_{x..s..x}$ is zero for $s = 2, \ldots, k$, and the G^k-conditions reduce to

$$
\begin{aligned}
\mathbf{p} &= \mathbf{q} \ , \\
\mathbf{p}_x &= \mathbf{q}_u \ \alpha \ + \ \mathbf{q}_v \ \beta \ , \\
\mathbf{p}_{xx} &= \mathbf{q}_{uu}\alpha^2 + 2\mathbf{q}_{uv}\alpha\beta + \mathbf{q}_{vv}\beta^2 \ , \\
&\vdots \\
\mathbf{p}_{x..k..x} &= \sum_{i+j=k} \binom{k}{i} \mathbf{q}_{u..i..uv..j..v}\alpha^i\beta^j \ , \qquad (1)
\end{aligned}
$$

where $\alpha = \alpha(y) = u_x(0, y)$ and $\beta = \beta(y) = v_x(0, y)$.

Note that the right hand sides also represent the partial derivatives of $\mathbf{q}$ with respect to the direction $[\alpha\ \beta]^t = \mathbf{u}_x$.

Remark 2: A mixed partial derivative $\mathbf{p}_{x..i..xy..j..y}$ can be expressed in terms of the mixed partial derivatives of $\mathbf{q}$ up to total order $i + j$ and the mixed partial derivatives of $\mathbf{u}(x, y)$ up to order (i, j). For example,

$$\mathbf{p}_{xy} = \mathbf{q}_{uu}u_x u_y + \mathbf{q}_{uv}(u_x v_y + u_y v_x) + \mathbf{q}_{vv}v_x v_y + \mathbf{q}_u u_{xy} + \mathbf{q}_v v_{xy} \ .$$

Remark 3: In particular, if $\mathbf{u}(x, y)$ is a dilation in x and y, i.e.,

$$\mathbf{u}(x, y) = [c_1 x\ c_2 y]^t \ ,$$

then all mixed partial derivatives $\mathbf{p}_{x..i..xy..j..y}$ can be expressed in terms of u_x, v_y and the mixed partial derivatives of $\mathbf{q}$ up to order (i, j).

14.4 G^k surfaces of arbitrary topology

In this section, we present a construction of smooth free-form surfaces. These surfaces interpolate the **vertices** $\mathbf{c}_i$ of a given quadrilateral net and smoothly contact prescribed polynomial surfaces $\mathbf{s}_i$ at these vertices.

The resulting surface is G^k-continuous and consists of tensor product patches parametrized over $[0, 1]^2$, where each patch corresponds uniquely to a quadrilateral of the given net and vice versa.

For notational simplicity, we assume that the given net is **orientable** and has no boundary.

We call a vertex **regular**, if it has exactly four neighbors and **irregular** otherwise. To simplify the complex construction, we assume further that

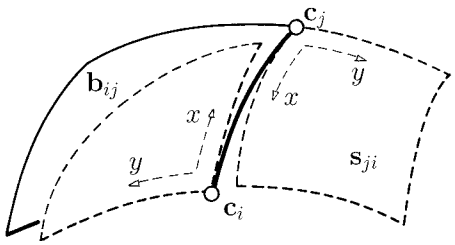

Figure 14.6: An edge polynomial.

are of minimal degree. Therefore, if $\mathbf{c}_i$ and $\mathbf{c}_j$ are regular, then $\mathbf{b}_{ij}$ has degree $2k+1$ and, otherwise, if $\mathbf{c}_i$ or $\mathbf{c}_j$ is irregular, then $\frac{\partial^r}{\partial y^r}\mathbf{b}_{ij}$ has the degree $3k+1-r$. The Bézier points of $\mathbf{b}_{ij}$ are shown schematically in Figure 14.7 for $k=2$, where $\mathbf{c}_i$ is irregular. The points determined by the C^{2k} contact at $\mathbf{c}_i$ are marked by triangles $\triangle$, the points determined by the $C^{k,k}$ contact at $\mathbf{c}_j$ by squares $\square$ and the points determined by the minimal degree constraints by circles $\circ$. The points marked by dots $\cdot$ are non-interesting.

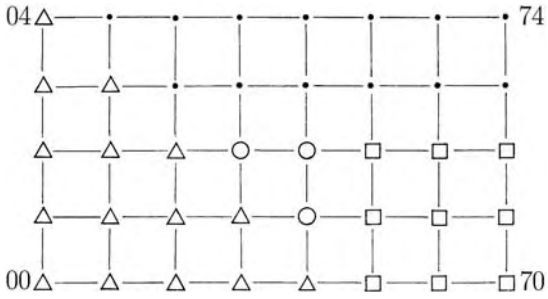

Figure 14.7: Schematic view of the Bézier points of an edge polynomial.

Analogously, we get a second polynomial $\mathbf{b}_{ji}$ for the oppositely directed edge $\mathbf{c}_j\mathbf{c}_i$. Due to our construction, both polynomials have a simple C^k contact along the parameter line $y=0$,

$$\mathbf{b}_{ij}(x,y) \underset{y=0}{\overset{k}{=}} \mathbf{b}_{ji}(1-x,-y) \ .$$

Further, due to our construction, any two polynomials $\mathbf{b}_{ij}$ and $\mathbf{b}_{ik}$ belonging to a vertex $\mathbf{c}_i$ have $G^{k,k}$- or G^{2k} contact at $\mathbf{c}_i$.

3. For each quadrilateral of the given net, we construct a patch $\mathbf{p}(u,v)$ of the final G^k surface from the four associated edge polynomials. For each edge $\mathbf{c}_i\mathbf{c}_j$, we use a reparametrization

$$\mathbf{x}_{ij}(u,v) = \sum \mathbf{b}_{rs} B_{rs}^{2k,2k}(u,v)$$

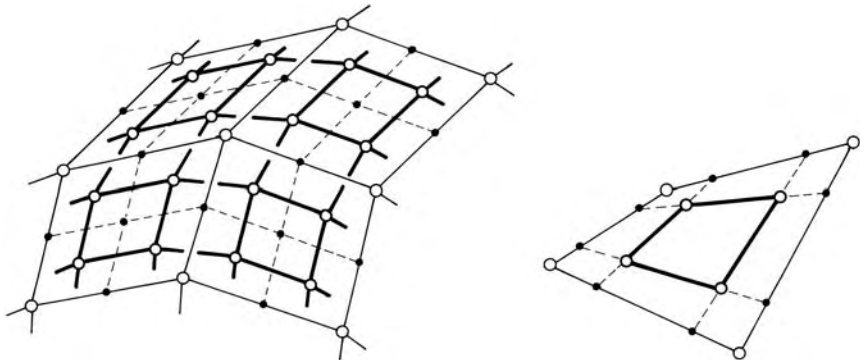

Figure 15.1: Refining and averaging a net.

$i+n+1$. Applying the convergence result in 6.3 twice, we obtain the estimate

$$\sup_{i,j} \|\mathbf{s}((i,j)/2^m) - \mathbf{c}_{ij}^m\| = O(1/4^m) \ ,$$

provided that the second derivatives of $\mathbf{s}$ are bounded over $\mathbb{R}^2$.

15.2 General stationary subdivision and masks

Any refinement equation

$$\mathbf{c}_\mathbf{i}^{m+1} = \sum_\mathbf{k} \mathbf{c}_\mathbf{k}^m \gamma_{\mathbf{i}-2\mathbf{k}}$$

with a finite number of non-zero and arbitrary coefficients $\gamma_\mathbf{i}$ represents a general **stationary subdivision scheme**. If the γ_{ij} are products of the form $\alpha_i\beta_j$, then this scheme is a tensor product scheme, as discussed in 15.1.

The refinement equation combines four different affine combinations: The indices $\mathbf{k}$ of the weights $\gamma_\mathbf{k}$ used to compute a point $\mathbf{c}_\mathbf{i}^{m+1}$ form the set $\mathbf{i}+2\mathbb{Z}^2$, which is either

$$2\mathbb{Z}^2, \quad \mathbf{e}_1 + 2\mathbb{Z}^2, \quad \mathbf{e}_2 + 2\mathbb{Z}^2 \quad \text{or} \quad \mathbf{e} + 2\mathbb{Z}^2 \ .$$

The four (finite) matrices $[\gamma_{-2\mathbf{k}}], [\gamma_{\mathbf{e}_1-2\mathbf{k}}], [\gamma_{\mathbf{e}_2-2\mathbf{k}}]$ and $[\gamma_{\mathbf{e}-2\mathbf{k}}]$ are called **masks**. They, too, represent the subdivision scheme.

Remark 2: A necessary condition for the convergence of a stationary subdivision scheme is that each mask defines an affine combination, see 15.3. This means that the weights of any mask must sum to one. To avoid fractions, it is common, therefore, to represent a mask by some multiple of it. The proper

mask is then obtained by dividing by the sum of all its weights. We will use this convention in the sequel.

Remark 3: The four masks of the refinement operator $\mathcal{M}_1$ defined in 15.1, are

$$\begin{bmatrix} 1 & 0 \\ 1 & 0 \end{bmatrix}, \begin{bmatrix} 1 & 1 \\ 1 & 1 \end{bmatrix}, \begin{bmatrix} 0 & 0 \\ 1 & 0 \end{bmatrix}, \begin{bmatrix} 0 & 0 \\ 1 & 1 \end{bmatrix} .$$

They are presented graphically on the left side of Figure 15.2. The right side of Figure 15.2 shows the four masks

$$\begin{bmatrix} 9 & 3 \\ 3 & 1 \end{bmatrix}, \begin{bmatrix} 3 & 9 \\ 1 & 3 \end{bmatrix}, \begin{bmatrix} 3 & 1 \\ 9 & 3 \end{bmatrix}, \begin{bmatrix} 1 & 3 \\ 3 & 9 \end{bmatrix}$$

of the operator $\mathcal{M}_2 = \mathcal{A}\mathcal{M}_1$ for biquadratic splines.

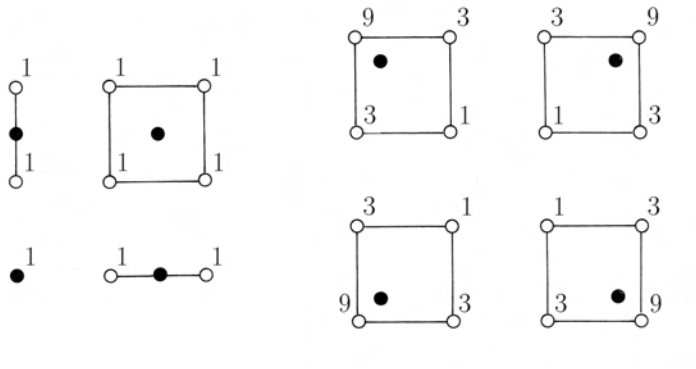

Figure 15.2: The four masks of the Lane-Riesenfeld algorithms $\mathcal{M}_1$ (left) and $\mathcal{M}_2$ (right).

Remark 4: The refinement operator $\mathcal{M}_1$ is described by four masks, whereas the averaging operator $\mathcal{A}$ is described by a single mask only. Figures 15.3 and 15.4 show the masks for $\mathcal{A}$ and $\mathcal{A}^2$.

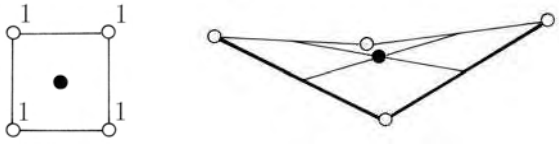

Figure 15.3: The mask of the averaging operator $\mathcal{A}$ (left) and its application (right).

tions $\mathbf{c}(\mathbf{x})$ and $\mathbf{d}(\mathbf{x})$, respectively, where $\mathbf{v} \in \mathbb{Z}^2$.

Then $\mathbf{d}(\mathbf{x})$ is the directional derivative of $\mathbf{c}(\mathbf{x})$ with respect to $\mathbf{v}$.

For a proof, choose $\mathbf{u} \in \mathbb{Z}^2$ be such that $\mathbf{u}$ and $\mathbf{v}$ are linearly independent. Clearly, the control nets

$$[c_{ij}^m] = [\mathbf{c}_{i\mathbf{u}+j\mathbf{v}}^m]$$

converge to $\mathbf{c}(x\mathbf{u}+y\mathbf{v})$ and the difference polygons $2^m \nabla_{\mathbf{v}}[c_{ij}^m]$ to $\mathbf{d}(x\mathbf{u}+y\mathbf{v})$. So, without loss of generality, we can and do assume $\mathbf{v} = \mathbf{e}_2$. Obviously the piecewise constant splines

$$\mathbf{d}_m(x,y) := \sum_{i,j} 2^m \nabla_{\mathbf{v}} \mathbf{c}_{ij}^m N_i^0(2^m x) N_j^0(2^m y)$$

and the splines

$$\mathbf{c}_m(x,y) := \int \mathbf{d}_m(x,y)dy = \sum_{i,j} \mathbf{c}_{ij}^m N_i^0(2^m x) N_j^1(2^m y)$$

converge uniformly to $\mathbf{d}(\mathbf{x})$ and $\mathbf{c}(\mathbf{x})$, respectively. Hence, $\mathbf{c}(x,y) = \int \mathbf{d}(x,y)dy$, which concludes the proof. $\diamond$

15.4 Increasing averages

In 15.3, divided differences of control nets are discussed. In contrast, we now study averaged nets.

If the polygons $C_m = [\mathbf{c_i}]_{\mathbf{i}\in\mathbb{Z}^2}$ converge uniformly to a Riemann integrable function $\mathbf{c}(\mathbf{x})$ with compact support, then the increasing averages

$$\mathbf{a}_{ij}^m = \frac{1}{4^m} \sum_{k,l=0}^{2^m-1} \mathbf{c}_{i-k,j-l}^m$$

converge uniformly to the uniformly continuous function

$$\mathbf{a}(\mathbf{x}) = \int_{[0,1]^2} \mathbf{c}(\mathbf{x}-\mathbf{t})d\mathbf{t} \ .$$

For a proof, let Ω be the interval $(\mathbf{i}-[0,1]^2)/2^m$, which depends on $\mathbf{i}$ and m. Since $\mathbf{c}(\mathbf{x})$ is Riemann integrable, the Riemann sums

$$\mathbf{r}_{\mathbf{i}}^m = 4^{-m} \sum_{k,l=0}^{2^m-1} \mathbf{c}((i-k,j-l)/2^m)$$

converge to $\mathbf{a}(\mathbf{i})$ uniformly for all $\mathbf{i}$, as m goes to infinity.

Since the $\mathbf{c}_\mathbf{i}^m$ converge uniformly to $\mathbf{c}(\mathbf{x})$, the averages $\mathbf{a}_\mathbf{i}^m$ converge uniformly to the Riemann sums $\mathbf{r}_\mathbf{i}^m$, which concludes the proof. $\diamond$

Similarly, one can prove the next result.

If the polygons $C_m = [\mathbf{c}_\mathbf{i}]_{\mathbf{i}\in\mathbb{Z}^2}$ converge uniformly over any compact set to a continuous function $\mathbf{c}(\mathbf{x})$, then the **increasing line averages**

$$\mathbf{b}_\mathbf{i}^m = \frac{1}{2^m}\sum_{k=0}^{2^m-1} \mathbf{c}_{\mathbf{i}-k\mathbf{v}}^m \quad , \quad \mathbf{v}\in\mathbb{Z}^2 \quad ,$$

converge uniformly over any compact set to the uniformly continuous function

$$\mathbf{b}(\mathbf{x}) = \int_0^1 \mathbf{c}(\mathbf{x}-t\mathbf{v})dt \quad .$$

Remark 5: The averages $\mathbf{a}_\mathbf{i}^m$ are line averages of line averages, since

$$\mathbf{a}_\mathbf{i}^m = \frac{1}{2^m}\sum_{k=0}^{2^m-1} \mathbf{b}_{\mathbf{i}-k\mathbf{e}_1}^m \quad , \quad \mathbf{e}_1 = [1\ 0] \quad ,$$

where

$$\mathbf{b}_\mathbf{i}^m = \frac{1}{2^m}\sum_{l=0}^{2^m-1} \mathbf{c}_{\mathbf{i}-l\mathbf{e}_2}^m \quad , \quad \mathbf{e}_2 = [0\ 1] \quad .$$

15.5 Computing the difference schemes

A stationary subdivision scheme can also be described by means of generating functions. As in 8.8, we multiply the refinement equation by the monomial $\mathbf{x}^\mathbf{i} = x^i y^j$ and sum over all $\mathbf{i}$. This results in

$$\begin{aligned}\sum_\mathbf{i} \mathbf{c}_\mathbf{i}^{m+1}\mathbf{x}^\mathbf{i} &= \sum_\mathbf{i}\sum_\mathbf{j} \mathbf{c}_\mathbf{j}^m \gamma_{\mathbf{i}-2\mathbf{j}}\mathbf{x}^{2\mathbf{j}}\mathbf{x}^{\mathbf{i}-2\mathbf{j}} \\ &= \sum_\mathbf{j} \mathbf{c}_\mathbf{j}^m \mathbf{x}^{2\mathbf{j}} \sum_\mathbf{k} \gamma_\mathbf{k}\mathbf{x}^\mathbf{k} \quad ,\end{aligned}$$

which we abbreviate by

$$\mathbf{c}^{m+1}(\mathbf{x}) = \mathbf{c}^m(\mathbf{x}^2)\gamma(\mathbf{x}) \quad .$$

The factor

$$\gamma(\mathbf{x}) = \sum_{\mathbf{k}} \gamma_{\mathbf{k}} \mathbf{x}^{\mathbf{k}}$$

represents the subdivision scheme, and it is called its **symbol** or **characteristic polynomial**. For a tensor product scheme, the characteristic polynomial is the product of two univariate polynomials $\alpha(x)$ and $\beta(y)$ representing two curve schemes.

Any stationary curve scheme has an underlying difference scheme, but for surface schemes this is not true in general. To study when a subdivision scheme has a difference scheme, we identify control nets and subdivision schemes with their generating polynomials.

Thus, given a control net

$$\mathbf{c}(\mathbf{x}) = \sum \mathbf{c}_{\mathbf{i}} \mathbf{x}^{\mathbf{i}} \ ,$$

its refinement under a stationary scheme $\gamma(\mathbf{x})$ is given by

$$\mathbf{b}(\mathbf{x}) = \mathbf{c}(\mathbf{x}^2)\gamma(\mathbf{x}) \ ,$$

and the differences $\nabla_{\mathbf{v}} \mathbf{c}_{\mathbf{i}} = \mathbf{c}_{\mathbf{i}} - \mathbf{c}_{\mathbf{i}-\mathbf{v}}, \mathbf{v} \in \mathbb{Z}^2$, form the polygon

$$\nabla_{\mathbf{v}} \mathbf{c}(\mathbf{x}) = \mathbf{c}(\mathbf{x})(1 - \mathbf{x}^{\mathbf{v}}) \ .$$

Hence, the differences of the refined polygon $\mathbf{b}(\mathbf{x}) = \mathbf{c}(\mathbf{x}^2)\gamma(\mathbf{x})$ are given by

$$\nabla_{\mathbf{v}} \mathbf{b}(\mathbf{x}) = \nabla_{\mathbf{v}} \mathbf{c}(\mathbf{x}^2)\gamma(\mathbf{x}) \frac{1 - \mathbf{x}^{\mathbf{v}}}{1 - \mathbf{x}^{2\mathbf{v}}} \ .$$

Thus, there exists a stationary scheme, the **$\nabla_{\mathbf{v}}$-difference scheme**, mapping $\nabla_{\mathbf{v}} \mathbf{c}$ onto $\nabla_{\mathbf{v}} \mathbf{b}$ if and only if

$$\delta(\mathbf{x}) = \gamma(\mathbf{x})/(1 + \mathbf{x}^{\mathbf{v}})$$

is a polynomial. In case $\delta(\mathbf{x})$ is a polynomial, it is the **characteristic polynomial of the difference scheme**.

Remark 6: Given a control net $C = [\mathbf{c}_{\mathbf{i}}]$, let ∇C be the control net whose "vertices" are the matrices

$$\nabla \mathbf{c}_{\mathbf{i}} = [\nabla_{\mathbf{e}_1} \mathbf{c}_{\mathbf{i}} \ \ \nabla_{\mathbf{e}_2} \mathbf{c}_{\mathbf{i}}] \ .$$

If the control net B is obtained by application of a stationary subdivision scheme from C, then ∇B is obtained from ∇C using a stationary scheme whose weights are 2×2 matrices, see [Kobbelt '00, Cavaretta et al. '91, Thm. 2.3].

Remark 7: The Lane-Riesenfeld scheme $\mathcal{M}_n$, see 15.1, has the characteristic polynomial

$$\gamma(x,y) = 4^{-n}(1+x)^{n+1}(1+y)^{n+1} \quad .$$

This follows directly from Remark 5 in 8.8.

15.6 Computing the averaging schemes

Using characteristic polynomials, it can be seen that for any stationary subdivision scheme there exists a stationary scheme for the averages considered in 15.4.

Let

$$\mathbf{c}^m(\mathbf{x}) = \gamma(\mathbf{x})\mathbf{c}^{m-1}(\mathbf{x}^2)$$

represent a sequence of control nets $[\mathbf{c}_\mathbf{i}^m]$ obtained under a stationary subdivision scheme γ. Using the variables

$$\mathbf{x}_k := \mathbf{x}^{2^k} \quad ,$$

this sequence can be written as

$$\mathbf{c}^m(\mathbf{x}) \quad = \quad \gamma(\mathbf{x}_0) \ldots \gamma(\mathbf{x}_{m-1})\mathbf{c}^0(\mathbf{x}_m) \quad .$$

Further, for any $\mathbf{v} \in \mathbb{Z}^2$, let the polynomial $\mathbf{b}^m(\mathbf{x}) = \sum \mathbf{b}_\mathbf{i}^m \mathbf{x}^\mathbf{i}$ represent the line averages

$$\mathbf{b}_\mathbf{i}^m = \frac{1}{2^m} \sum_{k=0}^{2^m-1} \mathbf{c}_{\mathbf{i}-k\mathbf{v}}^m \quad .$$

With $\mathbf{y}^k := \mathbf{x}^{k\mathbf{v}}$, this can be written as

$$\begin{aligned} \mathbf{b}^m(\mathbf{x}) &= 2^{-m}(1+\mathbf{y}+\mathbf{y}^2+\mathbf{y}^3+\cdots+\mathbf{y}^{2^m-1})\mathbf{c}^m(\mathbf{x}) \\ &= 2^{-m}(1+\mathbf{y})(1+\mathbf{y}^2)(1+\mathbf{y}^4)\ldots(1+\mathbf{y}^{2^{m-1}})\mathbf{c}^m(\mathbf{x}) \\ &= \beta(\mathbf{x}_0)\ldots\beta(\mathbf{x}_{m-1})\mathbf{c}^0(\mathbf{x}) \quad , \end{aligned}$$

where

$$\beta(\mathbf{x}) = \gamma(\mathbf{x})(1+\mathbf{x}^\mathbf{v})/2$$

is the characteristic polynomial of the **averaging scheme** obtained from the scheme γ.

This means that the scheme β is described by the following algorithm.

Given control points $\mathbf{b_i}$, $\mathbf{i} \in \mathbb{Z}^2$, and a vector $\mathbf{v} \in \mathbb{Z}^2$
repeat

1 For all $\mathbf{i}$, subdivide by the scheme γ, i.e.,
$$\mathbf{d_i} := \textstyle\sum_{\mathbf{j}} \mathbf{b_j} \gamma_{\mathbf{i}-2\mathbf{j}} \ .$$

2 For all $\mathbf{i}$, compute the line averages
$$\mathbf{b_i} := \tfrac{1}{2}(\mathbf{d_i} + \mathbf{d_{i-v}}) \ .$$

Similarly, it follows that the averages

$$\mathbf{a}_\mathbf{i}^m = \frac{1}{4^m} \sum_{k,l=0}^{2^m-1} \mathbf{c}_{i-k,j-l}^m$$

are obtained from the points $\mathbf{a}_\mathbf{i}^0 = \mathbf{c}_\mathbf{i}^0$ under the stationary scheme represented by

$$\alpha(\mathbf{x}) = \gamma(\mathbf{x})(1+x)(1+y)/4.$$

This scheme is described by the following algorithm.

Given control points $\mathbf{a_i}$, $\mathbf{i} \in \mathbb{Z}^2$
repeat
1 For all $\mathbf{i}$, subdivide by the scheme γ, i.e.,
$$\mathbf{d_i} := \textstyle\sum_{\mathbf{j}} \mathbf{a_j} \gamma_{\mathbf{i}-2\mathbf{j}} \ .$$
2 For all $\mathbf{i}$, compute the line averages
$$\mathbf{f_i} := \tfrac{1}{2}(\mathbf{d_i} + \mathbf{d_{i-e_1}}) \ .$$
3 For all $\mathbf{i}$, compute the line averages
$$\mathbf{a_i} := \tfrac{1}{2}(\mathbf{f_i} + \mathbf{f_{i-e_2}}) \ .$$

15.7 Subdivision for triangular nets

Every regular quadrilateral net can be transformed into a regular triangular net and vice versa by adding or deleting "diagonal" edges, as illustrated in Figure 15.5. Thus, we can represent any regular triangular net by a biinfinite matrix

$$C = \begin{bmatrix} & \vdots & \iddots \\ \cdots & \mathbf{c}_{ij} & \cdots \\ \iddots & \vdots & \end{bmatrix}$$

whose entries are the vertices of the net.

In particular, the three vectors

$$\mathbf{e}_1 = \begin{bmatrix} 1 \\ 0 \end{bmatrix} \ , \quad \mathbf{e}_2 = \begin{bmatrix} 0 \\ 1 \end{bmatrix} \ , \quad \mathbf{e}_3 = \begin{bmatrix} -1 \\ -1 \end{bmatrix}$$

represents a three direction averaging algorithm, and $C_m = \mathcal{B}_{\mathbf{n}}^m(C)$ represents the sequence of triangular nets obtained from C under the averaging algorithm $\mathcal{B}_{\mathbf{n}}$.

Remark 8: The doubling operator $\mathcal{D}$ is the Lane-Riesenfeld operator $\mathcal{M}_0$ given in Remark 7. Its characteristic polynomial is

$$\delta(x, y) = (1 + x)(1 + y) \ .$$

Remark 9: In particular, $\mathcal{B}_{001}$ represents the **refinement operator** $\mathcal{R}$ that subdivides all triangles of a regular net uniformly into four congruent triangles, as illustrated in Figure 15.7. The figure also depicts the four masks representing $\mathcal{B}_{001}$. The weights of these four masks form the coefficients of the characteristic polynomial of $\mathcal{B}_{001}$, see 15.2. This polynomial is

$$\begin{aligned} \gamma(x, y) &= (1 + x)(1 + y)(1 + \mathbf{x}^{\mathbf{e}_3})/2 \\ &= \frac{1}{2} \begin{bmatrix} x^{-1} & 1 & x \end{bmatrix} \begin{bmatrix} 1 & 1 & 0 \\ 1 & 2 & 1 \\ 0 & 1 & 1 \end{bmatrix} \begin{bmatrix} y^{-1} \\ 1 \\ y \end{bmatrix} \ . \end{aligned}$$

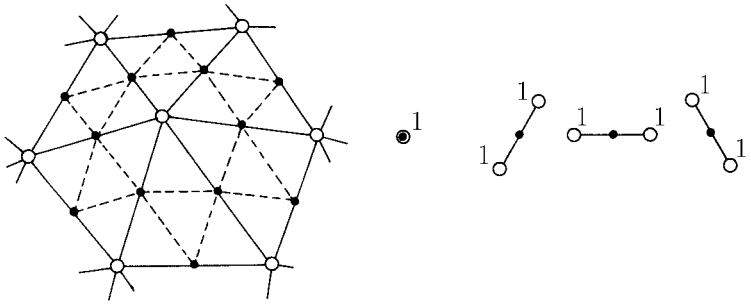

Figure 15.7: The refinement operator $\mathcal{R}$ applied to a regular triangular net and its four masks.

Remark 10: Any net obtained by successive application of the refinement operator $\mathcal{R}$ to a regular triangular net C represents the same continuous piecewise linear surface. Hence, a sequence of nets obtained under $\mathcal{R}$ converges.

Remark 11: The symmetric averaging operator $\mathcal{A}_{111} = \mathcal{A}_1\mathcal{A}_2\mathcal{A}_3$ is given by a single mask. The mask has been introduced in [Boehm '83] and is depicted

in Figure 15.8. The polynomial representing $\mathcal{A}_{111}$ is

$$\gamma(x,y) = \frac{1}{8}\begin{bmatrix}1 & x & x^2\end{bmatrix}\begin{bmatrix}0 & 1 & 1\\ 1 & 2 & 1\\ 1 & 1 & 0\end{bmatrix}\begin{bmatrix}1\\ y\\ y^2\end{bmatrix} \quad .$$

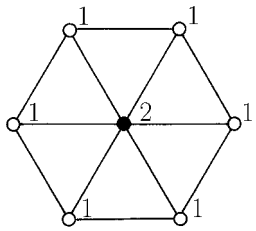

Figure 15.8: Boehm's mask of the symmetric averaging operator $\mathcal{A}_{111}$.

15.8 Box splines over triangular grids

Let C_m be a sequence of triangular nets obtained under repeated applications of the averaging operator $\mathcal{B}_{\mathbf{n}}$. If $\mathcal{B}_{\mathbf{n}}$ is the doubling operator, given by $\mathbf{n} = (0,0,0)$, or refinement operator, given by $\mathbf{n} = (0,0,1)$, then C_m converges to a piecewise constant or continuous piecewise linear spline, respectively.

In general, if

$$k := \min\{n_1{+}n_2,\, n_1{+}n_3{-}1,\, n_2{+}n_3{-}1\} \geq 0 \quad ,$$

then, over every compact domain, C_m converges uniformly to a C^k spline, which is polynomial of total degree $|\mathbf{n}| = n_1 + n_2 + n_3$ over each triangle of the grid spanned by $\mathbf{e}_1, \mathbf{e}_2$ and $\mathbf{e}_3$.

These splines are three-direction box splines, see Chapter 17.

For a proof, we apply repeatedly the results in 15.4 and 15.6 and take into account the following fact. If $f(\mathbf{x})$ is continuous, then the integral

$$\int_0^1\int_0^1\int_0^1 f(\mathbf{x} - u\mathbf{e}_1 - v\mathbf{e}_2 - w\mathbf{e}_3)dudvdw$$

has continuous mixed partial derivatives with respect to any two distinct directions $\mathbf{e}_i$ and $\mathbf{e}_j$. Since $\mathbf{e}_i = \mathbf{e}_j{+}\mathbf{e}_k$ for all permutations (i,j,k) of $(1,2,3)$, all second partial derivatives exist. Consequently, iterated integration with respect to two different directions raises the smoothness order by one, but iterated integration with respect to three directions raises it by two. $\diamond$

as the one illustrated in Figure 16.1. In this figure, the light edges form the net C, the light and broken edges form the net $\mathcal{R}C$ and the bold edges form the net $\mathcal{A}\mathcal{R}C$.

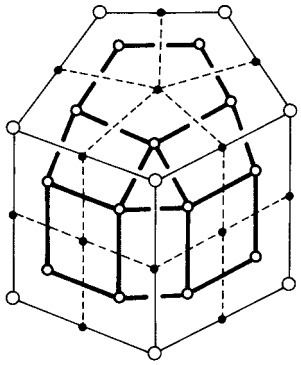

Figure 16.1: Refining and averaging a net.

We call the operator $\mathcal{M}_n = \mathcal{A}^{n-1}\mathcal{R}$, which refines a net and averages it $(n-1)$ times successively, the **midpoint operator** and say that any sequence of nets $\mathcal{M}_n^i C$ is obtained from C under the **midpoint** scheme $\mathcal{M}_n$.

In particular, if C is a regular quadrilateral net, then $\mathcal{M}_n$ represents the Lane-Riesenfeld algorithm for tensor product splines of bidegree n. Furthermore, for arbitrary nets, $\mathcal{M}_2$ and $\mathcal{M}_3$ represent specific instances of the **Doo-Sabin** [Doo et al. '78] and **Catmull-Clark algorithm** [Catmull et al. '78], respectively. A sequence of nets obtained by application of $\mathcal{M}_3$ is shown in Figure 16.2.

For odd and even n, the midpoint schemes $\mathcal{M}_n$ have dual properties. If n is odd, all nets $\mathcal{M}_n^i C, i \geq 1$, are quadrilateral and if n is even, all nets $\mathcal{M}_n^i C, i \geq 1$, have interior vertices of valence four only. Non-quadrilateral meshes and interior vertices of valence different from four are called **extraordinary meshes** and **extraordinary vertices**, respectively. In short, we refer to both types using the term **extraordinary elements**.

Furthermore, every extraordinary element of a net $\mathcal{M}_n^i C$ is obtained by an affine combination of a fixed number of vertices around a corresponding extraordinary element of the preceding net $\mathcal{M}_n^{i-1} C$. Since any extraordinary element in a net $\mathcal{M}_n^{i-1} C$ corresponds to at most one extraordinary element in $\mathcal{M}_n^i C$, the number of extraordinary elements in any net $\mathcal{M}_n^i C$ is bounded by the number of extraordinary elements in C. If C is a closed net, i.e., if C has no boundary, then the number of extraordinary elements is the same for all nets $\mathcal{M}_n^i C, i \geq 0$.

Remark 1: The distance between two extraordinary elements in some net $\mathcal{M}_n^i C$ is the number of edges of a shortest path connecting the two elements.

17 Box splines

Box splines are density functions of the shadows of higher dimensional polyhedra, namely boxes. For example, B-splines with equidistant knots are special univariate box splines, and the surfaces obtained by the averaging algorithm described in Section 15.7 are box spline surfaces over a regular triangular grid. This chapter (an abbreviated version of [Prautzsch et al. '02]) provides a brief introduction to general box splines. It also covers half-box splines. Symmetric half-box splines of degree $3n$ are more suitable for the construction of arbitrary G^{2n-1} free-form surfaces with triangular patches than box splines.

17.1 Definition of box splines

An s-variate **box spline** $B(\mathbf{x}|\mathbf{v}_1 \ \dots \ \mathbf{v}_k)$ is determined by k directions $\mathbf{v}_i$ in $\mathbb{R}^s$. For simplicity, we assume that $k \geq s$ and that $\mathbf{v}_1, \dots, \mathbf{v}_s$ are linearly independent. Under these assumptions, the box splines $B_k(\mathbf{x}) = B(\mathbf{x}|\mathbf{v}_1 \ \dots \ \mathbf{v}_k)$, $k = s, s+1, \dots$, are defined by successive convolutions, similarly to the definition given in 8.1,

$$B_s(\mathbf{x}) = \begin{cases} 1/|\det[\mathbf{v}_1 \ \dots \ \mathbf{v}_s]| & \text{if} \quad \mathbf{x} \in [\mathbf{v}_1 \ \dots \ \mathbf{v}_s][0,1)^s \\ 0 & \text{otherwise} \end{cases}$$

$$B_k(\mathbf{x}) = \int_0^1 B_{k-1}(\mathbf{x} - t\mathbf{v}_k)dt, \quad k > s \ .$$

which corresponds, up to a constant factor, to the inductive definition of box splines. Consequently, $\mathrm{vol}_{k-s}\beta_k(\mathbf{x})$ is a multiple of the box spline $B_k(\mathbf{x})$, and, since

$$\int_{\mathbb{R}^s} \mathrm{vol}_{k-s}\beta_k(\mathbf{x})\, d\mathbf{x} = \mathrm{vol}_k\beta_k \quad \text{and} \quad \int_{\mathbb{R}^s} B_k(\mathbf{x})d\mathbf{x} = 1 \ ,$$

equation (1) follows. $\diamond$

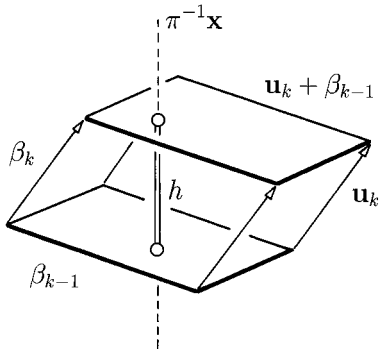

Figure 17.3: Measurements of the box β_k.

Remark 1: From the geometric definition (1), it follows that a box spline solves the functional equation

$$\int_{\mathbb{R}^s} B(\mathbf{x}|\mathbf{v}_1 \ \ldots \ \mathbf{v}_k) f(\mathbf{x}) d\mathbf{x} = \int_{[0,1)^k} f([\mathbf{v}_1 \ \ldots \ \mathbf{v}_k]\mathbf{t}) d\mathbf{t}$$

for all continuous test functions $f(\mathbf{x})$.

17.3 Properties of box splines

From the geometric construction (1) of box splines, it follows that $B(\mathbf{x}) = B(\mathbf{x}|\mathbf{v}_1 \ \ldots \ \mathbf{v}_k)$

- *does not depend on the* **ordering** *of the directions* $\mathbf{v}_i$,
- *is* **positive** *over the convex set* $[\mathbf{v}_1 \ldots \mathbf{v}_k][0,1)^k$,
- *has the* **support** $\mathrm{supp}B(\mathbf{x}) = [\mathbf{v}_1 \ \ldots \ \mathbf{v}_k][0,1]^k$,
- *is* **symmetric** *with respect to the center of its support.*

Further, let $B(\mathbf{x})$ be the shadow of a box β as in 17.2. The $(s-1)$-dimensional faces of β projected into $\mathbb{R}^s$ form a tessellation of the support. It is illustrated

is linearly dependent if $|\det[\mathbf{v}_1 \dots \mathbf{v}_s]| \neq 1$. Since the ordering of the $\mathbf{v}_i$ does not matter, this sequence is also linearly dependent if there is any independent subsequence $\mathbf{v}_{i_1} \dots \mathbf{v}_{i_s}$ with

$$|\det[\mathbf{v}_{i_1} \dots \mathbf{v}_{i_s}]| \neq 1 \ .$$

The converse is also true [**?**, '85]. One can prove it, for example, by induction, see [Jia '83, '85]. We leave it as an exercise. In summary, we have the following theorem.

> *$B(\mathbf{x}-\mathbf{i}|\mathbf{v}_1 \dots \mathbf{v}_k), \mathbf{i} \in \mathbb{Z}^s$, is linearly independent over each open subset of $\mathbb{R}^s$ if and only if $[\mathbf{v}_1 \dots \mathbf{v}_k]$ is* **unimodular**,

which means that the determinant of any submatrix $[\mathbf{v}_{i_1} \dots \mathbf{v}_{i_s}]$ is $1, 0$ or -1.

If the directions $\mathbf{v}_1, \dots, \mathbf{v}_{k-1}$ span $\mathbb{R}^s$, then we can compute the **directional derivative** $D_{\mathbf{v}_k}\mathbf{s}$ of $\mathbf{s}$ with respect to $\mathbf{v}_k$. Using derivative formula (3) from 17.3, we obtain

$$D_{\mathbf{v}_k}\mathbf{s}(\mathbf{x}) = \sum_{\mathbf{i}\in\mathbb{Z}^s} \nabla_{\mathbf{v}_k}\mathbf{c}_\mathbf{i} B(\mathbf{x}-\mathbf{i}|\mathbf{v}_1 \ \dots \ \mathbf{v}_{k-1}) \ , \tag{5}$$

where $\nabla_\mathbf{v}\mathbf{c}_\mathbf{i} = \mathbf{c}_\mathbf{i} - \mathbf{c}_{\mathbf{i}-\mathbf{v}}$. Further, if for all $j = 1, \dots, k$ the $k-1$ directions $\mathbf{v}_1, \dots, \mathbf{v}_j^*, \dots, \mathbf{v}_k$ span $\mathbb{R}^s$, then $B(\mathbf{x})$ is continuous, as shown in 17.3, and the span of its shifts contains the linear polynomials. In particular, if

$$\mathbf{m}_\mathbf{i} = \mathbf{i} + \frac{1}{2}(\mathbf{v}_1 + \dots + \mathbf{v}_k)$$

is the **center** of $\mathrm{supp} B(\mathbf{x} - \mathbf{i})$, then

$$\sum_{\mathbf{i}\in\mathbb{Z}^s} \mathbf{m}_\mathbf{i} B(\mathbf{x} - \mathbf{i}) = \mathbf{x} \ . \tag{6}$$

Namely, because of symmetry, this equation holds for $\mathbf{x} = \mathbf{m}_\mathbf{o}$, and for all $j = 1, \dots, s$, we obtain

$$D_{\mathbf{v}_j} \sum \mathbf{m}_\mathbf{i} B(\mathbf{x} - \mathbf{i}) = \mathbf{v}_j \ .$$

Since the box spline representation is affinely invariant, we obtain for any linear polynomial $l(\mathbf{x})$ that

$$l(\mathbf{x}) = \sum l(\mathbf{m}_\mathbf{i}) B(\mathbf{x} - \mathbf{i}) \ .$$

This property is referred to as the **linear precision** of the box spline representation, see also Problems 1 and 2.

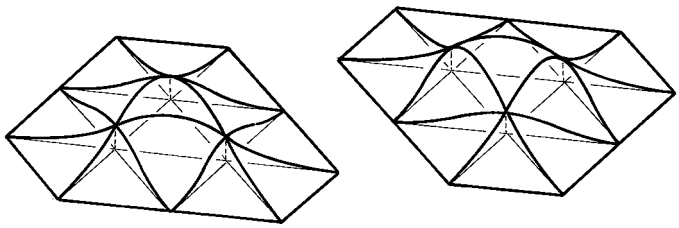

Figure 17.6: The two piecewise cubic C^1half-box splines.

The half-box splines are **normalized** such that

$$\int_{\mathbb{R}^2} H(\mathbf{x})d\mathbf{x} = 1/2 \ .$$

Any k independent directions $\mathbf{u}_1, \ldots, \mathbf{u}_k \in \mathbb{R}^k$ define a half-box

$$\vartheta = \{\sum \mathbf{u}_i \alpha_i | 0 \leq \alpha_1 \leq \alpha_2 \quad \text{and} \quad \alpha_2, \ldots, \alpha_k \in [0,1]\} \ .$$

The **density of a shadow** of this half-box represents a half-box spline: If π denotes the orthogonal projection from $\mathbb{R}^k$ onto $\mathbb{R}^2$ mapping $\mathbf{u}_1, \ldots, \mathbf{u}_k$ to $\mathbf{e}_1, \mathbf{e}_2, \mathbf{v}_3, \ldots, \mathbf{v}_k$, then

$$H(\mathbf{x}|\mathbf{v}_3 \ \ldots \ \mathbf{v}_k) = \frac{1}{2 \operatorname{vol}_k \vartheta} \operatorname{vol}_{k-2}(\pi^{-1}\mathbf{x} \cap \vartheta) \ .$$

From this geometric construction it follows that $H(\mathbf{x})$

- *does not depend on the* **ordering** *of* $\mathbf{v}_3 \ \ldots \ \mathbf{v}_k$,
- *is* **positive** *over the convex set* $\Delta + [\mathbf{v}_3 \ldots \mathbf{v}_k](0,1)^{k-2}$,
- *has the* **support** $\operatorname{closure}(\Delta) + [\mathbf{v}_3 \ldots \mathbf{v}_k][0,1]^{k-2}$,
- *has the* **directional derivative**

  $$D_{\mathbf{v}_r} H(\mathbf{x}) = H(\mathbf{x}|\mathbf{v}_3 \ \ldots \ \mathbf{v}_r^* \ \ldots \ \mathbf{v}_k) - H(\mathbf{x} - \mathbf{v}_r|\mathbf{v}_3 \ \ldots \ \mathbf{v}_r^* \ \ldots \ \mathbf{v}_k)$$

  with respect to $\mathbf{v}_r$, $r \geq 3$,
- *is* r *times* **continuously differentiable**, *provided that all subsets of* $\{\mathbf{v}_3, \ \ldots \ , \mathbf{v}_k\}$ *obtained by deleting* $r+1$ *vectors* $\mathbf{v}_i$ *span* $\mathbb{R}^2$,
- *is polynomial of total degree* $\leq k-2$ *over each triangle* $\mathbf{i} + \Delta$ *and* $\mathbf{i} + \nabla, \mathbf{i} \in \mathbb{Z}^2$.

derivative formula given in 17.8 for a single half-box spline. It is given by

$$D_{\mathbf{v}_r}\mathbf{s}(\mathbf{x}) = \sum_{\mathbf{i}\in\mathbb{Z}^s} \left(\nabla_{\mathbf{v}_r}\mathbf{c}_\mathbf{i}^\Delta H_\Delta(\mathbf{x}-\mathbf{i}|\mathbf{v}_3 \ \dots \ \mathbf{v}_r^* \dots \mathbf{v}_k) + \nabla_{\mathbf{v}_r}\mathbf{c}_\mathbf{i}^\nabla H_\nabla(\mathbf{x}-\mathbf{i}|\mathbf{v}_3 \ \dots \ \mathbf{v}_r^* \dots \mathbf{v}_k)\right) \ ,$$

where $\nabla_\mathbf{v}\mathbf{c}_\mathbf{i} = \mathbf{c}_\mathbf{i} - \mathbf{c}_{\mathbf{i}-\mathbf{v}}$.

If $H_\Delta(\mathbf{x})$ is continuous or, equivalently, if there exist two independent directions among $\mathbf{v}_3, \dots, \mathbf{v}_k$, then all directional derivatives of the sum of all shifts, $\sum H_\Delta(\mathbf{x}-\mathbf{i})$, are zero. Therefore, this sum is a constant function. Because of symmetry, and since the shifts of both half-box splines H_Δ and H_∇ form a partition of unity, we obtain

$$\sum_{\mathbf{i}\in\mathbb{Z}^2} H_\Delta(\mathbf{x}-\mathbf{i}) = \sum_{\mathbf{i}\in\mathbb{Z}^2} H_\nabla(\mathbf{x}-\mathbf{i}) = 1/2 \ . \tag{8}$$

In particular, this implies that the shifts of H_Δ and H_∇ are **linearly dependent**.

Further, if the box spline

$$B(\mathbf{x}) = B(\mathbf{x}|\mathbf{e}_1\mathbf{e}_2\mathbf{v}_3 \ \dots \ \mathbf{v}_k) = H_\Delta(\mathbf{x}) + H_\nabla(\mathbf{x})$$

is continuous, then we recall from (6) in 17.5 that

$$\sum_{\mathbf{i}\in\mathbb{Z}^2} \mathbf{m}_\mathbf{i}\left(H_\Delta(\mathbf{x}-\mathbf{i}) + H_\nabla(\mathbf{x}-\mathbf{i})\right) = \mathbf{x} \ ,$$

where $\mathbf{m}_\mathbf{i}$ is the center of $\mathrm{supp}B(\mathbf{x}-\mathbf{i})$. If H_Δ is continuous, we can use (8) and obtain for any $\mathbf{v} \in \mathbb{R}^2$

$$\sum_{\mathbf{i}\in\mathbb{Z}^2} \left((\mathbf{m}_\mathbf{i}+\mathbf{v})H_\Delta(\mathbf{x}-\mathbf{i}) + (\mathbf{m}_\mathbf{i}-\mathbf{v})H_\nabla(\mathbf{x}-\mathbf{i})\right) = \mathbf{x} \ .$$

For example, if $\mathbf{v} = (\mathbf{e}_2 - \mathbf{e}_1)/6$, then the points $\mathbf{m}_\mathbf{i}^\Delta = \mathbf{m}_\mathbf{i} + \mathbf{v}$ and $\mathbf{m}_\mathbf{i}^\nabla = \mathbf{m}_\mathbf{i} - \mathbf{v}$ form a regular hexagonal grid, as illustrated in Figure 17.8.

Since the half-box spline representation is affinely invariant, we obtain for any linear polynomial $l(\mathbf{x})$ the half-box spline representation

$$l(\mathbf{x}) = \sum_{\mathbf{i}\in\mathbb{Z}^2} \left(l(\mathbf{m}_\mathbf{i}^\Delta)H_\Delta(\mathbf{x}-\mathbf{i}) + l(\mathbf{m}_\mathbf{i}^\nabla)H_\nabla(\mathbf{x}-\mathbf{i})\right) \ .$$

This property is referred to as the **linear precision** of the half-box spline representation.

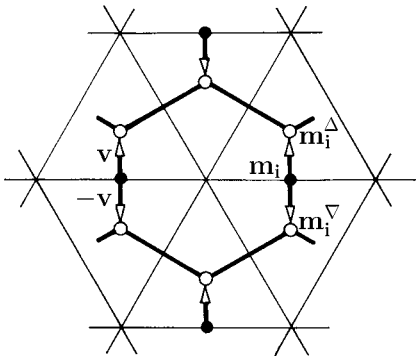

Figure 17.8: The hexagonal grid of the "centers" $\mathbf{m}_\mathbf{i}^\Delta$ and $\mathbf{m}_\mathbf{i}^\nabla$.

Remark 11: Any half-box spline surface

$$\mathbf{s}(\mathbf{x}) = \sum_{\mathbf{i}\in\mathbb{Z}^2} \left(\mathbf{c}_\mathbf{i}^\Delta H_\Delta(\mathbf{x}-\mathbf{i}) + \mathbf{c}_\mathbf{i}^\nabla H_\nabla(\mathbf{x}-\mathbf{i})\right)$$

has also a "finer" representation

$$\mathbf{s}(\mathbf{x}) = \sum_{\mathbf{i}\in\mathbb{Z}^2} \left(\mathbf{d}_\mathbf{i}^\Delta H_\Delta(m\mathbf{x}-\mathbf{i}) + \mathbf{d}_\mathbf{i}^\nabla H_\nabla(m\mathbf{x}-\mathbf{i})\right)$$

for any $m \in \mathbf{N}$. In particular, for $m = 2^k, k \in \mathbf{N}$, the new control points $\mathbf{d}_\mathbf{i}^\Delta$ and $\mathbf{d}_\mathbf{i}^\nabla$, which depend on m, can be computed by k repeated applications of the subdivision algorithm 15.9. Similar to the subdivision algorithm for box splines as described in Section 17.6, this algorithm has an obvious generalization that generates the points $\mathbf{d}_\mathbf{i}^\Delta$ and $\mathbf{d}_\mathbf{i}^\nabla$ for any arbitrary $m \in \mathbf{N}$. We leave it as an exercise to work out this generalization.

17.10 Problems

1 Let the directions $\mathbf{v}_1, \ldots, \mathbf{v}_k \in \mathbb{Z}^s$ span $\mathbb{R}^s$, and assume that the associated box spline $B(\mathbf{x}) = B(\mathbf{x}|\mathbf{v}_1 \ldots \mathbf{v}_k)$ is r times continuously differentiable. Use the derivative formula (5) given in 17.5 to show, by induction over k, that for any polynomial $c(\mathbf{x})$ of total degree $d \le r+1$ the spline

$$s(\mathbf{x}) = \sum_{\mathbf{i}\in\mathbb{Z}^s} c(\mathbf{i})B(\mathbf{x}-\mathbf{i})$$

is also a polynomial of degree d.

18.5 A recurrence relation

If the new knot $\mathbf{a}_{k+1}$ coincides with $\mathbf{x}$, then the knot insertion formula (1) from 18.4 represents a simplex spline at $\mathbf{x}$ as an affine combination of simplex splines with $\mathbf{x}$ as a knot, i.e.,

$$M(\mathbf{x}|\mathbf{a}_0 \ \dots \ \mathbf{a}_k) = \sum_{i=0}^{k} \xi_i M(\mathbf{x}|\mathbf{x}\,\mathbf{a}_0 \ \dots \ \mathbf{a}_i^* \ \dots \ \mathbf{a}_k) \ ,$$

where $\mathbf{x} = \sum \xi_i \mathbf{a}_i$ and $1 = \sum \xi_i$.

This leads to a recursive formula since the simplex splines on the right are simplex splines of lower degree. For example, let σ_0 be the simplex $\mathbf{p}\ \mathbf{p}_1 \ \dots \ \mathbf{p}_k$ in $\mathbb{R}^k$ with shadow

$$M_{\sigma_0}(\mathbf{x}) = M(\mathbf{x}|\mathbf{x}\,\mathbf{a}_1 \dots \mathbf{a}_k) \ ,$$

where $\pi\mathbf{p}, \pi\mathbf{p}_1, \dots, \pi\mathbf{p}_k$ are the knots $\mathbf{x}, \mathbf{a}_1, \dots, \mathbf{a}_k$. We assume that the "base simplex" ρ with the vertices $\mathbf{p}_1, \dots, \mathbf{p}_k$ lies in a hyperplane orthogonal to the fibers of the projection π.

Hence, if h denotes the Euclidean distance between $\mathbf{p}$ and ρ, we obtain

$$\mathrm{vol}_k \sigma_0 = \frac{1}{k} h \cdot \mathrm{vol}_{k-1} \rho$$

and

$$\mathrm{vol}_{k-s}(\sigma_0 \cap \pi^{-1}\mathbf{x}) = \frac{1}{k-s} h \cdot \mathrm{vol}_{k-s-1}(\rho \cap \pi^{-1}\mathbf{x})$$

as illustrated in Figure 18.6 for $k = 3$ and $s = 1$.

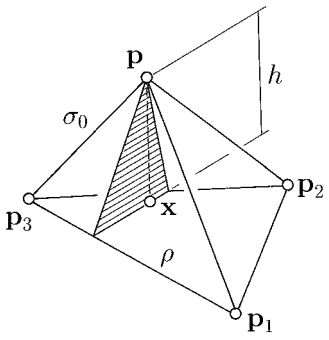

Figure 18.6: Computing the volumes of σ_0 and $\sigma_0 \cap \pi^{-1}\mathbf{x}$.

Dividing the second by the first equation, we obtain

$$M(\mathbf{x}|\mathbf{x}\,\mathbf{a}_1 \ \dots \ \mathbf{a}_k) = \frac{k}{k-s} M(\mathbf{x}|\mathbf{a}_1 \ \dots \ \mathbf{a}_k) \ .$$

Hence, we can transform the knot insertion formula (1) into **Micchelli's recurrence relation**

$$M(\mathbf{x}|\mathbf{a}_0 \ldots \mathbf{a}_k) = \frac{k}{k-s} \sum_{i=0}^{k} \xi_i M(\mathbf{x}|\mathbf{a}_0 \ldots \mathbf{a}_i^* \ldots \mathbf{a}_k) \ , \tag{2}$$

which represents a simplex spline with $k+1$ knots as a linear combination of simplex splines with k knots, see [Micchelli '80]. Since the weights ξ_i depend linearly on $\mathbf{x}$, repeated application of this recurrence relation shows that

> *an s-variate simplex spline with $k+1$ knots is piecewise polynomial of total degree $\leq k-s$.*

Remark 4: Comparing the recurrence relations for simplex splines and Bernstein polynomials, see 10.1, we see that an s-variate simplex spline with only $s+1$ distinct knots is a Bernstein polynomial, i.e.,

$$M(\mathbf{x}|\mathbf{a}_0 \overset{i_0+1}{\ldots} \mathbf{a}_0 \ldots \mathbf{a}_s \overset{i_s+1}{\ldots} \mathbf{a}_s) = \frac{\binom{k}{s}}{\mathrm{vol}_s \Delta} B_{\mathfrak{i}}^{k-s}(\mathfrak{u}) \ ,$$

where $\mathfrak{i} = (i_0 \ldots i_s), k = i_0 + \cdots + i_s + s, \Delta$ denotes the simplex $\mathbf{a}_0 \ldots \mathbf{a}_s$ and $\mathfrak{u}$ the barycentric coordinate column of $\mathbf{x}$ with respect to Δ, see Figure 18.7.

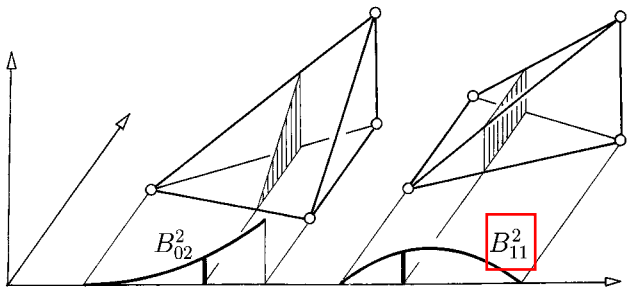

Figure 18.7: Quadratic Bernstein polynomials.

Remark 5: Repeated application of the recursion formula(2) also shows that each polynomial segment of a multivariate B-spline can be written as a product of k weights ξ, which represent $\mathbf{x}$ as certain affine combinations of all or some knots $\mathbf{a}_i$. Since these weights depend continuously on the knots $\mathbf{a}_i$ (or on the vertices $\mathbf{p}_i$ of some associated simplex), it follows that each polynomial segment depends continuously on the knots $\mathbf{a}_i$.

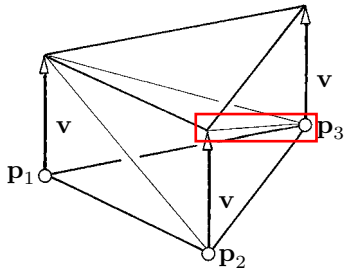

Figure 18.8: Triangulation of a prism.

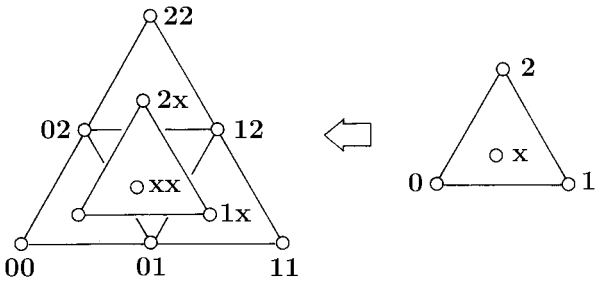

Figure 19.1: De Casteljau's algorithm for a quadratic.

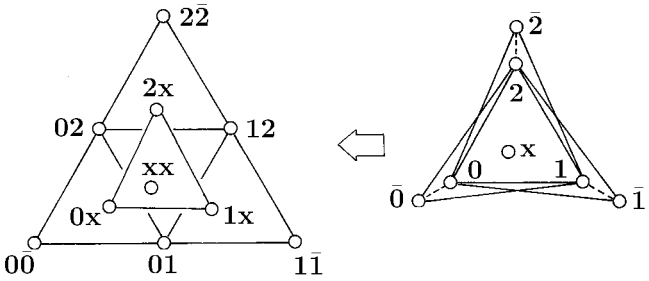

Figure 19.2: Seidel's generalization of de Casteljau's algorithm for a quadratic.

$\mathbf{c}[\bar{1}\bar{2}]$, $\mathbf{c}[\bar{2}\mathbf{2}]$ and $\mathbf{c}[\bar{2}\bar{0}]$, we compute the three points $\mathbf{c}[\mathbf{i}\,\mathbf{x}]$ and then compute from these three points the point $\mathbf{c}(\mathbf{x}) = \mathbf{c}[\mathbf{x}\,\mathbf{x}]$.

To present the generalization of de Casteljau's algorithm, let $\mathbf{a}_i^0, \ldots, \mathbf{a}_i^{n-1}$ denote a sequence, also called **chain** or **cloud of knots**, for $i = 0, \ldots, s$. If these knots are in general position, then any s-variate polynomial surface $\mathbf{c}(\mathbf{x})$ with polar form $\mathbf{c}[\mathbf{x}_1 \ldots \mathbf{x}_n]$ is completely defined by its **B-points**

$$\mathbf{c}_{\mathbb{i}} = \mathbf{c}[\mathbf{a}_0^0 \ldots \mathbf{a}_0^{i_0-1} \ldots \mathbf{a}_s^0 \ldots \mathbf{a}_s^{i_s-1}] \ ,$$

where $\mathbb{i} = [i_0 \ldots i_s] \in \Delta_n$ and

$$\Delta_n = \{\mathbb{i} | \mathbb{i} \in \mathbb{Z}^{s+1}, \mathbb{0} \leq \mathbb{i}, i_0 + \cdots + i_s = n\} \ .$$

Namely, $\mathbf{c}(\mathbf{x})$ can be computed by means of the recursion formula

$$\mathbf{c}_{\mathbb{j}} = \xi_0 \mathbf{c}_{\mathbb{j}+\mathbb{e}_0} + \cdots + \xi_s \mathbf{c}_{\mathbb{j}+\mathbb{e}_s} \quad \mathbb{j} \in \Delta := \Delta_{n-1} \cup \cdots \cup \Delta_0 \ ,$$

where the ξ_k are the barycentric coordinates of $\mathbf{x}$ with respect to the simplex

$$S_{\mathbb{j}} = [\mathbf{a}_0^{j_0} \ldots \mathbf{a}_s^{j_s}]$$

and $\mathbb{e}_k$ denotes the kth unit vector in $\mathbb{R}^{s+1}$ as before. This means that

$$\mathbf{c}_{\mathbb{j}} = \mathbf{c}[\mathbf{a}_0^0 \dots \mathbf{a}_0^{j_0-1} \dots \mathbf{a}_s^0 \dots \mathbf{a}_s^{j_s-1} \mathbf{x} \dots \mathbf{x}]$$

and that the knots are in **general position** if all simplices $S_{\mathbb{j}}$ are non-degenerate.

Remark 1: If $\mathbf{c}(\mathbf{x})$ is quadratic, then its Bézier points $\mathbf{b}_{\mathbb{i}}$ over the simplex $S_{\mathbb{o}}$ satisfy

$$\mathbf{b}_{\mathbb{e}_i+\mathbb{e}_j} = \mathbf{c}_{\mathbb{e}_i+\mathbb{e}_j} \quad \text{for all} \quad i \neq j \ ,$$

and $\mathbf{b}_{\mathbb{e}_i+\mathbb{e}_i}$ lies in the plane spanned by the points $\mathbf{c}_{\mathbb{e}_i+\mathbb{e}_j}$, $j = 0, \dots, s$. An example is shown in Figure 19.5.

19.2 B-polynomials and B-patches

We can apply the generalized de Casteljau algorithm from Section 19.1 to any arbitrary net of control points $\mathbf{c}_{\mathbb{i}}, |\mathbb{i}| \in \Delta_n$. If we start with the control points

$$c_{\mathbb{i}} = \begin{cases} 1 & \text{if} \quad \mathbb{i} = \mathbb{k} \\ 0 & \text{otherwise} \end{cases} \quad , \quad \mathbb{i} \in \Delta_n \ ,$$

then the resulting scalar valued polynomials $C^n_{\mathbb{k}}(\mathbf{x})$ form a basis for the space of all nth degree polynomials. Namely, since the generalized de Casteljau algorithm in 19.1 is linear in the control points, any polynomial $\mathbf{c}(\mathbf{x})$ of degree $\leq n$ can be written as

$$\mathbf{c}(\mathbf{x}) = \sum_{\mathbb{i} \in \Delta_n} \mathbf{c}_{\mathbb{i}} C^n_{\mathbb{i}}(\mathbf{x}) \ ,$$

where $\mathbf{c}_{\mathbb{i}}$ is defined as in 19.1. Further, the $C^n_{\mathbb{i}}$ are linearly independent since their number $\binom{n+s}{s}$ equals the dimension of the space of all polynomials of total degree $\leq n$.

The polynomials $C^n_{\mathbb{i}}$ are called the **B-polynomials** and the representation of a polynomial as a linear combination of B-polynomials is referred to as a **B-patch representation**. From their construction above, we obtain the following properties, which are similar to the properties of Bernstein polynomials, given in Section 10.1. The s-variate B-polynomials of degree n

- *form a* **basis** *for all s-variate polynomials of total degree $\leq n$,*
- *form a* **partition of unity**, *i.e.,*

$$\sum_{\mathbb{i} \in \Delta_n} C^n_{\mathbb{i}}(\mathbf{x}) = 1 \ ,$$

- *are* **positive** *for all* $\mathbf{x}$ *in the interior of the intersection* Γ *of all simplices* $S_{\mathbb{j}}, |\mathbb{j}| \leq n-1$,
- *and satisfy the* **recursion**

$$C^n_{\mathbb{i}}(\mathbf{x}) = \sum_{k=0}^{s} \xi_k C^{n-1}_{\mathbb{i}-\mathbf{e}_k}(\mathbf{x}) \ ,$$

where ξ_k is the kth barycentric coordinate of $\mathbf{x}$ with respect to $S_{\mathbb{i}-\mathbf{e}_k}$ and $C^n_{\mathbb{j}} = 0$ if $\mathbb{j}$ has a negative coordinate.

The intersection Γ of the simplices $S_{\mathbb{j}}, \mathbb{j} \in \Delta$, is illustrated in Figure 19.3 for $n = 2$ and $s = 2$. It can be empty, depending on the knot positions.

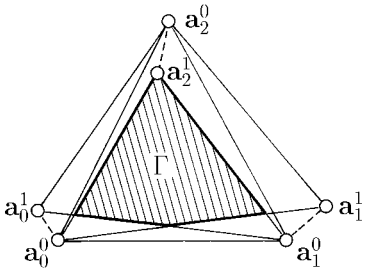

Figure 19.3: The region Γ over which all B-polynomials are positive for $n = s = 2$.

Since the B-polynomials form a partition of unity, any polynomial surface $\mathbf{c}(\mathbf{x})$ is an affine combination of its B-points $\mathbf{c}_{\mathbb{i}}$. Consequently, a B-patch representation is affinely invariant. Furthermore, the patch $\mathbf{c}(\mathbf{x}), \mathbf{x} \in \Gamma$, lies in the convex hull of the B-points $\mathbf{c}_{\mathbb{i}}$ since the B-polynomials sum to one and are non-negative over Γ.

Remark 2: If all knots of each knot chain are equal, i.e., $S_{\mathbb{o}} = S_{\mathbb{j}}$ for all $\mathbb{j}$, then the B-polynomials $C^n_{\mathbb{i}}$ are the Bernstein polynomials $B^n_{\mathbb{i}}$ over the simplex $S_{\mathbb{o}}$ since both sets of polynomials satisfy the same recursion.

19.3 Linear precision

The linear polynomial $\mathbf{x}$, which is the identity map on $\mathbb{R}^s$, has a B-patch representation of degree n with respect to the knots $\mathbf{a}^j_i$ introduced in 19.1. Since $\mathbf{x}$ has the polar form

$$\mathbf{x}[\mathbf{x}_1 \ \ldots \ \mathbf{x}_n] = \frac{1}{n}(\mathbf{x}_1 + \cdots + \mathbf{x}_n) \ ,$$

its B-points are

$$\mathbf{x}_{\mathbb{i}} := \frac{1}{n}(\mathbf{a}^0_0 + \cdots + \mathbf{a}^{i_0-1}_0 + \cdots + \mathbf{a}^0_s + \cdots + \mathbf{a}^{i_s-1}_s) \ ,$$

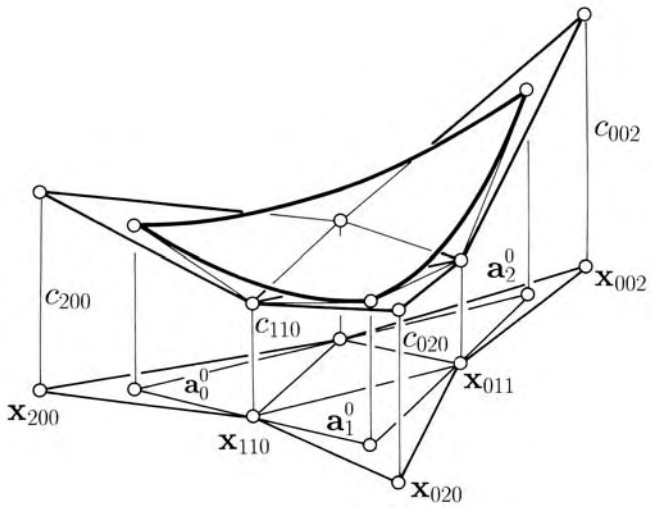

Figure 19.5: A quadratic polynomial with its B-patch and Bézier ordinates.

denote the directional derivative of $\mathbf{c}$ with respect to $\Delta\mathbf{x}$ at $\mathbf{x}$. Furthermore, let $\mathbf{c}[\mathbf{x}_1 \ \dots \ \mathbf{x}_n]$ be the symmetric polynomial of $\mathbf{c}(\mathbf{x})$. Then, the symmetric polynomial of $\dot{\mathbf{c}}(\mathbf{x})$ is given by

$$\dot{\mathbf{c}}[\mathbf{x}_2 \ \dots \ \mathbf{x}_n] = n\mathbf{c}[\Delta\mathbf{x} \ \mathbf{x}_2 \ \dots \ \mathbf{x}_n] \ ,$$

as explained in 11.6. Hence, the B-points of $\dot{\mathbf{c}}(\mathbf{x})$ are given by

$$n\dot{\mathbf{c}}_{\mathbb{j}} = n\mathbf{c}[\Delta\mathbf{x} \ \mathbf{a}_0^0 \dots \mathbf{a}_0^{i_0-1} \dots \mathbf{a}_s^0 \dots \mathbf{a}_s^{i_s-1}] \ , \quad \mathbb{j} \in \Delta_{n-1} \ .$$

Expressing $\Delta\mathbf{x}$ with respect to $S_{\mathbb{j}}$, i.e., writing $\Delta\mathbf{x}$ as

$$\Delta\mathbf{x} = \sum_{k=0}^{s} \nu_k \mathbf{a}_k^{j_k}, \quad 0 = \sum_{k=0}^{s} \nu_k \ ,$$

and using the fact that polar forms are multiaffine, we obtain for the control points $\dot{\mathbf{c}}_{\mathbb{j}}$ of the derivative

$$\dot{\mathbf{c}}_{\mathbb{j}} \quad = \quad \sum_{k=0}^{s} \nu_k \mathbf{c}_{\mathbb{j}+\mathbb{e}_k} \ .$$

This result is illustrated in Figure 19.6 for $s = n = 2$.

Remark 4: Let $\mathbf{x}_{\mathbb{i}}$ be the B-points of the identity polynomial $\mathbf{p}(\mathbf{x}) = \mathbf{x}$ with respect to the knots $\mathbf{a}_k^i$ and view the B-net of $\mathbf{c}(\mathbf{x})$ as the collection of the

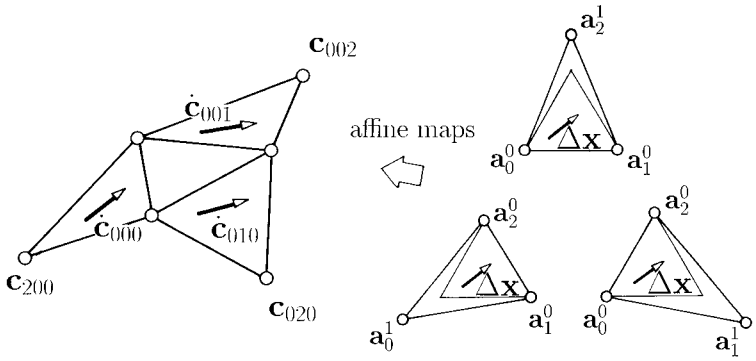

Figure 19.6: The differences $\dot{\mathbf{c}}_{\mathbb{j}}$.

linear patches

$$\mathbf{c}_{\mathbb{j}}(\mathbf{x}) := \sum_{k=0}^{s} \gamma_k \mathbf{c}_{\mathbb{j}+\mathbb{e}_k} \quad , \quad \mathbb{j} \in \Delta_{n-1} \quad ,$$

over the simplices $\mathbf{x}_{\mathbb{j}+\mathbb{e}_0} \ \ldots \ \mathbf{x}_{\mathbb{j}+\mathbb{e}_s}$, where $\gamma_0, \ldots, \gamma_s$ are the barycentric coordinates of $\mathbf{x}$ with respect to $\mathbf{x}_{\mathbb{j}+\mathbb{e}_0} \ \ldots \ \mathbf{x}_{\mathbb{j}+\mathbb{e}_s}$.

Since $\dot{\gamma}_k = n\nu_k$, the directional derivative of $\mathbf{c}_{\mathbb{j}}(\mathbf{x})$ with respect to $\Delta\mathbf{x}$ is $n\dot{\mathbf{c}}_{\mathbb{j}}$. Hence,

> *the derivative of the B-net consists of the B-points of the derivative* $\dot{\mathbf{c}}(\mathbf{x})$.

This is illustrated in Figure 19.7 for a functional bivariate quadratic surface.

19.5 Multivariate B-splines

The B-polynomials $C_{\mathbb{i}}$, $\mathbb{i} \in \Delta_n$, are defined with respect to the knots

$$\mathbf{a}_0^0, \ \ldots \ , \mathbf{a}_0^{n-1}, \ \ldots \ , \mathbf{a}_s^0, \ \ldots \ , \mathbf{a}_s^{n-1} \quad .$$

Here, we add $s+1$ knots $\mathbf{a}_0^n, \ldots, \mathbf{a}_s^n$ and show that

> *the normalized simplex splines*
>
> $$N_{\mathbb{i}} := \frac{\text{vol } S_{\mathbb{i}}}{\binom{n+s}{s}} M(\mathbf{x}|A_{\mathbb{i}}) \quad , \quad \mathbb{i} \in \Delta_n \quad ,$$
>
> *with the knot sequences* $A_{\mathbb{i}} = \mathbf{a}_0^0 \ \ldots \ \mathbf{a}_0^{i_0} \ \ldots \mathbf{a}_s^0 \ldots \mathbf{a}_s^{i_s}$ *coincide with*

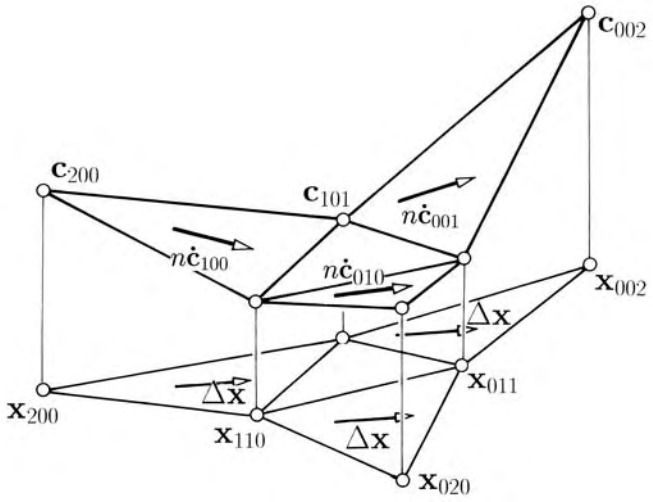

Figure 19.7: The directional derivative of a B-net for $n = s = 2$.

the B-polynomials $C_{\mathbb{i}}(\mathbf{x})$ *for all*

$$\mathbf{x} \in \Omega := \text{interior} \left(\bigcap_{\mathbb{j} \in \Delta_0 \cup \cdots \cup \Delta_n} S_{\mathbb{j}} \right) .$$

This result is due to [Dahmen et al. '92].

The splines $N_{\mathbb{i}}$ are multivariate **B-splines** with properties similar to those of univariate B-splines. In fact, for $s = 1$ the B-splines $N_{\mathbb{i}}(x)$ are the univariate B-splines defined in 5.3.

Proof: From the definition of constant simplex splines in 18.1 and from the recurrence formula (2) in 18.5 for simplex splines, we obtain for $\mathbf{x} \in \mathbb{R}^s$ the recurrence relation

$$N^0_{\mathbb{o}}(\mathbf{x}) = \begin{cases} 1 & \text{if} \quad \mathbf{x} \in S_{\mathbb{o}} \\ 0 & \text{otherwise} \end{cases} ,$$

$$N_{\mathbb{j}}(\mathbf{x}) = \sum_{k=0}^{s} \frac{\text{vol } S_{\mathbb{j}}}{\binom{j+s}{s}} \frac{j+s}{s} \frac{\sigma^k_{\mathbb{j}} \text{vol } S^k_{\mathbb{j}}}{\sigma_{\mathbb{j}} \text{vol } S_{\mathbb{j}}} M(\mathbf{x} | A_{\mathbb{j}-\mathbb{e}_k}) , \quad j := |\mathbb{j}| ,$$

where $S^k_{\mathbb{j}}$ is obtained from $S_{\mathbb{j}}$ by replacing $\mathbf{a}^{j_k}_k$ by $\mathbf{x}$. The orientations -1 or $+1$ of the sequences $S_{\mathbb{j}}$ and $S^k_{\mathbb{j}}$ are denoted by $\sigma_{\mathbb{j}}$ and $\sigma^k_{\mathbb{j}}$, respectively.

Since both simplices $S_{\mathbb{j}}$ and $S_{\mathbb{j}-\mathbb{e}_k}$ contain Ω, their orientations are equal and the equation above is equivalent to

$$\begin{aligned} N_{\mathbb{j}}(\mathbf{x}) &= \sum_{k=0}^{s} \frac{\sigma_{\mathbb{j}}^k}{\sigma_{\mathbb{j}-\mathbb{e}_k}} \frac{\text{vol } S_{\mathbb{j}}^k}{\text{vol } S_{\mathbb{j}-\mathbb{e}_k}} N_{\mathbb{j}-\mathbb{e}_k}(\mathbf{x}) \\ &= \sum_{k=0}^{s} \xi_{\mathbb{j}-\mathbb{e}_k}^k N_{\mathbb{j}-\mathbb{e}_k}(\mathbf{x}) \quad , \end{aligned} \tag{1}$$

where $\xi_{\mathbb{j}-\mathbb{e}_k}^k$ is the kth barycentric coordinate of $\mathbf{x}$ with respect to $S_{\mathbb{j}-\mathbb{e}_k}$. To have all terms well-defined, we define, for $j_k = 0$,

$$\begin{aligned} \xi_{\mathbb{j}-\mathbb{e}_k}^k &= \sigma_{\mathbb{j}}^k \text{vol} S_{\mathbb{j}}^k / \sigma_{\mathbb{j}} \quad , \quad \sigma_{\mathbb{j}-\mathbb{e}_k} \text{vol } S_{\mathbb{j}-\mathbb{e}_k} = 1 \qquad \text{and} \\ N_{\mathbb{j}-\mathbb{e}_k}(\mathbf{x}) &= \frac{1}{\binom{j+s-1}{s}} M(\mathbf{x}|A_{\mathbb{j}-\mathbb{e}_k}) \quad . \end{aligned} \tag{2}$$

If $j_k = 0$, then $N_{\mathbb{j}-\mathbb{e}_k}$ is a simplex spline over the knot sequence $A_{\mathbb{j}-\mathbb{e}_k}$, which does not contain any knot from the kth knot cloud $\mathbf{a}_k^0 \ldots \mathbf{a}_k^n$. Its support and Ω are disjoint, which we prove next.

The support of $N_{\mathbb{j}-\mathbb{e}_k}$ is the convex hull of all knots in $A_{\mathbb{j}-\mathbb{e}_k}$. Hence, every point in this support is a convex combination of some points $\mathbf{a}_0, \ldots, \mathbf{a}_k^*, \ldots, \mathbf{a}_s$, where $\mathbf{a}_i$ lies in the convex hull of the first $j_i + 1$ knots $\mathbf{a}_i^0, \ldots, \mathbf{a}_i^{j_i}$ of the ith knot chain.

We need to show that any such simplex $\mathbf{a}_0 \ldots \mathbf{a}_k^* \ldots \mathbf{a}_s$ does not intersect Ω. Since Ω is contained in all simplices $S_{\mathbb{k}}$, where $\mathbb{o} \leq \mathbb{k} \leq \mathbb{j}$, it is also contained in any simplex $\mathbf{a}_0 \, \mathbf{a}_1^0 \ldots \mathbf{a}_s^0$. Applying this argument repeatedly, we find that the open set Ω is contained in the interior of the simplex $\mathbf{a}_0 \ldots \mathbf{a}_s$, which implies that Ω and the support of $N_{\mathbb{j}-\mathbb{e}_k}$ are disjoint.

So, for all $\mathbf{x}$ in Ω, the recurrence formula of the B-splines $N_{\mathbb{j}}$ coincides with the recurrence formula of the B-polynomials $C_{\mathbb{j}}$. Hence, it follows that $N_{\mathbb{i}}(\mathbf{x}) = C_{\mathbb{i}}(\mathbf{x})$ for all $\mathbf{x} \in \Omega$. $\diamond$

19.6 Linear combinations of B-splines

We have discussed multivariate B-splines over one complex of $s+1$ knot chains. However, the true value of these B-splines is that they define useful spline spaces over the entire $\mathbb{R}^s$ partitioned into complexes of such knot chains.

Let $\mathbf{a}_k^0$, $k \in \mathbb{Z}$, be the vertices of a triangulation of $\mathbb{R}^s$, and let $K \subset \mathbb{Z}^{s+1}$ represent the simplices

$$\mathbf{a}_{k_0}^0 \ldots \mathbf{a}_{k_s}^0 \quad , \quad \mathbb{k} = [k_0 \ldots k_s] \in K \quad ,$$

and, consequently,

$$\xi^0_{\mathbb{k}\mathbb{j}} = -\xi^0_{\bar{\mathbb{k}}\mathbb{j}} \ .$$

Since the control net is connected and $N_{\mathbb{k}\mathbb{j}} = N_{\bar{\mathbb{k}}\mathbb{j}}$, see (2), we obtain, therefore,

$$\xi^0_{\mathbb{k}\mathbb{j}}\mathbf{c}_{\mathbb{k},\mathbb{j}+\mathbb{e}_0}N_{\mathbb{k}\mathbb{j}} + \xi^0_{\bar{\mathbb{k}}\mathbb{j}}\mathbf{c}_{\bar{\mathbb{k}},\mathbb{j}+\mathbb{e}_0}N_{\bar{\mathbb{k}}\mathbb{j}} = 0 \ ,$$

which concludes the proof. $\diamond$

19.8 Derivatives of a spline

The recurrence relation (2) in 18.5 and the derivative formula (3) in 18.6 for simplex splines are similar. One obtains the derivative formula up to a constant factor just by differentiating the weights in the recurrence formula although one might expect further terms due to the product rule.

Because of this, we can transform the recurrence (1) in 19.5 for multivariate splines to a derivative formula. Differentiating the barycentric coordinates ξ in the proof of the recurrence formula in 19.7, we obtain that the directional derivative with respect to a direction $\Delta\mathbf{x}$ of a spline

$$\mathbf{s}(\mathbf{x}) = \sum_{\mathbb{k}\in K}\sum_{\mathbb{i}} \mathbf{c}_{\mathbb{k}\mathbb{i}}N_{\mathbb{k}\mathbb{i}}(\mathbf{x})$$

of degree $n = |\mathbb{i}|$ with connected control net is given by

$$\frac{d}{dt}\mathbf{s}(\mathbf{x}+t\Delta\mathbf{x})|_{t=0} = n\sum_{\mathbb{k}\in K}\sum_{\mathbb{j}\in\Delta}\dot{\mathbf{c}}_{\mathbb{k}\mathbb{j}}N_{\mathbb{k}\mathbb{j}}(\mathbf{x}) \ ,$$

where

$$\dot{\mathbf{c}}_{\mathbb{k}\mathbb{j}} = \sum_{l=0}^{s}\nu_l\mathbf{c}_{\mathbb{k},\mathbb{j}+\mathbb{e}_l}$$

and $\nu_0,\ldots,\nu_s$ are the barycentric coordinates of the direction $\Delta\mathbf{x}$ with respect to the simplex $S_{\mathbb{k}\mathbb{j}}$, see also 19.4.

Remark 5: As already observed in 19.4, the directions $\dot{\mathbf{c}}_{\mathbb{k}\mathbb{j}}$ are part of the directional derivatives with respect to $\Delta\mathbf{x}$ of the control nets $\mathbf{c}_{\mathbb{k}\mathbb{j}}(\mathbf{x})$ of $\mathbf{s}(\mathbf{x})$ over the simplices $\mathbf{x}_{\mathbb{k},\mathbb{j}+\mathbb{e}_0}\ \ldots\ \mathbf{x}_{\mathbb{k},\mathbb{j}+\mathbb{e}_s}$.

19.9 The main theorem

We use the notation from 19.6 and assume that the first r knots $\mathbf{a}^0_k,\ldots,\mathbf{a}^{r-1}_k$ of every knot cluster coincide. Still, the simplices $S_{\mathbb{k}\mathbb{o}}$ form a triangulation of $\mathbb{R}^s$. We show that any C^{n-r} piecewise polynomial function over this

triangulation is a linear combination of the B-splines $N_{\mathbb{k}\mathbb{i}}$ and relate its control points to the polar forms of its polynomial segments.

Let $\mathbf{s}(\mathbf{x})$ be any $(n-r)$ times differentiable spline which, over each simplex $S_{\mathbb{k}\mathbb{o}}$, is identical with some polynomial $\mathbf{s}_{\mathbb{k}}(\mathbf{x})$ of degree $\leq n$. Then, the multivariate version of the **main theorem** 5.5 is as follows [Seidel '92].

The spline $\mathbf{s}(\mathbf{x})$ *can be written as*

$$\mathbf{s}(\mathbf{x}) = \sum_{\mathbb{k}\in K} \sum_{\mathbb{i}\in\Delta_n} \mathbf{s}_{\mathbb{k}}[A_{\mathbb{k},\mathbb{i}-\mathbb{e}}] N_{\mathbb{k}\mathbb{i}}(\mathbf{x}) \quad , \tag{4}$$

where $\mathbf{s}_{\mathbb{k}}[\mathbf{x}_1 \ \ldots \ \mathbf{x}_n]$ *is the polar form of* $\mathbf{s}_{\mathbb{k}}$.

We prove this by induction over $n-r$. If $n-r=-1$, then the B-splines $N_{\mathbb{k}\mathbb{i}}$ are the Bernstein polynomials over $S_{\mathbb{k}\mathbb{o}}$, see 19.5 and Remark 2 in 19.2. In this case, identity (4) follows from the main theorem 11.2. Now let $n-r \geq 0$ and let $D\mathbf{s}(\mathbf{x})$ be the directional derivative of $\mathbf{s}(\mathbf{x})$ with respect to some non-zero vector $\Delta\mathbf{x}$ and assume that

$$D\mathbf{s}(\mathbf{x}) = \sum_{\mathbb{k}\in K} \sum_{\mathbb{j}\in\Delta_{n-1}} D\mathbf{s}_{\mathbb{k}}[A_{\mathbb{k},\mathbb{j}-\mathbb{e}}] N_{\mathbb{k}\mathbb{j}}(\mathbf{x}) \quad .$$

According to Section 11.6, the polar form of $D\mathbf{s}_{\mathbb{k}}$ can be expressed by the polar form of $\mathbf{s}_{\mathbb{k}}$, i.e.,

$$\begin{aligned} D\mathbf{s}_{\mathbb{k}}[A_{\mathbb{k},\mathbb{j}-\mathbb{e}}] &= n\mathbf{s}_{\mathbb{k}}[\Delta\mathbf{x}\ A_{\mathbb{k},\mathbb{j}-\mathbb{e}}] \\ &= n\sum_{l=0}^{s} \nu_l \mathbf{s}_{\mathbb{k}}[A_{\mathbb{k},\mathbb{j}-\mathbb{e}+\mathbb{e}_l}] \quad , \end{aligned}$$

where $\nu_0, \ldots, \nu_s$ are the barycentric coordinates of $\Delta\mathbf{x}$ with respect to $S_{\mathbb{k}\mathbb{j}}$.

Because of Remark 7 in 11.7, the control points $\mathbf{s}_{\mathbb{k}}[A_{\mathbb{k},\mathbb{i}-\mathbb{e}}]$ form a connected net. Hence, it follows from 19.8 that

$$D\sum_{\mathbb{k}}\sum_{\mathbb{i}} \mathbf{s}_{\mathbb{k}}[A_{\mathbb{k},\mathbb{i}-\mathbb{e}}] N_{\mathbb{k}\mathbb{i}} = D\mathbf{s} \quad .$$

Therefore, (4) is true up to some constant term. Since (4) holds over every $\Omega_{\mathbb{k}}$, see 19.4 and 19.5, this constant is zero, which concludes the proof. $\diamond$

In particular, it follows that the B-splines form a **partition of unity**, i.e.,

$$\sum_{\mathbb{k}\in K} \sum_{\mathbb{i}\in\Delta_n} N_{\mathbb{k}\mathbb{i}} = 1 \quad .$$

C